
Lime Microsystems Limited

Surrey Tech Centre
Occam Road
The Surrey Research Park
Guildford, Surrey GU2 7YG
United Kingdom



Tel: +44 (0) 1483 685 063
Fax: +44 (0) 1428 656 662
e-mail: enquiries@limemicro.com

LMS7002M Field Programmable RF MIMO Transceiver Integrated Circuit

- RF and Analog Measurement Results -

Chip version: LMS7002M
Chip revision: 01
Document version: 01
Document revision: 04
Last modified: 24/08/2015 10:50:00

Contents

| | |
|--|-----------|
| 1. Introduction | 6 |
| 2. PLL Synthesizer Measurements | 7 |
| 2.1 Frequency Coverage..... | 8 |
| 2.2 Phase Noise Measurements | 10 |
| 2.3 PLL Spur Measurements | 14 |
| 3. TX Measurements | 17 |
| 3.1 TX LPF Measurements | 18 |
| 3.2 TX RF Gain Measurements..... | 21 |
| 3.3 TX OIP3 Measurements..... | 22 |
| 3.4 Optimum TX ACPR Measurements | 24 |
| 3.5 Using the TSP NCO for Quick Linearity test | 26 |
| 3.6 TX Output Harmonics | 28 |
| 3.7 TX Noise Measurements | 29 |
| 3.8 TX EVM Measurements | 32 |
| 3.9 TX Output Power vs Frequency..... | 35 |
| 3.10 TX Noise Leakage into RX Band | 36 |
| 3.11 TX Peak Detector Measurements..... | 38 |
| 3.12 TX-TX TX-RX Isolation at RF Port | 40 |
| 4. RX Measurements | 41 |
| 4.1 RX Low Pass Filters..... | 42 |
| 4.2 RX Noise Figure and Inband IIP3 Measurement | 45 |
| 4.3 RX Out of band IIP2 and IIP3 Measurement | 48 |
| 4.4 Variation of RX Gain and Noise Figure with Temperature | 52 |
| 4.5 RX LTE EVM Measurement | 54 |
| 4.6 RX GSM Blocker EVM Measurements | 57 |
| 4.7 RX W-CDMA Blocker Test..... | 60 |
| 4.8 Out of Band P1dB | 63 |
| 4.9 Comparison of LNA gains | 64 |
| 4.10 RSSI | 65 |
| 4.11 RX Gain step accuracy | 67 |
| 4.12 RX LO Leakage at RF Port | 69 |
| 5. Loop Back Measurements | 70 |
| 5.1 Baseband Loopback | 70 |
| 5.2 RF Loopback | 73 |
| 6. Miscellaneous Measurements..... | 76 |
| 6.1 Power dissipation | 76 |
| 6.2 ‘On Chip’ LDO Measurements..... | 81 |
| 6.3 LMS7002M Internal LDO Noise Measurement | 82 |

List of Figures

| | |
|--|----|
| Figure 1. Simplified block diagram of the LMS7002M MIMO Software defined radio transceiver chip. | 6 |
| Figure 2. Block diagram of PLL | 7 |
| Figure 3. Test bench for temperature measurements on the TX PLL | 8 |
| Figure 4. Phase noise regions of a PLL synthesizer..... | 10 |
| Figure 5. Test configuration for plateau region phase noise measurements | 11 |
| Figure 6. Plateau phase noise measurements for various LO frequencies with a 30.72MHz TXCO crystal reference. | 12 |
| Figure 7. Plateau phase noise measurements for various LO frequencies with a 52.00MHz discrete crystal reference. | 12 |
| Figure 8. Test configuration for measuring far out phase of the LMS7002M. | 13 |
| Figure 9. shows the amplitude of typical charge pump spurs 900MHz, RefFreq 30.72MHz.... | 14 |
| Figure 10. shows the amplitude of typical charge pump spurs 900MHz, RefFreq 52.00MHz.. | 14 |
| Figure 11. shows the amplitude of typical charge pump spurs 2650MHz, RefFreq 30.72MHz.15 | 15 |
| Figure 12. shows the amplitude of typical charge pump spurs 2650MHz, RefFreq 52.00MHz.15 | 15 |
| Figure 13. shows the amplitude of DSM boundary spurs | 15 |
| Figure 14. shows the amplitude of TX and RX VCO coupling spurs at the TX output (relative to the TX output) with varying RX frequency when TX LO=2649.6MHz | 16 |
| Figure 15. Block diagram of the Transmitter..... | 18 |
| Figure 16. Test bench used to test TX LPF Low Band | 19 |
| Figure 17. Filter responses of the TX LPF Low Band including de-emphasis pole. | 19 |
| Figure 18. 10MHz Filter responses of the TX LPF Low Band with de-emphasis de-embedded | 19 |
| Figure 19. Test bench used to test TX LPF High Band | 20 |
| Figure 20. Filter responses of the TX LPF High Band | 20 |
| Figure 21. Test bench used to measure TX RF Gain Control | 21 |
| Figure 22. Variation of output power and gain step accuracy with TX RF Gain Control. | 21 |
| Figure 23. Test bench for measuring two tone OIP3. | 22 |
| Figure 24. Variation of OIP3 with output power at 900MHz as input level is varied for 3 different bias/gain settings in GUI | 23 |
| Figure 25. Test bench used for ACPR measurements with output power. | 25 |
| Figure 26. Measured ACPR vs output power with optimum gain controls. | 25 |
| Figure 27 Test bench for ‘quick linearity’ test..... | 27 |
| Figure 28 Testbench for measuring TX output harmonics | 29 |
| Figure 29 Test bench for transmitter noise measurement. | 30 |
| Figure 30. Test Bench used for TX EVM measurements with output power..... | 32 |
| Figure 31. LTE EVM Measurement at 860MHz | 33 |
| Figure 32. LTE EVM Measurement at 2140MHz | 33 |
| Figure 33. LTE EVM Measurement at 2610MHz | 34 |
| Figure 34. Test bench for broadband software defined radio output power measurements. | 35 |
| Figure 35. TX power output vs frequency for an unmatched evaluation board in broadband operation with W-CDMA signal with -50dBc ACPR..... | 35 |
| Figure 36. Test bench for measuring TX Noise in the RX band..... | 36 |
| Figure 37. Test bench used to measure peak detector performance..... | 38 |
| Figure 38. Typical output of peak detector with TX output power while varying the peak detector preamplifier gain. | 39 |

| | |
|--|----|
| Figure 39. Typical output of peak detector with TX output power while varying the peak detector load..... | 39 |
| Figure 40. Test bench for TX-TX and TX-RX coupling using the LMS7002M evaluation board..... | 40 |
| Figure 41. Simplified block diagram of a single receiver channel..... | 42 |
| Figure 42. Test bench for testing low pass filters..... | 42 |
| Figure 43. Variable bandwidth of low frequency low pass filter (LPFL)..... | 43 |
| Figure 44. 600kHz Low pass filter (LPFH) | 43 |
| Figure 45. 2.5MHz Lowpass filter (LPFL) | 44 |
| Figure 46. Variable bandwidth of the high frequency low pass filter (LPFH) | 44 |
| Figure 47. Test Bench for Noise Figure and Inband Linearity | 45 |
| Figure 48. DSB Noise figure and inband IIP3 measurements vs gain at 800MHz..... | 45 |
| Figure 49. DSB Noise figure and inband IIP3 measurements vs gain at 1850MHz..... | 46 |
| Figure 50. DSB Noise figure and inband IIP3 measurements vs gain at 2600MHz..... | 46 |
| Figure 51. Noise figure and S_{11} vs frequency for best match at 850MHz..... | 47 |
| Figure 52. Noise figure and S_{11} vs frequency for minimum noise at 850MHz..... | 47 |
| Figure 53. Test bench for the out of band two tone receiver measurements..... | 48 |
| Figure 54. Comparsion of out of band IIP3 with gain of LMS7002M with a competing part at 850MHz with 600kHz LPF..... | 50 |
| Figure 55. Comparsion of out of band IIP3 with gain of LMS7002M with a competing part at 915MHz with 600kHz LPF..... | 50 |
| Figure 56. Comparsion of out of band IIP3 with gain of LMS7002M with a competing part at 1980MHz with 2.5MHz LPF | 51 |
| Figure 57. Comparsion of out of band IIP3 with gain of LMS7002M with a competing part at 2400MHz with 2.5MHz LPF | 51 |
| Figure 58 Test bench for gain over temperature measurements | 52 |
| Figure 59 Test Bench for noise figure over temperature measurements..... | 52 |
| Figure 60 Gain vs Frequency for different temperatres | 53 |
| Figure 61 Noise Figure vs Frequency for different temperatures | 53 |
| Figure 62. Test bench for RX EVM measurements | 54 |
| Figure 63. Low IF EVM performance at 860MHz | 55 |
| Figure 64. Low IF LTE EVM at 2140MHz | 55 |
| Figure 65. Low IF LTE EVM at 2600MHz | 56 |
| Figure 66. Test bench used to measure RX EVM with CW blocker. | 57 |
| Figure 67. RX GSM 900 EVM with CW blocker..... | 58 |
| Figure 68. RX GSM 900 EVM with CW blocker..... | 58 |
| Figure 69. RX GSM 1850 EVM with CW blocker..... | 59 |
| Figure 70. RX GSM 1850 EVM with CW blocker..... | 59 |
| Figure 71. Test bench configuration for W-CDMA blocker case..... | 61 |
| Figure 72. Spectrum of IF output without blocker present (signal -94dBm). | 61 |
| Figure 73. Spectrum of IF output with blocker present (signal -94dBm, blocker -15.6dBm)... | 62 |
| Figure 74. W-CDMA Code Domain View (signal -94dB, blocker -15.6dBm) | 62 |
| Figure 75. Out of band P1dB compression point vs LNA gain control code. Measured with 2.5MHz LPF and blocker at 20MHz offset for different PGA gains. | 63 |
| Figure 76. Variation of gain vs frequency of LNAH, LNAW and LNAL on LMS7002M evaluation board with each input matched at each frequency..... | 64 |
| Figure 77. RSSI measurement test setup..... | 65 |
| Figure 78. RSSI output value vs input power @ 2.14GHz | 66 |
| Figure 79. Test bench for measuring RX gain step accuracy..... | 67 |
| Figure 80. LNA Gain step accuracy for different RF frequencies | 68 |

| | |
|--|----|
| Figure 81. Gain step accuracy for PGA at 1MHz and 10MHz. | 68 |
| Figure 82. Test bench for measuring RX LO leakage..... | 69 |
| Figure 83 Test bench for baseband loop back testing. | 71 |
| Figure 84 Frequency response of baseband loopback..... | 71 |
| Figure 85. Test bench used to measure RF loopback..... | 73 |
| Figure 86. Variation of RF loopback gain for two different frequencies..... | 74 |
| Figure 87 Typical RX LPF response measured with RF loop back..... | 74 |
| Figure 88. Test bench used to measure power dissipation..... | 78 |
| Figure 89 Test configuration used to measure noise..... | 83 |
| Figure 90 AC coupling circuit used for LDO noise measurement..... | 83 |
| Figure 91 Measured LDO noise of the LDO with LNA for different LDO modes. | 83 |

Revision History

Version 01r00

Started: 1 Nov, 2014

Finished: 11 Nov, 2014

Initial version.

Version 01r01

Started: 11 Nov, 2014

Finished: 19 Nov, 2014

Added: Sections 3.11, 3.12, 4.7, 4.11, 4.12, 6.2.

1

Introduction

The LMS7002M is a software defined radio transceiver integrated circuit radio system which can be divided into a number of simpler sections as shown in Figure 1. The phase locked loop synthesizer (PLL) generates the frequency to be modulated or demodulated in the transmitter (TX) and receiver (RX) respectively. The transmitter and receiver can be subdivided into RF, baseband (BB) and digital signal processing blocks (RSP/TSP). Measurements of the TX/RX synthesizer performance are presented in Chapter 2. Measurements of transmitter and receiver performance are presented in Chapter 3 and Chapter 4 respectively. Loop back paths exist between the transmitter and receiver at RF, analog baseband and digital baseband to allow calibration and testing. Measurements of the loop back performance are presented in Chapter 5. The LMS7002M can be operated in either single input single output (SISO) or multiple input multiple output (MIMO) configurations. Miscellaneous measurements, such as power dissipation and LDO noise, can be found in Chapter 6.

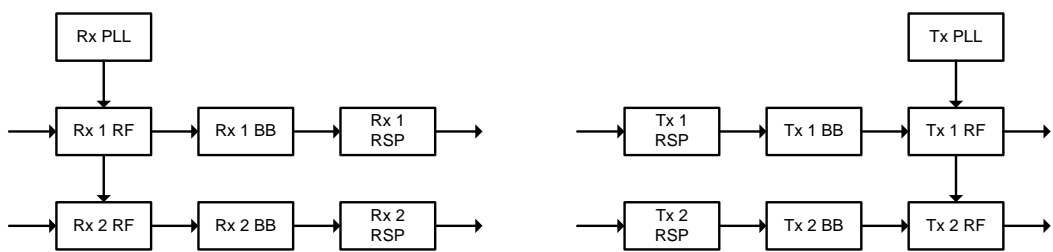


Figure 1. Simplified block diagram of the LMS7002M MIMO Software defined radio transceiver chip.

In all the measurements the LMS7002M Evaluation board (LMS7002EVB) was used, together with the Graphical User Interface (GUI) software called LMS7002M Control.

2

PLL Synthesizer Measurements

The Phase Locked Loop (PLL) Synthesizer plays a major role in determining a number of key performance parameters of a radio, such as Error Vector Magnitude (EVM) and RX sensitivity in the presence of continuous wave (CW) blockers etc. A good PLL will cover a wide range of frequencies and have low integrated phase noise, low far out phase noise, and low spurs. In these measurements we show the LMS7002M is able to fulfil these demanding requirements.

A block diagram of the LMS7002M synthesizer is shown in Figure 2 and consists of voltage controlled oscillators (VCOs), programmable output (feedforward) divider, programmable feedback divider (/N), delta sigma modulator ($\Delta\Sigma$), phase frequency detector (PFD), charge pump (CHP) and lock detectors and reference buffers. The GUI is used to set up each of the blocks for the required operation.

This section describes measured performance of the LMS7002M including frequency coverage in Section 2.1, phase noise in Section 2.2, and spurs in Section 2.3.

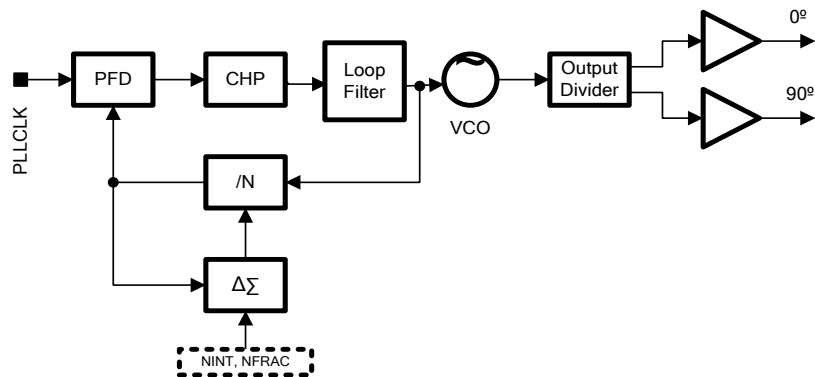


Figure 2. Block diagram of PLL

2.1 Frequency Coverage

The VCOs and feedforward dividers determine the range of local oscillator (LO) frequencies that the LMS7002M synthesizer can generate. The highest LO frequency generated is limited by the highest frequency of VCOH. The lowest frequency generated is limited by the lowest frequency of VCOL and the maximum value of feedforward division (64). The three VCOs provide over an octave of coverage, ensuring the frequency range is continuous over the working range. The frequency ranges achievable with different VCO and feedforward divider settings are shown in Table 1.

Table 1. LO Frequency ranges for each VCO for different divider settings.

| DIV_LOCH_SX | 0 | 1 | 2 | 3 | 4 | 5 | 6 | |
|----------------|------|--------|--------|---------|--------|--------|-------|-----|
| div Ratio_LOCH | 1 | 2 | 4 | 8 | 16 | 32 | 64 | |
| VCOL | 1900 | 950 | 475 | 237.5 | 118.75 | 59.38 | 29.69 | MHz |
| | 2611 | 1305.5 | 652.75 | 326.375 | 163.19 | 81.59 | 40.80 | |
| VCOM | 2481 | 1240.5 | 620.25 | 310.125 | 155.06 | 77.53 | 38.77 | MHz |
| | 3377 | 1688.5 | 844.25 | 422.125 | 211.06 | 105.53 | 52.77 | |
| VCOH | 3153 | 1576.5 | 788.25 | 394.125 | 197.06 | 98.53 | 49.27 | MHz |
| | 3857 | 1928.5 | 964.25 | 482.125 | 241.06 | 120.53 | 60.27 | |

The DSM determines the resolution of frequency in each range as specified in the data sheet.

Temperature measurements were made on the TX PLL using the test configuration of Figure. A programmable DC voltage is applied to the V_{tune} pin of the VCO using the internal test bus to measure kVCO. The charge pump is disabled during kVCO measurements. The Evaluation board is placed in an Heraeus Votsch environmental chamber so that temperature could be varied. At each temperature, the nominal oscillation frequency with $V_{tune}=0.6V$ is recorded for each VCO for different CSW values. Additionally V_{tune} is varied and the kVCO is calculated.

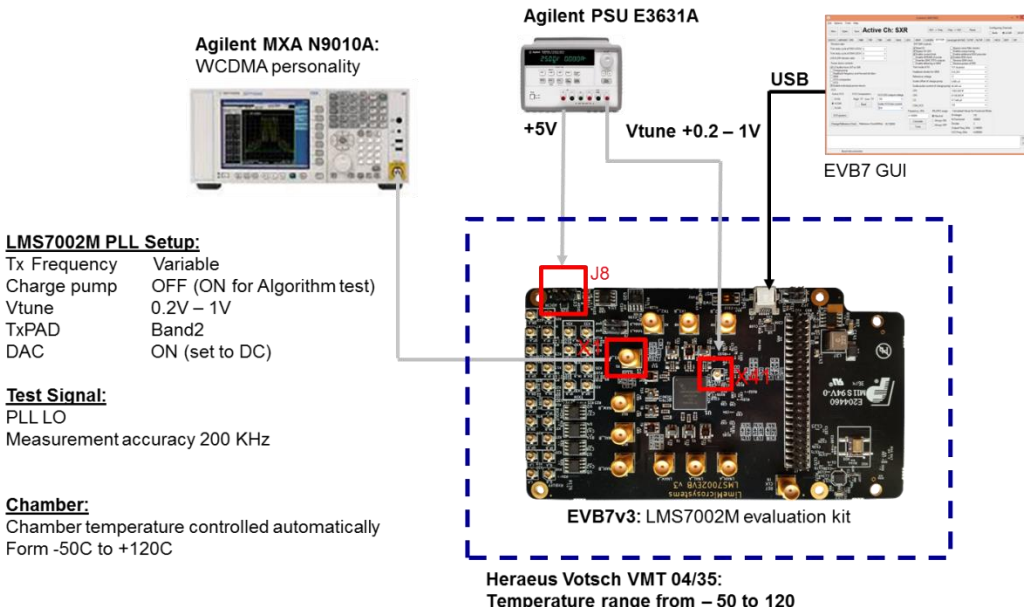


Figure 3. Test bench for temperature measurements on the TX PLL

Table 2. Summary of temperature drift of VCOs over temperature, kVCO and tuning voltage requirements.

| Temp | VCO | CSW | fVCO | fLO | dfLO/dT | kVCO | kLO | dVtune/dT |
|-------------|------------|------------|-------------|------------|----------------|-------------|------------|------------------|
| -50 °C | VCOL | 0 | 3809 | 1904.5 | -10.5 | 35.2 | 17.6 | 0.62 |
| 90 °C | | | 3788 | 1894 | | 34 | 17 | |
| -50 °C | | 255 | 5336 | 2668 | -32 | 84.8 | 42.4 | 0.78 |
| 90 °C | | | 5272 | 2636 | | 81.6 | 40.8 | |
| -50 °C | VCOM | 0 | 5066 | 2533 | -26 | 45.25 | 22.625 | 1.04 |
| 90 °C | | | 5014 | 2507 | | 50 | 25 | |
| -50 °C | | 255 | 6921 | 3460.5 | -57 | 108.8 | 54.4 | 0.96 |
| 90 °C | | | 6807 | 3403.5 | | 118.2 | 59.1 | |
| -50 °C | | 0 | 6442 | 3221 | -30 | 103 | 51.5 | 0.57 |
| 90 °C | | | 6382 | 3191 | | 105 | 52.5 | |
| -50°C | VCOH | 255 | 7896 | 3948 | -53 | 177 | 88.5 | 0.57 |
| 90 °C | | | 7790 | 3895 | | 184.5 | 92.25 | |

2.2 Phase Noise Measurements

The phase noise of the PLL synthesizer can be divided into four main regions as shown in Figure 4. The noise in each region being dominated by different parts of the PLL system. The first region is the drift region which is normally below 1kHz. The second region, the plateau region, approximately covers 1-100kHz region. The third region, the VCO/DSM region, is where the phase noise begins to fall sharply away from the plateau region. The fourth region is the far out noise which approximately covers 10-100MHz region which is very low and largely constant with frequency.

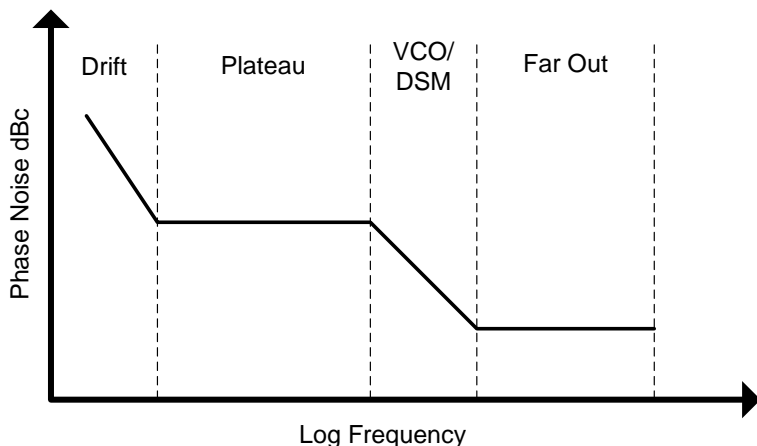


Figure 4. Phase noise regions of a PLL synthesizer.

In the first region, the drift region, the phase noise is dominated by the phase noise of the frequency reference (multiplied by the feedback divider value, N). Modulations such as OFDM inherently remove this noise through their pilot tones. Since this noise does not originate from the LMS7002M, no measurements are made here.

In the second region, the plateau region, phase noise is dominated by the charge pump noise (and noise from the crystal reference if its phase noise is above about -145dBc/Hz). The plateau region phase noise is measured with the phase noise personality of a Spectrum Analyzer as shown in Figure 5 which can measure accurately down to about -130dBc. The LMS7002M is configured as a transmitter with a DC input from the MXG (a low frequency single sideband input could also be used). Measurements of plateau region noise are presented in Figure 6 and Figure 7 for a number of different LO frequencies for two reference frequency sources. The first reference frequency is with a Rakon 30.72MHz commercial temperature stable crystal oscillator (TXCO). The second is for a discrete transistor very low phase noise 50MHz crystal reference. The integrated phase noise results are given in Table 3.

In the third region, VCO/DSM region, the phase noise is dominated by the noise of the VCO and the DSM. For higher LO frequencies, the loop filter poles CP2 and CP3 in the SXT/SXR tab of the GUI can be used to reduce the DSM noise. It may also be necessary to reduce the charge pump current as CP2 and CP3 are increased to prevent noise peaking in the plateau region.

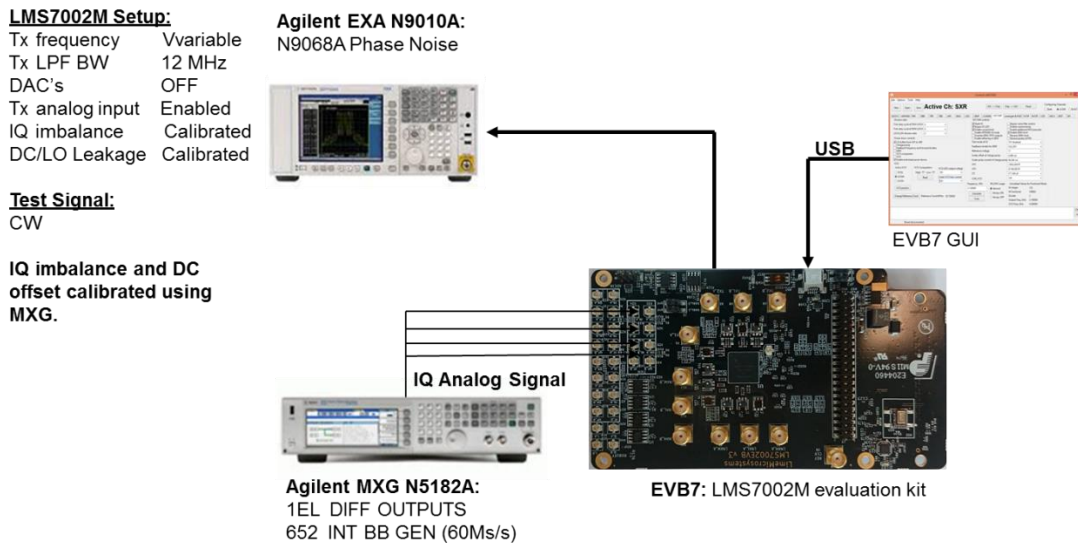


Figure 5. Test configuration for plateau region phase noise measurements

Table 3. Integrated phase noise for different Synthesizer frequencies (TXCO=50MHz)

| Tx LO, MHz | PN@ 1kHz, dBc | PN@ 10kHz, dBc | PN@ 100kHz, dBc | PN@ 1MHz, dBc | PN@ 10MHz, dBc | Integrated PN, deg* |
|------------|---------------|----------------|-----------------|---------------|----------------|---------------------|
| 2665 | -87.23 | -92.54 | -98.28 | -123.63 | -136.15 | 0.5 |
| 2140 | 90.71 | -92.57 | -102.45 | -127.67 | -137.46 | 0.4 |
| 1000 | -96.46 | -99.24 | -107.78 | -131.17 | -138.8 | 0.2 |
| 300 | -97.88 | -104.08 | -113.42 | -128.14 | -138.57 | 0.13 |

Table 4 Typical required integrated phase noise performance for OFDM

| Modulation | Required Integrated Phase Noise | Application |
|--------------|---------------------------------|-------------|
| OFDM QAM64 | 1° | LTE, WiMAX |
| OFDM QAM256 | 0.5° | CATV, DVB |
| OFDM QAM1024 | 0.25° | DVB-C2 |

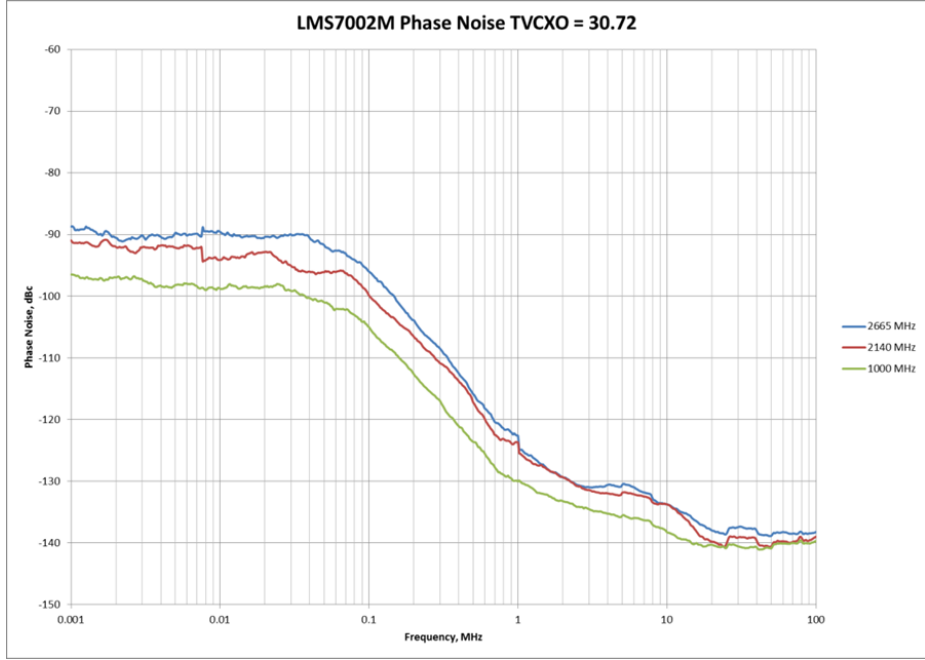


Figure 6. Plateau phase noise measurements for various LO frequencies with a 30.72MHz TXCO crystal reference.

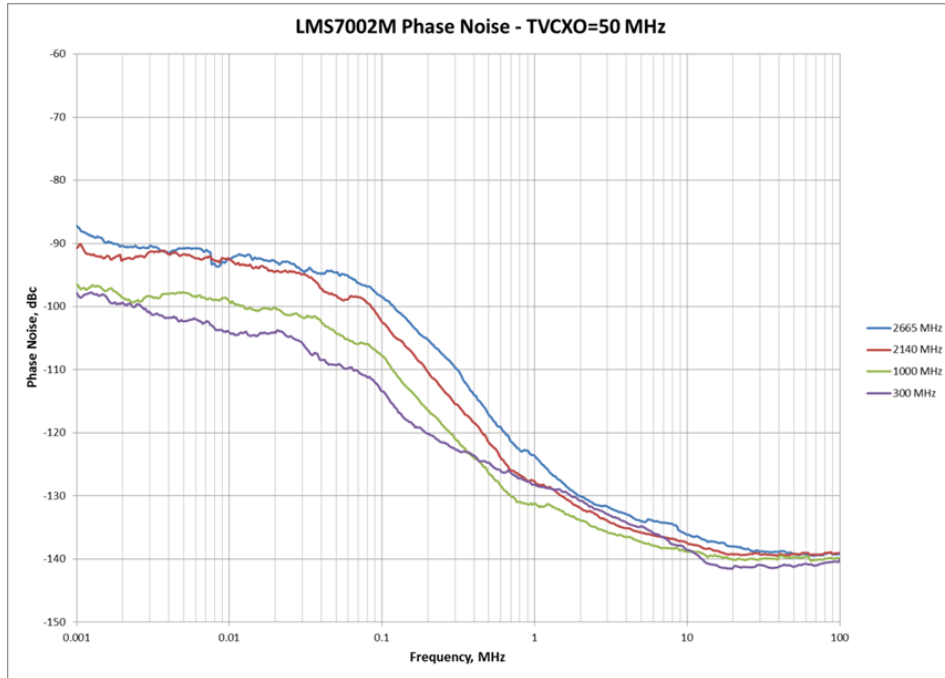


Figure 7. Plateau phase noise measurements for various LO frequencies with a 52.00MHz discrete crystal reference.

The fourth region, the far out noise, is dominated by the feedforward divider noise. Far out phase noise needs to be very low to avoid losing receiver sensitivity with large out of band blockers. It is also needed to prevent loss of sensitivity during FDD operation. The far out phase noise is very low, and cannot be measured directly with the phase noise personalities of a spectrum analyzer. A special test configuration, shown in Figure 8, is used, consisting of a duplexing filter to prevent the LO leakage overloading the spectrum analyzer and a low noise amplifier to lift the far out phase noise above the noise floor of the spectrum analyzer. The LMS7002M is configured as CW transmitter with a DC analog input. The measured far out

phase noise of the LMS7002M for Band I and Band V (W-CDMA frequencies) is shown in Table 5. The far out noise is calculated with the following formula.

$$N_{FarOut(dBc)} = N_{MeasuredRx(dBm)} + L_{FilterRX} + L_{CableX} - (P_{TXOut(dBm)} + L_{FilterTX} + L_{CableTX}) - G_{LNARX}$$

Where:

$N_{MeasuredRx(dBm)}$ is the measured transmitter noise in the RX band at the duplexer's RX output.

$L_{FilterRX}$ is the loss in the duplexer filter in the Ant-RX path.

L_{CableX} is the loss in the duplexer filter in the Ant-RX path.

$P_{TXOut(dBm)}$ is the measured transmitter power in the TX band at the TX output of the duplexer.

$L_{FilterTX}$ is the loss in the duplexer filter in the Ant-TX path.

$L_{CableTX}$ is the loss in the duplexer filter in the Ant-TX path.

G_{LNARX} is the gain of the external low noise amplifier in dB.

$N_{FarOut(dBc)}$ is the measured transmitter far out noise in dBc.

LMS7002M Setup:

| | |
|------------------|------------|
| Tx frequency | Band I, V |
| Tx LPF BW | 12 MHz |
| DAC's | OFF |
| Tx analog output | Enabled |
| IQ imbalance | Calibrated |
| DC/LO leakage | Calibrated |

Test Equipment Setup:

- Test signal 1MHz CW
- External LNA used to push the Tx noise above EXA noise floor
- SAW filter used to filter TX band

IQ Analog Signal



Stub Tuner

Duplexer:
Tx to Rx isolation
>55 dB

Triple-Stub:
Muaray
Microwave
1878B

Rx port

Tx port

50 Ω

Agilent MXA N9020A:

N9080 LTE option

Max BW 10 MHz



Ext. LNA 1:
Gain ~16dB
NF 3.8 dB



EVB7 GUI

EVB7: LMS7002M evaluation kit

Figure 8. Test configuration for measuring far out phase of the LMS7002M.

Table 5. Far Out Phase Noise for Band I and Band V

| Band | Tx Freq., MHz | Cable Loss, dB | Tx Output, dBm | Filter Insertion Loss, dB | Ext. LNA Gain, dB | Measured Noise Freq., MHz | Measured Noise, dBm/Hz | Tx Far-Out Noise, dBc/Hz |
|------|---------------|----------------|----------------|---------------------------|-------------------|---------------------------|------------------------|--------------------------|
| I | 2122 | -0.3 | 4.88 | -0.5 | 15.41 | 1932 | -141.3 | -160.79 |
| | 2140 | -0.3 | 5.1 | -0.5 | 14.7 | 1950 | -141.1 | -160.1 |
| | 2160 | -0.3 | 4.05 | -0.5 | 15.25 | 1970 | -141.01 | -159.51 |
| II | 870 | -0.08 | 9 | -1.46 | 15.1 | 820 | -135.9 | -158.46 |
| | 880 | -0.08 | 8.9 | -1.46 | 15.12 | 830 | -135.4 | -157.88 |
| | 890 | -0.08 | 8.6 | -1.46 | 15 | 840 | -136.9 | -158.96 |

2.3 PLL Spur Measurements

PLL Spurs arise from a number of sources. The main source is the charge pump, whose spurs are at an offset from the LO frequency related to the reference clock frequency and change frequency with the LO frequency. The second source of spurs is the DSM modulator when the synthesizer is operating close to integer multiples of the reference clock and are normally controlled by the charge pump offset current in the SXT/SXR tab of the GUI. The third source are spurs at harmonics of the clock frequency and generally arise from PCB layout. The fourth source of spurs arise from magnetic coupling of the TX and RX synthesizers which only occurs in full duplex mode and are usually small if the FDD frequencies are sufficiently apart. The test bench of Figure 47 was used for the measurements.

Spur levels from the charge pump are shown in Figure 9 to Figure 12. The position of these spurs depend on LO frequency and reference frequency. The amplitude of these spurs is reduced when the feedforward dividers are engaged.

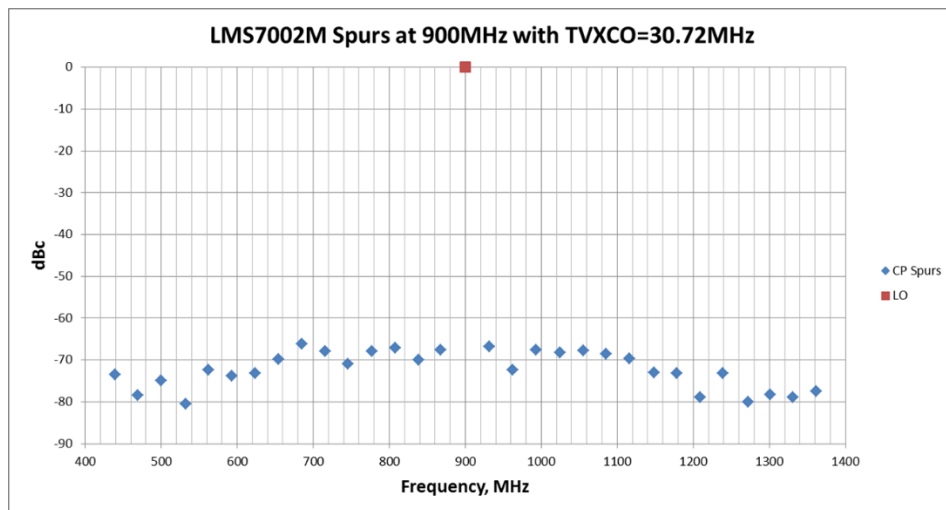


Figure 9. shows the amplitude of typical charge pump spurs 900MHz, RefFreq 30.72MHz.

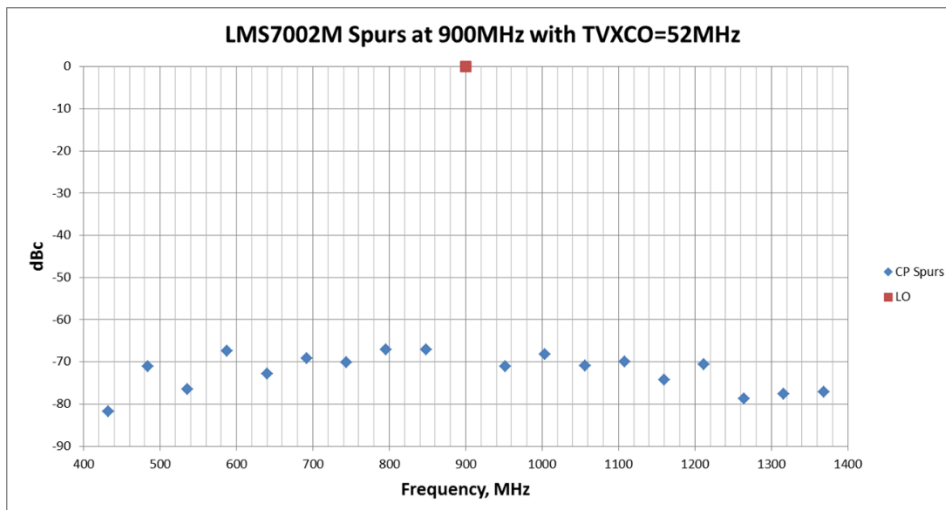


Figure 10. shows the amplitude of typical charge pump spurs 900MHz, RefFreq 52.00MHz.

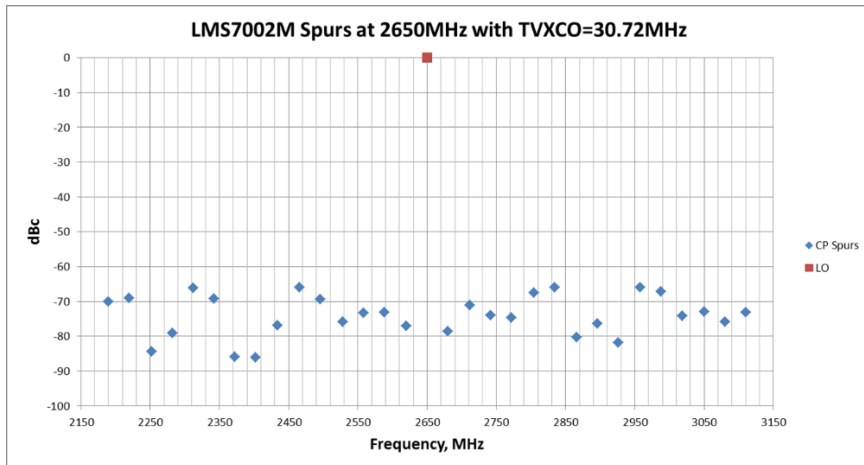


Figure 11. shows the amplitude of typical charge pump spurs 2650MHz, RefFreq 30.72MHz.

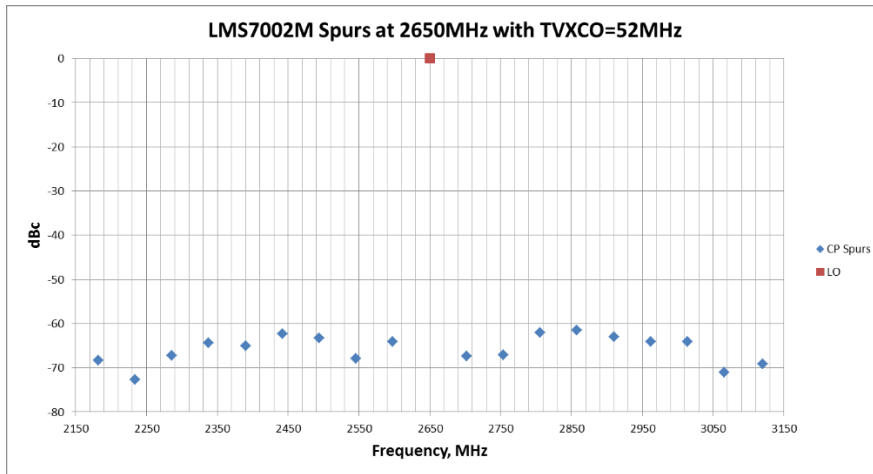


Figure 12. shows the amplitude of typical charge pump spurs 2650MHz, RefFreq 52.00MHz.

When the DSM operates close to integer, spurs fall into the pass band of the PLL loop filter, leading to high boundary spurs. Boundary spur levels are shown in Figure 13. The level of the boundary spur can be reduced by optimising the charge pump offset current in the SXR/SXT panel of the GUI.

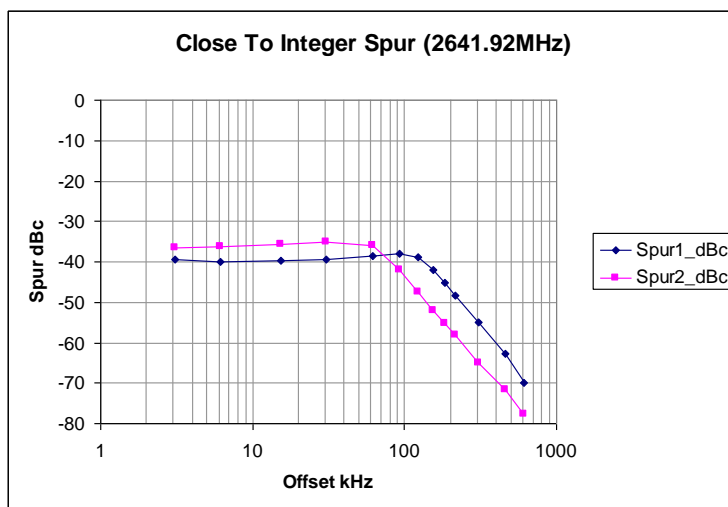


Figure 13. shows the amplitude of DSM boundary spurs

VCO coupling spurs occur when the TX and RX PLL are operating at similar frequencies, typically less than 100MHz apart. Typical VCO coupling spur levels are shown in Figure 14. It can be seen as the RX frequency is moved away from the TX frequency the amplitude of the spur falls. With typical LTE/W-CDMA duplexing frequencies the VCO coupling spur is smaller than the charge pump spurs. When the feedforward dividers are engaged the separation frequency is scaled by the division ratio e.g. if the PLL is at 850MHz (Band V), the PLL uses divide by 2, and the RX and TX LO are 50MHz apart. This corresponds to 100MHz in Figure 14.

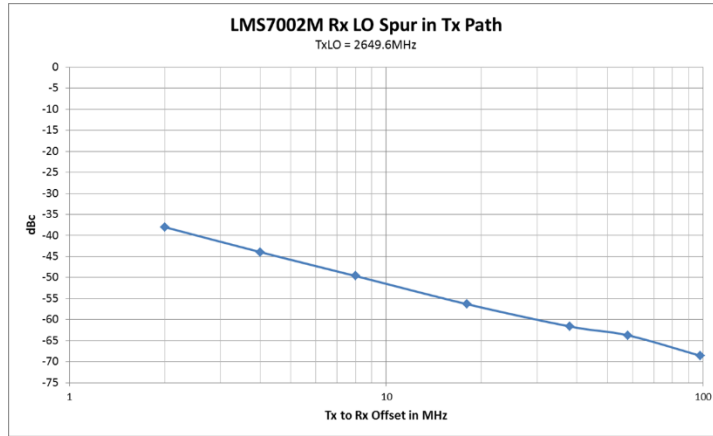


Figure 14. shows the amplitude of TX and RX VCO coupling spurs at the TX output (relative to the TX output) with varying RX frequency when TX LO=2649.6MHz

3

TX Measurements

The transmitter (TX) must modulate the information to be transmitted onto the TX synthesizer output with almost no degradation of the information quality and with no interference to users of other frequency bands, especially at nearby frequencies. The quality of the information being transmitted is usually described by the error vector magnitude (EVM). EVM includes the effect of phase noise from the synthesizer plateau region as well as signal to noise ratio, IQ mismatch, group delay mismatch and nonlinearity of the transmitter and any external power amplifier. The level of interference to users of other frequency bands is usually described by the adjacent channel power ratio (ACPR) which gives a measure of the signal to noise ratio available in the next channel. ACPR is degraded by nonlinearity and noise from the transmitter and external power amplifier and the far out phase noise from the synthesiser. Additionally the transmitter must maintain performance over a range of output powers, depending on its application (e.g. amplitude matching of multiple users in up-links, and maximum output power control in down-links).

A simplified block diagram of one of the transmitter (TX) channels is shown in Figure 15. The analog part of the TX consists of a programmable current amplifier (IAMP) to optimally match the input with the analog IF stage. A programmable analog IF filter (LPF), an RF mixer, a pair of programmable RF amplifier (PAD) to vary the RF output level. The TX digital signal processing block (TSP) includes inverse sync correction, digital filtering, dc offset adjustment for LO leakage cancellation, interpolation for improved signal to noise ratio, amplitude and phase correction for image rejection and digital upconversion. The performance of the TSP will be described in another test document.

The following sections describe the measured performance of the transmitter blocks. Section 3.1 describes the frequency response of the transmitter lowpass filters. Section 3.2 describes the power control of the TX. Sections 3.3 and 3.4 describes optimisation of the TX linearity for optimum OIP3 and ACPR with W-CDMA respectively. Section 3.5 describes how to use the internal numerically controlled oscillator (NCO) to optimise linearity. Section 3.6 and 3.7 measure output harmonics and noise respectively. Section 3.8 describes the EVM performance of the TX with LTE modulation. Section 3.9 describes output power vs frequency on the evaluation board. Section 3.10 describes the TX noise leakage into the RX.

Section 3.11 describes the peak detector performance. Section 3.12 describes the port isolation on the evaluation board.

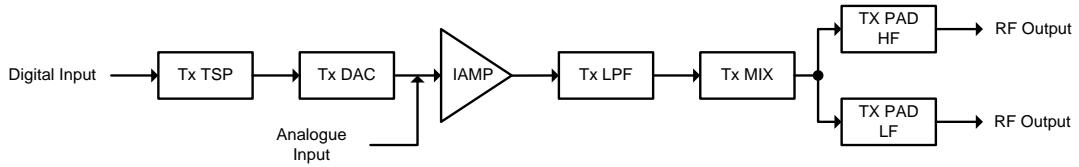


Figure 15. Block diagram of the Transmitter.

3.1 TX LPF Measurements

All DACs produces multiple aliases of the wanted output at frequencies above the Nyquist frequency. Additionally DACs produce broadband quantisation noise. The transmitter low pass filter (LPF) provides a convenient way of reducing these unwanted outputs to prevent interference to users of other bands. Further reduction of quantisation noise is possible by increasing the sample rate and using the interpolation filters in the TSP which will be described in another document.

The LMS7002M has a LPF in the TX which has two operating modes. It has a low frequency mode which covers 1MHz to 20MHz with a 4th order chebychev response, and a high frequency mode which covers 20MHz to 100MHz with a 2nd order chebychev response. The low frequency mode has an additional de-emphasis filter to further reduce transmit noise in the receive band by using a noise shaping scheme in basedband. The low frequency mode is primarily intended to be used with systems without predistortion. The high frequency mode is intended to be used with predistortion based transmitters where outputs beyond the intended channel bandwidth are transmitted to provide linearization of an external power amplifier.

The low frequency mode of the low pass filter was tested with the test bench shown in Figure 16, where the TX analog inputs are driven by a signal generator (MXG). A common mode voltage is applied to the chip from the MXG. The frequency responses of the filter for a range of bandwidths is shown in Figure 17. When the input response is correctly shaped for the de-emphasis filter, the correct frequency response can be seen as in Figure 18.

The high frequency mode of the low pass filter was tested by using the test bench shown in Figure 19 where the TX analog inputs are driven by the internal TX TSP numerically controlled oscillator (NCO) and DAC. The frequency response of the filter for a range of bandwidths is shown in Figure 20.

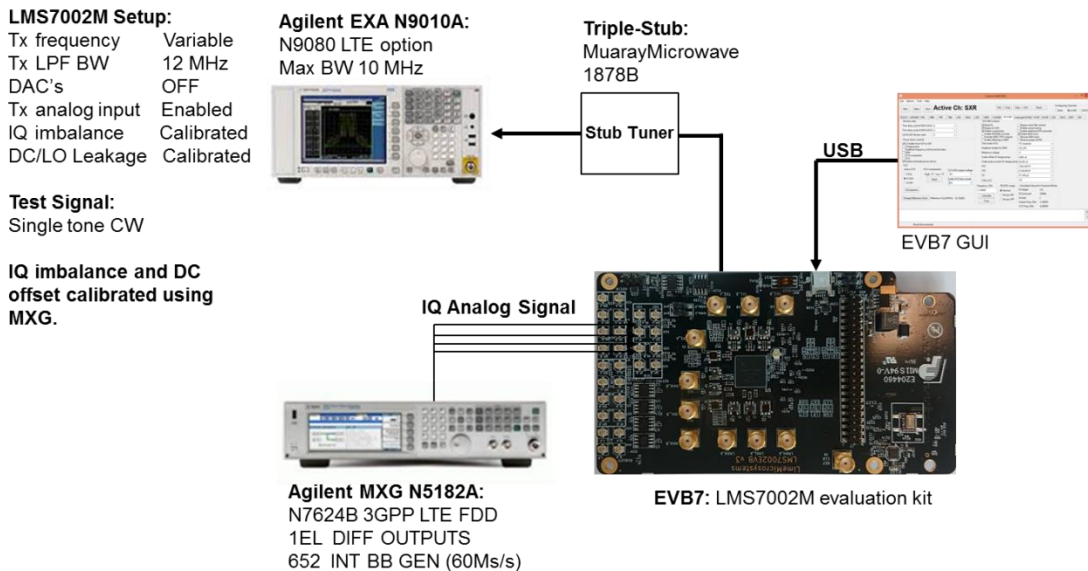


Figure 16. Test bench used to test TX LPF Low Band

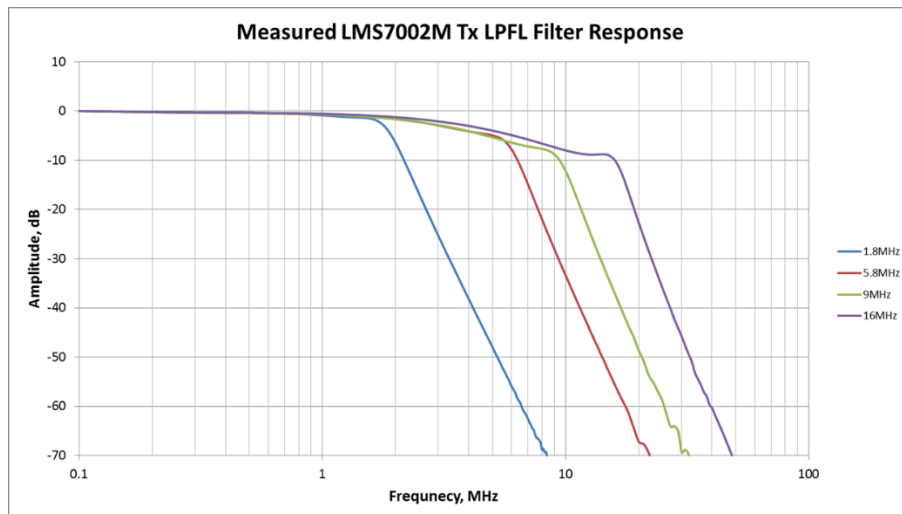


Figure 17. Filter responses of the TX LPF Low Band including de-emphasis pole.

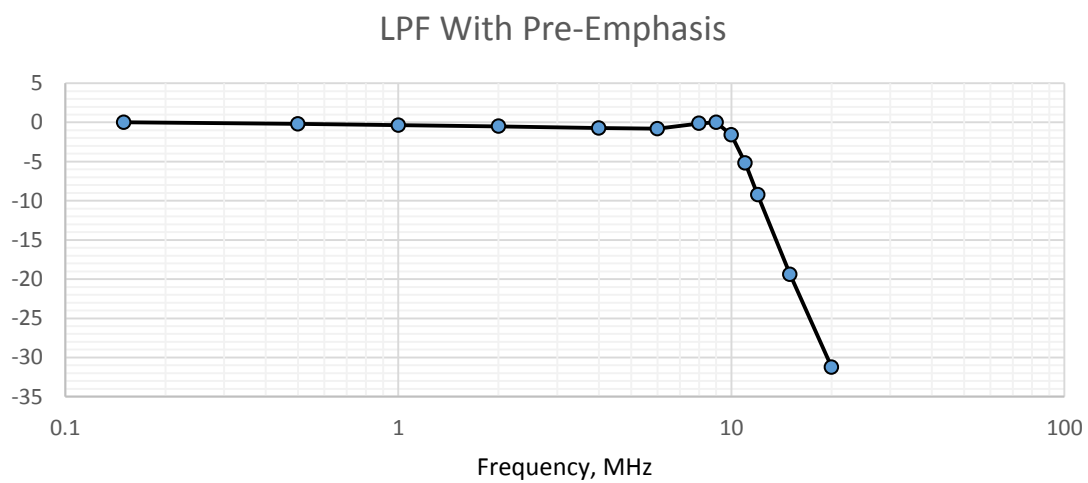
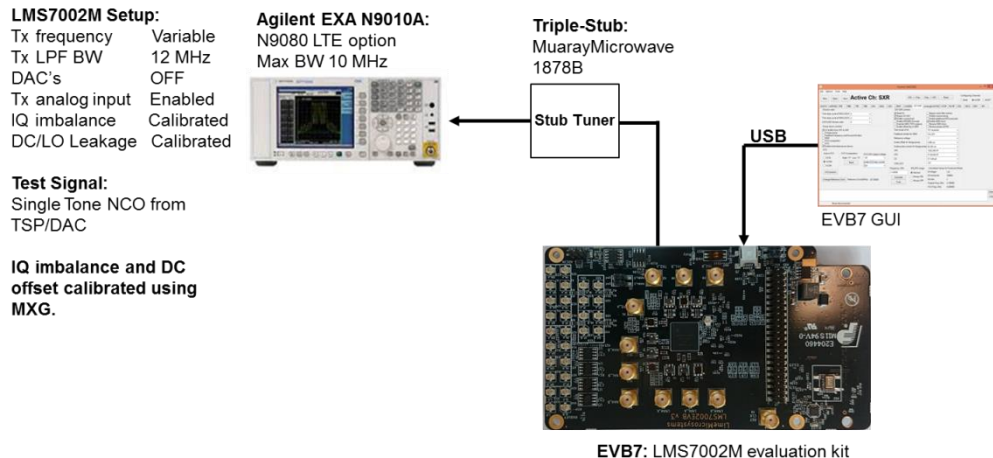


Figure 18. 10MHz Filter responses of the TX LPF Low Band with de-emphasis de-embedded



EVB7: LMS7002M evaluation kit

Figure 19. Test bench used to test TX LPF High Band

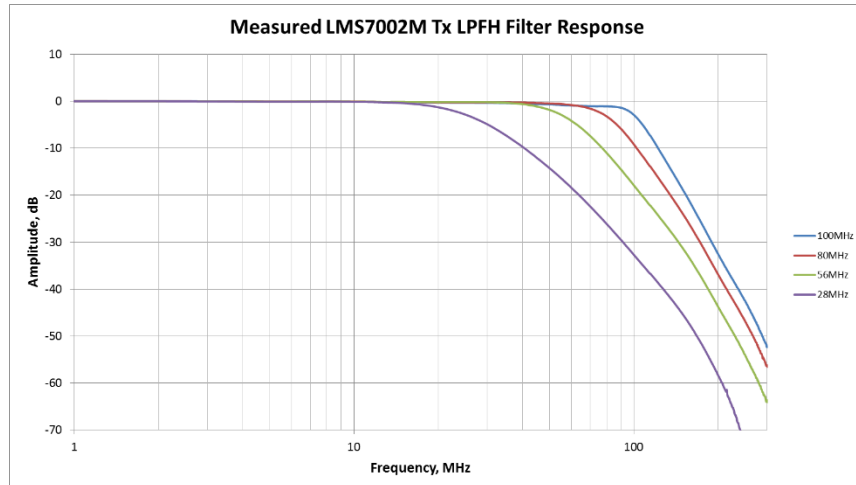


Figure 20. Filter responses of the TX LPF High Band

3.2 TX RF Gain Measurements

The transmitter TX PAD includes gain control function. This can be found in the TXRF tab of the GUI. This consists of two parts, the main gain control, and the lineariser gain control. These are intended to be adjusted together. This is demonstrated using the test bench shown in Figure 21. The variation of output power and gain step accuracy is shown in Figure 22. The first 10 steps are 1dB steps, subsequent steps are 2dB steps.

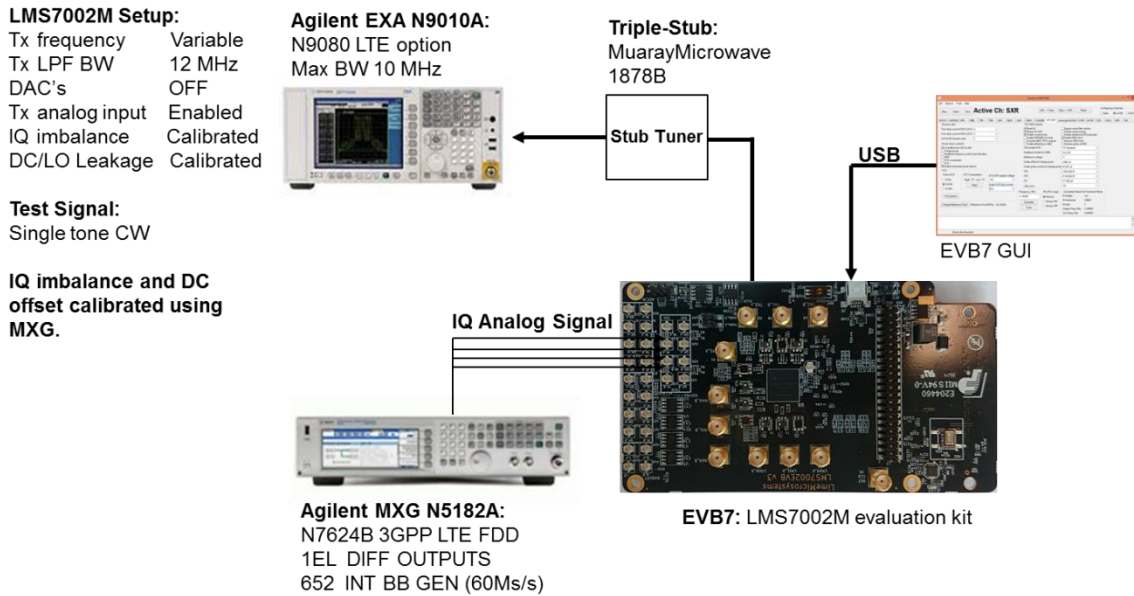


Figure 21. Test bench used to measure TX RF Gain Control

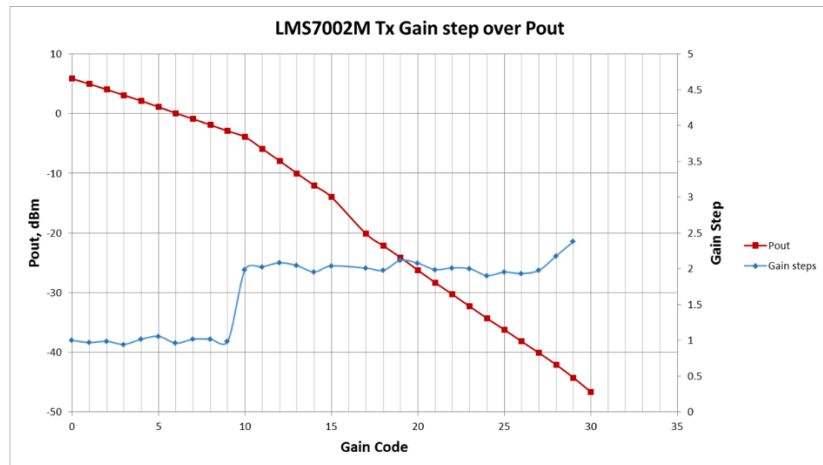


Figure 22. Variation of output power and gain step accuracy with TX RF Gain Control.

3.3 TX OIP3 Measurements

The TX RF output stage has a linearizer which can be used to optimize OIP3 over a range of output amplitudes. Using the test set of Figure 23 with a two tone output from the MXG differential IQ generator. A common mode voltage (0.3V) is applied to the chip from the MXG. For optimum OIP3 both the TXBB and TXRF have to be carefully aligned to avoid overloading critical blocks.

First the TXLPF resistors and TXIAMP are set to the required bandwidth (TXBB tab of the GUI).

Next, the MXG output level and current amplifier IAMP gain (TXBB tab of GUI) are carefully adjusted to give the lowest IM3 when TXPAD and linearizer gain are both 10dB backed off from max gain. (This removes the output nonlinearity of the TXPAD, allowing the TXBB to be optimized for lowest distortion.)

Next, the TXPAD gain is increased to max gain. The RF output power is tuned with the stub tuner first to achieve maximum output power, and then returned to allow the output power to fall by 2-3 dB from maximum output power and the tuner carefully adjusted for the position with lowest distortion at this output power. The distortion is further minimized using the TXRF tab in the GUI control software using the TXPAD bias currents and gain settings.

The variation of OIP3 at 900MHz is shown in Figure 24 for different gain and bias of the transmitter.

Table 6. Gain and Bias Settings used to adjust OIP3 maximum.

| Pout at OIP3 Peak | 0.6 | 0.7 | 0 |
|-------------------|-----|-----|----|
| IAMP_GAIN | 31 | 31 | 31 |
| IAMP_ICT2 | 3 | 3 | 3 |
| TXPAD_GAIN | 0 | 3 | 3 |
| TXPAD_LINGAIN | 3 | 6 | 6 |
| TXPAD_ICT | 14 | 15 | 19 |
| TXPAD_LIN_ICT | 31 | 28 | 31 |

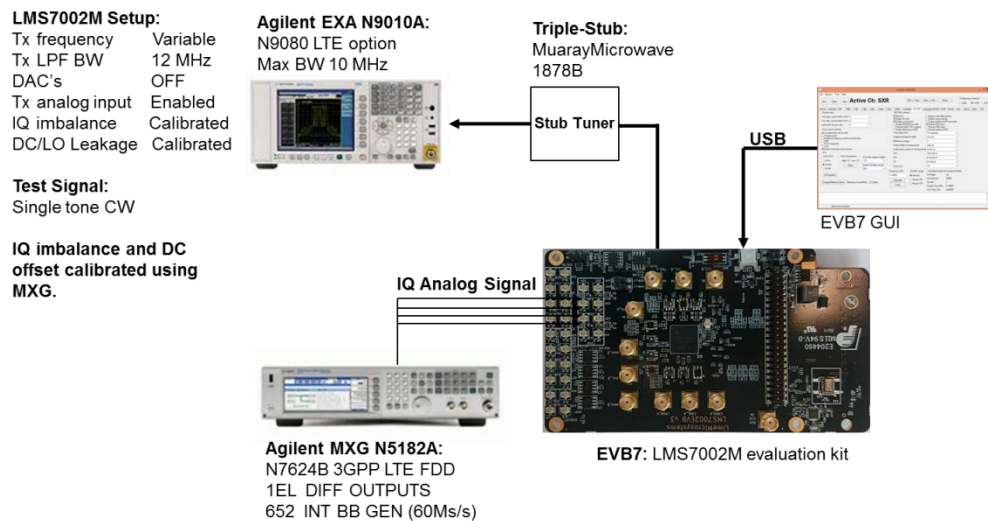


Figure 23. Test bench for measuring two tone OIP3.

Variation of OIP3 with Output Power

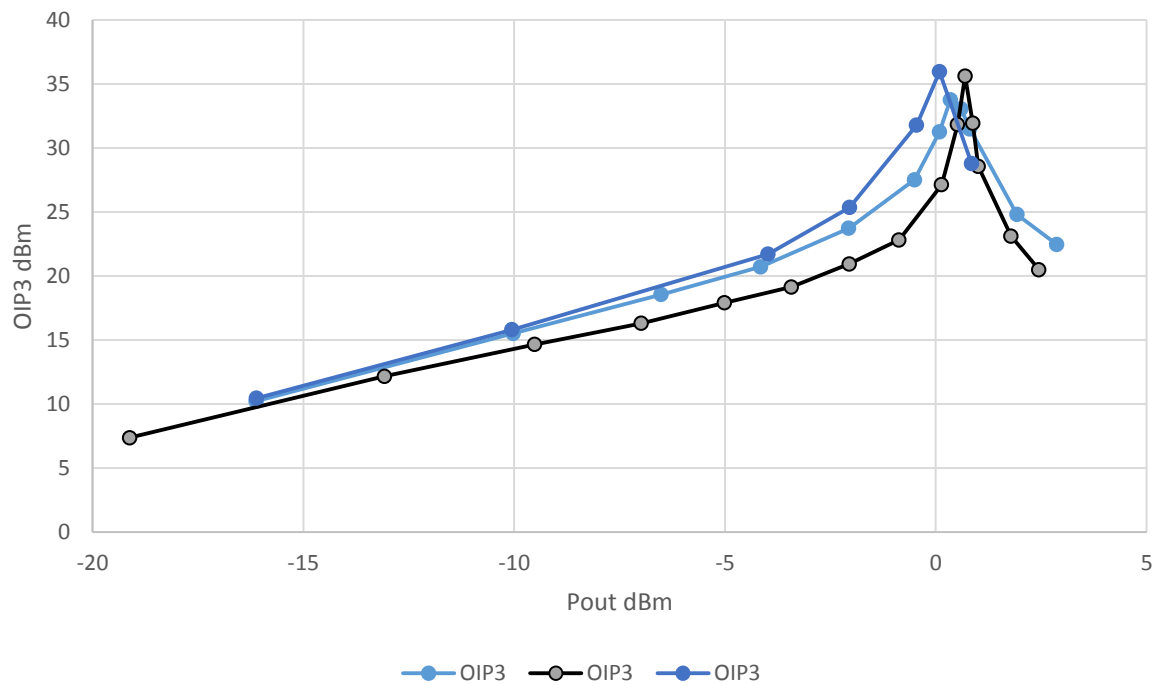


Figure 24. Variation of OIP3 with output power at 900MHz as input level is varied for 3 different bias/gain settings in GUI

3.4 Optimum TX ACPR Measurements

The TX RF output stage has a linearizer which can be used to optimize ACPR over a range of output amplitudes using the test set of Figure 25. A W-CDMA signal loaded into the MXG differential IQ generator. A common mode voltage (0.3V) is applied to the chip from the MXG. For optimum ACPR both the TXBB and TXRF have to be carefully aligned to avoid overloading critical blocks.

First the TXLPF resistors and TXIAMP are set to the required bandwidth (TXBB tab of the GUI).

Next, the MXG output level and current amplifier IAMP gain (TXBB tab of GUI) are carefully adjusted to give the best ACPR when TXPAD and linearizer gain are both 10dB backed off from max gain. (this removes the output nonlinearity of the TXPAD, allowing the TXBB to be optimized for lowest distortion).

Next, the TXPAD gain is increased to max gain. The RF output power is tuned with the stub tuner first to achieve maximum output power, and then returned to allow the output power to fall by 2-3 dB and the tuner carefully adjusted for the position with lowest ACPR at this output power (alternatively the tuner settings from the OIP3 can also be used). The ACPR is further minimized using the TXRF tab in the GUI control software using the TXPAD bias currents and gain settings. For most gain steps, the lineariser gain is simply a fixed offset from the TXPAD gain, the bias currents are held in a constant ratio. For highest output powers some further adjustment may be needed. The values used here are given in Table 7.

The measured variation of ACPR with RF output power at 900MHz is shown in Figure 26. Best ACPR is achieved at -5dBm output power.

Further improvements in ACPR measurements could be achieved by using a LNA in front of the spectrum analyser for low power outputs to reduce the effect of spectrum analyser noise floor. Same ACPR measurements were done with DAC enabled which results correspond to the shown below.

Table 7. Gain and bias settings used for optimum ACPR with output power.

| TPAD_Lin | 0 | 0 | 0 | 0 | 3 | 4 | 7 | 8 | 10 | 9 | 11 | 12 | 13 |
|-------------------------|------|------|------|------|------|------|------|------|------|------|------|------|------|
| TPAD_Main | 0 | 1 | 2 | 3 | 4 | 5 | 6 | 7 | 8 | 9 | 10 | 11 | 12 |
| TPAD_casc | 3 | 3 | 3 | 3 | 3 | 3 | 3 | 3 | 3 | 3 | 3 | 3 | 3 |
| ICT_LIN | 28 | 28 | 28 | 28 | 28 | 28 | 28 | 28 | 28 | 28 | 28 | 28 | 28 |
| ICT_PA | 12 | 12 | 12 | 12 | 12 | 12 | 12 | 12 | 12 | 12 | 12 | 12 | 12 |
| NMOS | 18 | 18 | 18 | 18 | 18 | 18 | 18 | 18 | 18 | 18 | 18 | 18 | 18 |
| PMOS | 24 | 24 | 24 | 24 | 24 | 24 | 24 | 24 | 24 | 24 | 24 | 24 | 24 |
| MXG_VCM | 0.31 | 0.31 | 0.31 | 0.31 | 0.31 | 0.31 | 0.31 | 0.31 | 0.31 | 0.31 | 0.31 | 0.31 | 0.31 |
| MXG_Scale | 6.5 | 6.5 | 6.5 | 6.5 | 6.5 | 6.5 | 6.5 | 6.5 | 6.5 | 6.5 | 6.5 | 6.5 | 6.5 |
| TBB_IAMP_Gain | 32 | 32 | 32 | 32 | 32 | 32 | 32 | 32 | 32 | 32 | 32 | 32 | 32 |
| TBB_IAMP_RefBias | 3 | 3 | 3 | 3 | 3 | 3 | 3 | 3 | 3 | 3 | 3 | 3 | 3 |
| TBB_IAMP_CalBias | 12 | 12 | 12 | 12 | 12 | 12 | 12 | 12 | 12 | 12 | 12 | 12 | 12 |
| TBB_LPF_C | 12 | 12 | 12 | 12 | 12 | 12 | 12 | 12 | 12 | 12 | 12 | 12 | 12 |
| TBB_LPF_RLAD | 171 | 171 | 171 | 171 | 171 | 171 | 171 | 171 | 171 | 171 | 171 | 171 | 171 |
| TBB_LPF_RRP | 135 | 135 | 135 | 135 | 135 | 135 | 135 | 135 | 135 | 135 | 135 | 135 | 135 |

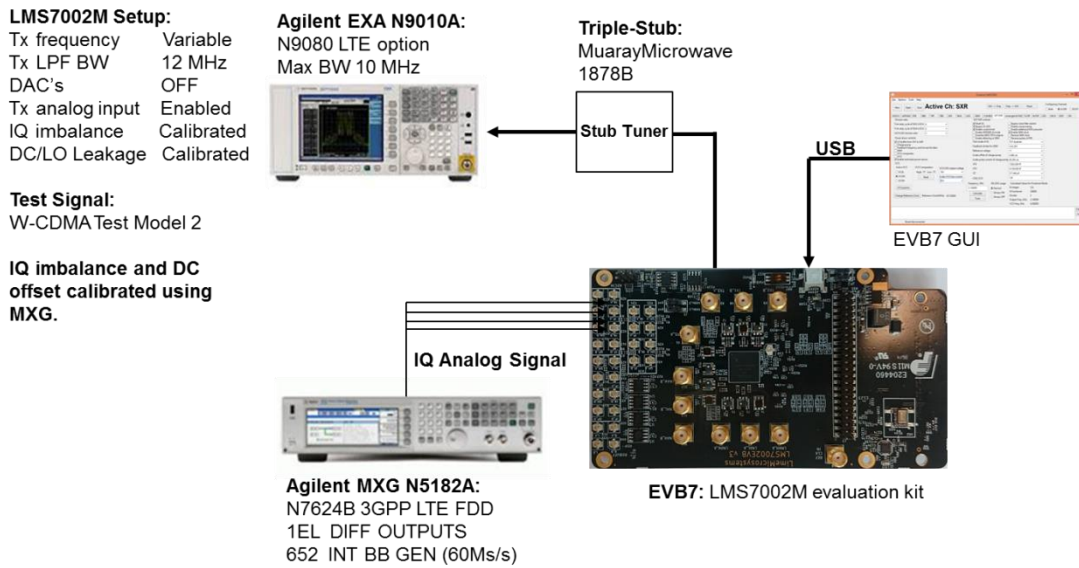


Figure 25. Test bench used for ACPR measurements with output power.

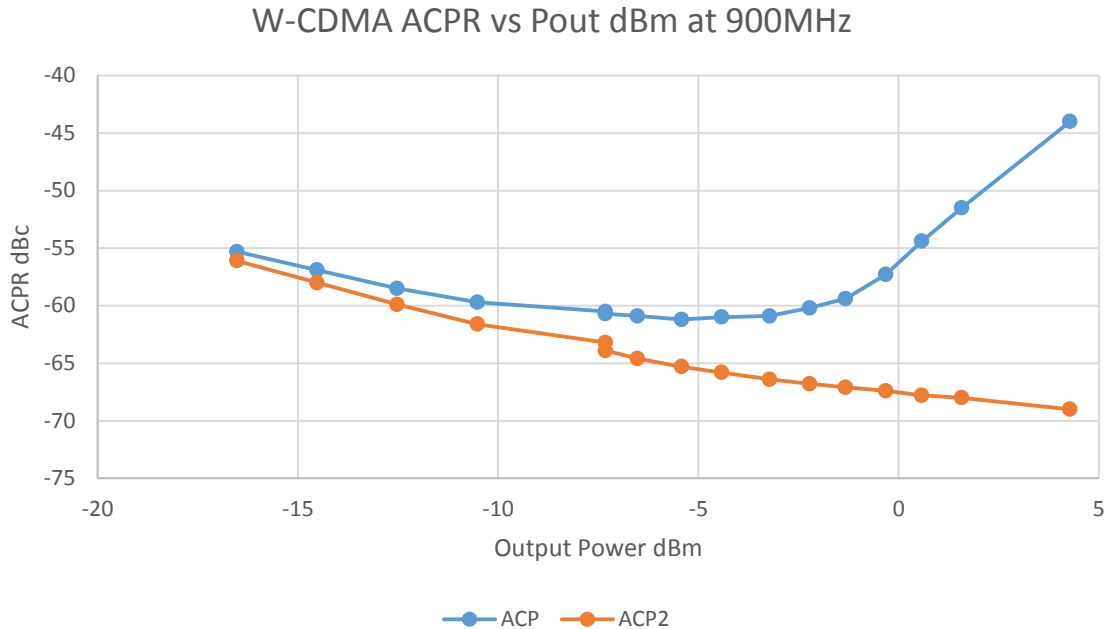


Figure 26. Measured ACPR vs output power with optimum gain controls.

3.5 Using the TSP NCO for Quick Linearity test

For the best performance from the TX, it is necessary to ensure the TX baseband is not overloading. The most effective way to set up the TX gains is with a 2 tone signal.

The LMS7002 contains a digital signal processing block (TSP) with a numerically controlled oscillator (NCO). Normally this digital test signal generates a SSB signal for calibration of LO leakage and image rejection. But by setting either the I or Q gain in the TSP to 0, it is possible to use this to generate DSB signal in the mixer, giving a two tone signal at the TX RF amplifier. This digital test signal can be used to generate test signals to correctly set up the gain in the TX IF chain.

Depending on the matching and gain set ups, the LMS7002M linearity can either be limited by the TX baseband blocks (TXBB) or the the TX RF blocks. By setting the TX RF gain to be approx. 12dB below max gain (or if the TX RF matching is unmatched), the TX RF nonlinearity can be made very small. This allows the TXBB to be correctly set up. The DAC has a programmable current output, normally 625uA is selected. By setting the TSP I Q registers to 7FFF, a full scale waveform can be generated from the DAC. The TX LPF is a transimpedance stage, converting the DAC output current into a voltage. If the output voltage is too large, clipping will occur leading to distortion. If this output voltage is too low, the signal to noise ratio (SNR) will be degraded. The TX current amplifier (IAMP) provides a means of scaling the DAC output for optimum dynamic range.

Once the TX LPF frequency response has been set, the IAMP gain can be adjusted for the inband IM3 to be approximately 60dBc. If the TXRF gain is then changed, the IM3 in dBc should remain unaltered. Once the TXBB is set up, the TX RF gain can be increased to measure OIP3. The optional stub tuner could then also be used to match TX RF output for best compromise of output power and OIP3.

The test bench used for the quick linearity test is shown in Figure 27. In Table 8 we show typical settings and measured results from setting up the TX IF. The first set of measurements show how IAMP gain changes IM3. The second set of measurements shows how changing RF gain does not change IM3 in dBc. The final measurements show how IAMP gain has to be changed if the TX LPF frequency or band is changed.

Note that the optimum settings shown here are meant for signals with low peak to average ratio (PAR), such as two tone test signals. OFDM modulation signals, which have a high PAR, are tolerant to a small amount of clipping of the peaks. One approach is to provide peak clipping in digital signal processing external to the LMS7002M. Some advance DSP tools can also give PAR optimized OFDM waveforms. Another approach is to operate the LMS7002M with a higher IAMP gain than used for the measurements here, and peak clipping will occur in the analog environment. Error Vector Magnitude (EVM) gives a sensitive measure of waveform quality and will indicate if digital or analog clipping is too severe compared to the unclipped waveform.

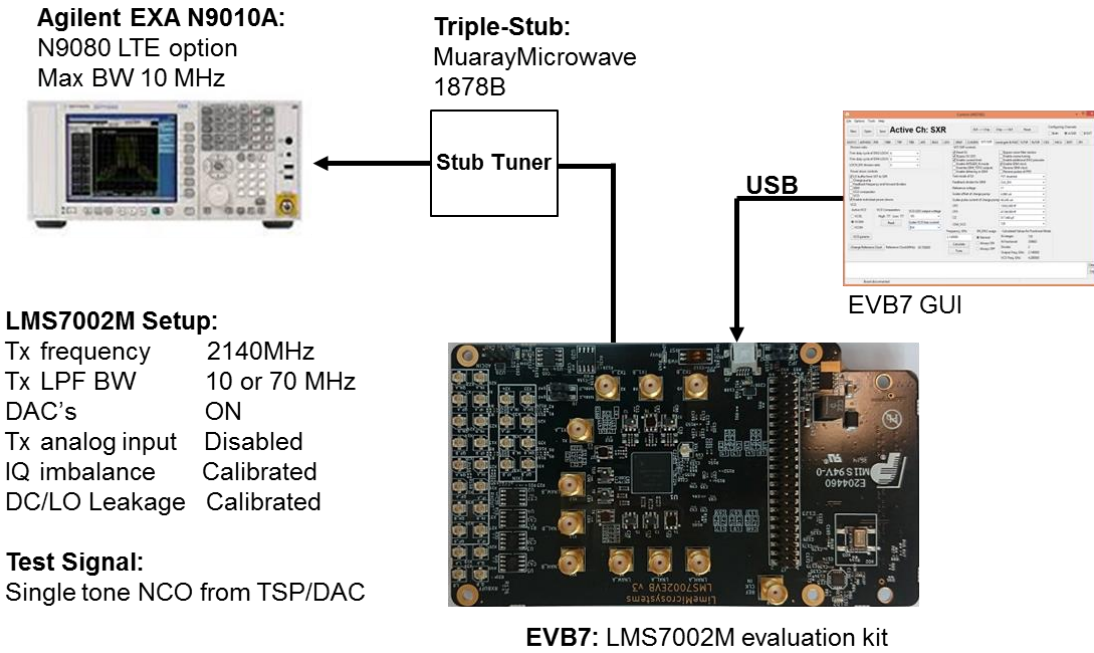


Figure 27 Test bench for 'quick linearity' test.

Table 8 Settings and measured IM3 for ‘quick linearity’ test.

| | | | | | | | | | |
|-----|------------------|-------|-------|-------|-------|-------|-------|-------|-------|
| TSP | FCW | 1 | 1 | 1 | 1 | 1 | 1 | 1 | 1 |
| TSP | Gain Q | 2047 | 2047 | 2047 | 2047 | 2047 | 2047 | 2047 | 2047 |
| TSP | Gain I | 0 | 0 | 0 | 0 | 0 | 0 | 0 | 0 |
| TSP | DC I | -99 | -99 | -99 | -99 | -99 | -99 | -87 | -84 |
| TSP | DC Q | -106 | -106 | -106 | -106 | -106 | -106 | -101 | -84 |
| TSP | DC_REG I, Q | 7FFF |
| TBB | IAMP Gain | 7 | 11 | 15 | 11 | 11 | 11 | 8 | 25 |
| TBB | IAMP Ref | 3 | 3 | 3 | 3 | 3 | 3 | 3 | 3 |
| TBB | IAMP Cascode | 12 | 12 | 12 | 12 | 12 | 12 | 12 | 12 |
| TBB | PD_LPFH_biquad | y | y | y | y | y | y | y | |
| TBB | PD_LPFIAMP | | | | | | | | |
| TBB | PD_LPFLAD | | | | | | | | y |
| TBB | PD_LPFS5 | | | | | | | | y |
| TBB | LPFH | 97 | 97 | 97 | 97 | 97 | 97 | 97 | 97 |
| TBB | LPFLAD | 171 | 171 | 171 | 171 | 171 | 171 | 85 | 171 |
| TBB | LPFS5 | 135 | 135 | 135 | 135 | 135 | 135 | 67 | 135 |
| TBB | Cap | 12 | 12 | 12 | 12 | 12 | 12 | 12 | 12 |
| TRF | TXPAD lin | 0 | 0 | 0 | 0 | 2 | 4 | 0 | 0 |
| TRF | TXPAD gain | 2 | 2 | 2 | 2 | 4 | 6 | 2 | 2 |
| TRF | TXPAD Cascode | 3 | 3 | 3 | 3 | 3 | 3 | 3 | 3 |
| TRF | Bias gm section | 48.3 | 48.3 | 48.3 | 48.3 | 48.3 | 48.3 | 48.3 | 48.3 |
| TRF | Bias lin section | 12 | 12 | 12 | 12 | 12 | 12 | 12 | 12 |
| SXT | LO | 2140 | 2140 | 2140 | 2140 | 2140 | 2140 | 2140 | 2140 |
| | | | | | | | | | |
| | IM3 2143MHz | -78.1 | -69.2 | -64.0 | -69.2 | -70.9 | -73.6 | -69.2 | -70.0 |
| | USB 2141MHz | -16.6 | -12.9 | -11.3 | -12.9 | -14.6 | -16.6 | -12.3 | -10.0 |
| | LSB 2139MHz | -16.4 | -12.7 | -11.1 | -12.7 | -14.4 | -16.4 | -12.0 | -9.9 |
| | IM3 2137MHz | -78.1 | -68.5 | -62.7 | -68.5 | -70.0 | -72.8 | -68.2 | -68.7 |
| | | | | | | | | | |
| | IM3 dBc | -61.5 | -56.3 | -52.7 | -56.3 | -56.3 | -57.0 | -56.9 | -60.0 |
| | IM3 dBc | -61.7 | -55.8 | -51.6 | -55.8 | -55.6 | -56.4 | -56.2 | -58.8 |

3.6 TX Output Harmonics

The transmitter produces harmonics of the wanted output. The even harmonic levels are low due to the use of differential outputs, which reduces filtering requirements.

The transmitter harmonic responses are measured with the test set shown in Figure 28. The NCO is used to produce a 1-tone test signal. The stub tuner is used to ensure the output power is the maximum value possible at the wanted frequency. The largest spur at each harmonic frequency is measured. Measured harmonic outputs at maximum TX RF gain are

shown in Table 9. It can be seen the 2nd harmonic output is very low, typically 60dBc. Whereas the 3rd harmonic output can be relatively large when the LO is at low frequency.

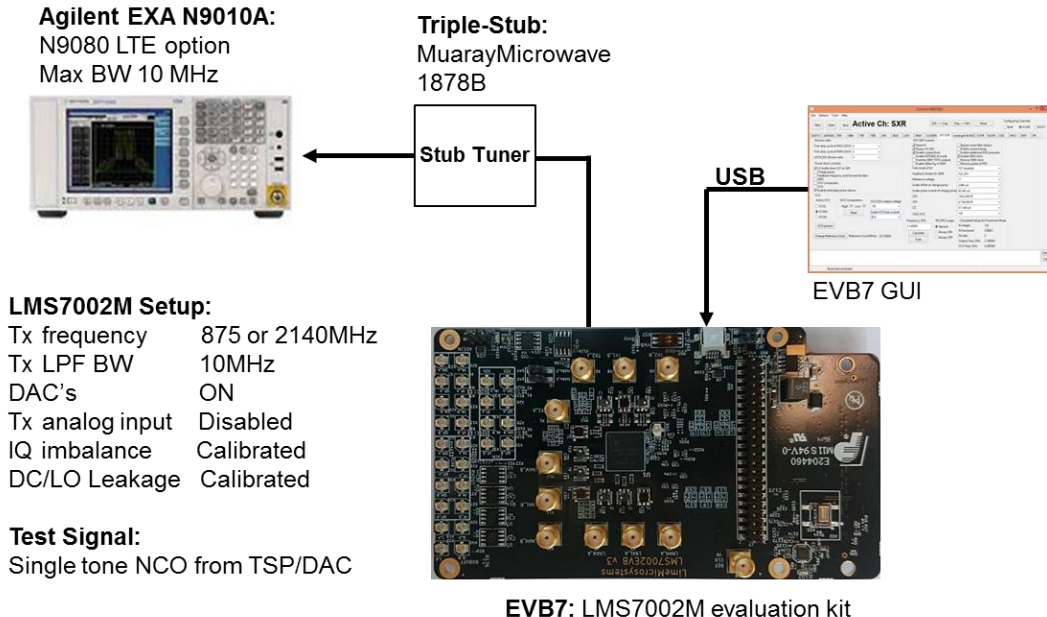


Figure 28 Testbench for measuring TX output harmonics

Table 9 Harmonic levels with large CW output

| Output Frequency | Fundamental | 2nd Harmonic | 3rd Harmonic |
|------------------|-------------|--------------|--------------|
| MHz | dBm | dBm | dBm |
| 876 | 10.1 | -60.0 | -15.4 |
| 2141 | -2.0 | -63.0 | -58.0 |

3.7 TX Noise Measurements

The transmitter produces several kinds of noise. When the output signal is large, PLL phase noise can contribute. But when the digital input is made zero, the thermal noise of the transmitter dominates residual noise. The thermal noise predominately comes from the TX low pass filters and depends on both TX RF gain and filter bandwidth.

Transmitter noise is measured with the test set shown in Figure 29. The NCO is used to produce 2-tone and 1-tone test signals. The stub tuner is used to ensure the output power is close to the maximum value possible level. The baseband is aligned so that the intermodulation distortion is around -60dBc.

First the RF power is measured at full RF gain and minimum RF gain. Then the noise to one side of the LO leakage spur is measured for both full RF gain and minimum RF gain with the digital gain set to 0. The measurement results are shown in Table 10. It can be seen at minimum RF gain the noise measurement is limited by the spectrum analyser. It can also be seen the absolute noise density depends on transmit frequency and choice of low pass filter.

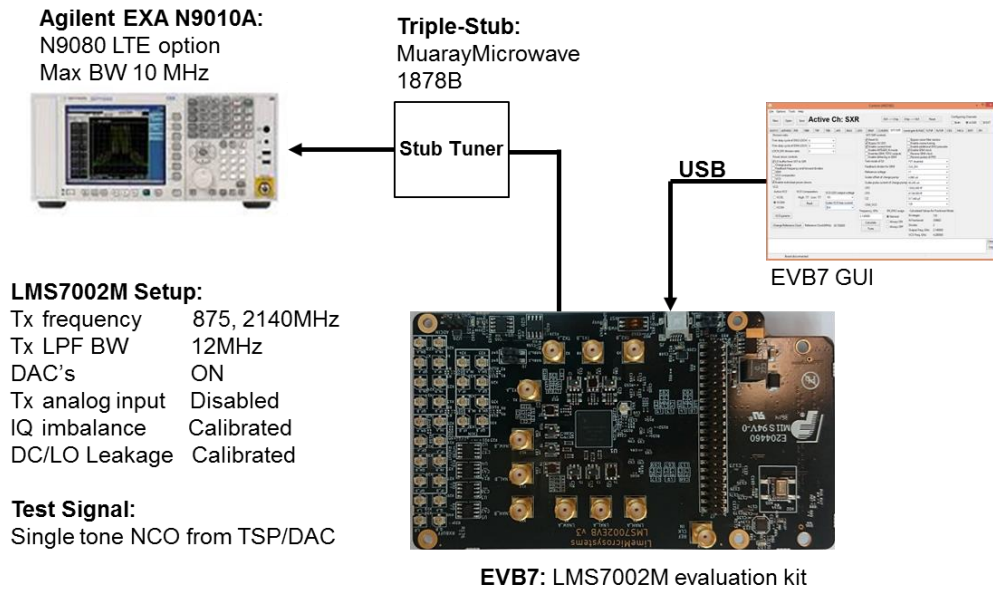


Figure 29 Test bench for transmitter noise measurement.

Table 10 Measured transmitter noise

| SXT | I, Q gain | IAMP Gain | LPF | TPAD Gain | TPAD Gain LIN | Output | Measurement | Measurement | Measurement | Measurement |
|------|--------------|--------------|-----|--------------|------------------|--------|-------------|-------------|-------------|-------------|
| MHz | Code | Code | MHz | Code | Code | | MHz | MHz | dBm | dBm/Hz |
| 2140 | 2047 | 11 | 10 | 0 | 0 | CW | 2141 | | -4.5 | |
| 2140 | 2047 | 11 | 10 | 31 | 31 | CW | 2141 | | -53 | |
| 2140 | 0 | 11 | 10 | 0 | 0 | No CW | 2137.2 | 5 | -69.5 | -136.4 |
| 2140 | 0 | 11 | 10 | 0 | 0 | No CW | 2132.2 | 5 | -74.6 | -141.5 |
| 2140 | 0 | 11 | 10 | 31 | 31 | No CW | 2137.2 | 5 | -81.7 | -148.5 |
| 2140 | 0 | 11 | 10 | 31 | 31 | No CW | 2132.2 | 5 | -80.7 | -147.6 |
| | | | | | | | | | | |
| 875 | 2047 | 11 | 10 | 0 | 0 | CW | 876 | | 4.5 | |
| 875 | 2047 | 11 | 10 | 31 | 31 | CW | 876 | | -46.2 | |
| 875 | 0 | 11 | 10 | 0 | 0 | No CW | 872.2 | 5 | -61.6 | -128.6 |
| 875 | 0 | 11 | 10 | 0 | 0 | No CW | 867.2 | 5 | -66.2 | -133.2 |
| 875 | 0 | 11 | 10 | 31 | 31 | No CW | 872.2 | 5 | -82.1 | -149.1 |
| 875 | 0 | 11 | 10 | 31 | 31 | No CW | 867.2 | 5 | -81.9 | -149 |
| | | | | | | | | | | |
| 875 | 2047 | 31 | 75 | 3 | 0 | CW | 876 | | 7.8 | |
| 875 | 2047 | 31 | 75 | 31 | 31 | CW | 876 | | -40 | |
| 875 | 0 | 31 | 75 | 3 | 0 | No CW | 853 | 40 | -58.1 | -134.1 |
| 875 | 0 | 31 | 75 | 3 | 0 | No CW | 811 | 40 | -59.6 | -135.6 |
| 875 | 0 | 31 | 75 | 31 | 31 | No CW | 853 | 40 | -73.3 | -149.3 |
| 875 | 0 | 31 | 75 | 31 | 31 | No CW | 811 | 40 | -73.6 | -149.6 |

3.8 TX EVM Measurements

EVM provides a measure of the quality of the signal being transmitted. It includes effects such as image rejection, LO leakage, plateau phase noise, group delay mismatch and nonlinearity. Typically EVM performance of <3% is required.

The test bench used for the LTE EVM measurements is shown in Figure 30.

First a 10MHz LTE signal was loaded into the MXG. A common mode voltage (0.3V) is applied to the chip from the MXG. The spectrum analyzer is set up for LTE demodulation.

Next the TXLPF resistors and TXIAMP are set to the required bandwidth (TXBB tab of the GUI).

Then the transmitter was calibrated to minimize LO leakage and image rejection using a single tone signal (for example from the ‘on chip’ NCO). LO leakage is minimized by applying DC offset to the MXG signal generator through the analog inputs. Image rejection is controlled using the duty cycle controls in SXT and TXRF tabs of the GUI (if digital signals are applied the TSP tab of the GUI provides DC offset and IQ corrector controls to reduce LO leakage and image rejection respectively).

The TXBB controls were optimized for lowest ACPR and EVM when the TXRF gain controls are set for 10dB back off from maximum gain.

In this case the output power was not optimized with a tuner, neither was the TXRF gain and bias optimized as done previously in Sections 3.3 and 3.4.

EVM was measured at 860MHz, 2100MHz and 2640MHz using a 30.72MHz TXCO.

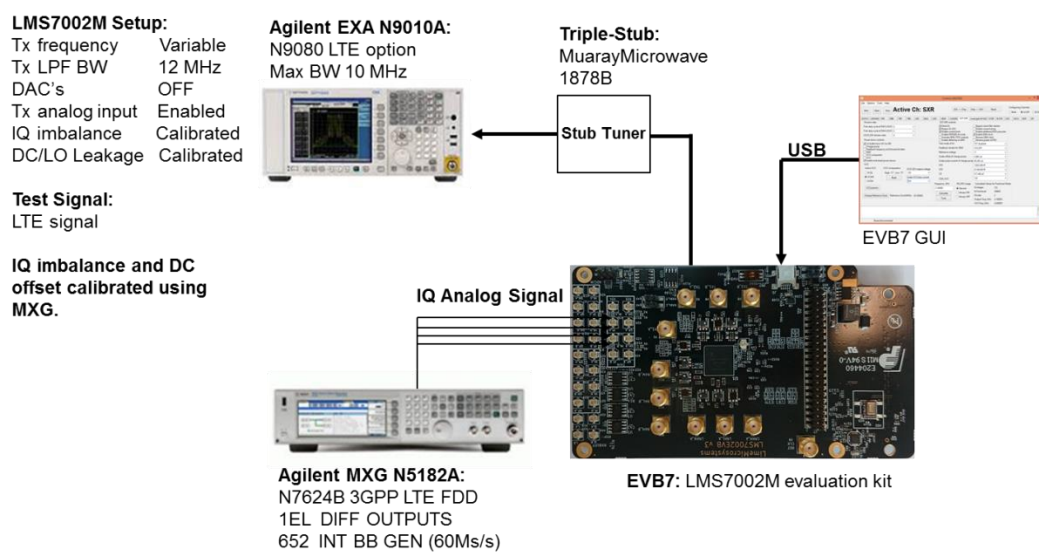
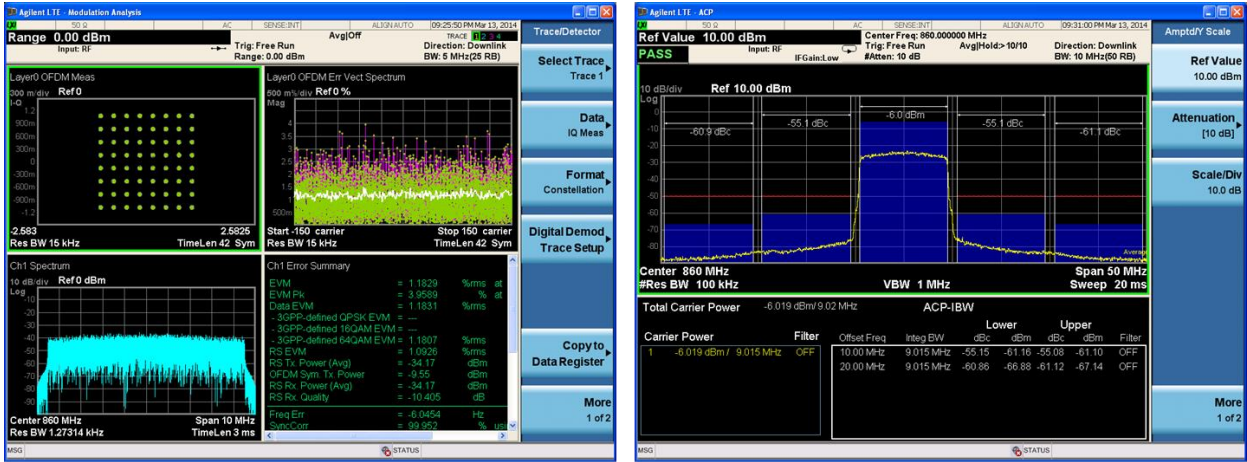
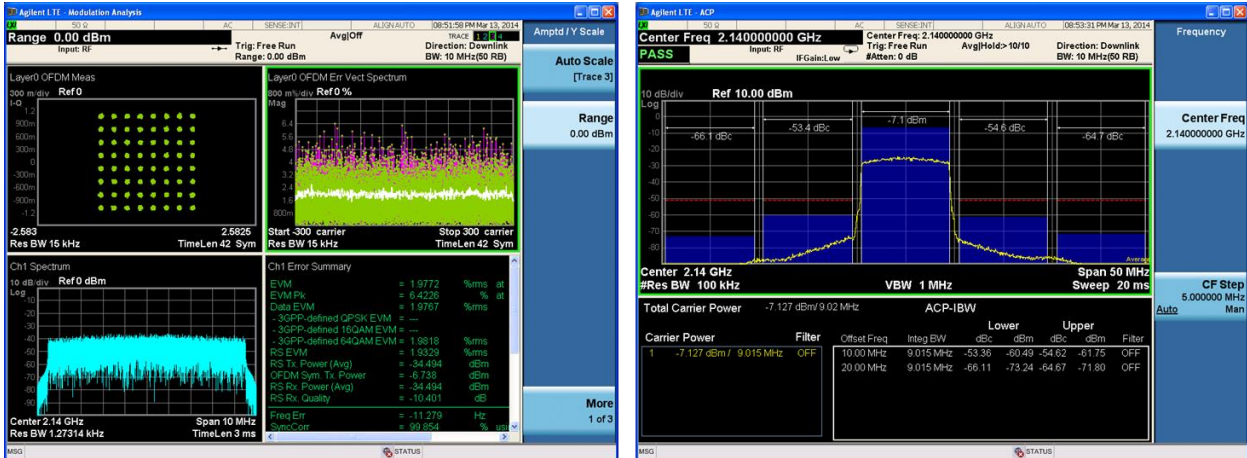


Figure 30. Test Bench used for TX EVM measurements with output power



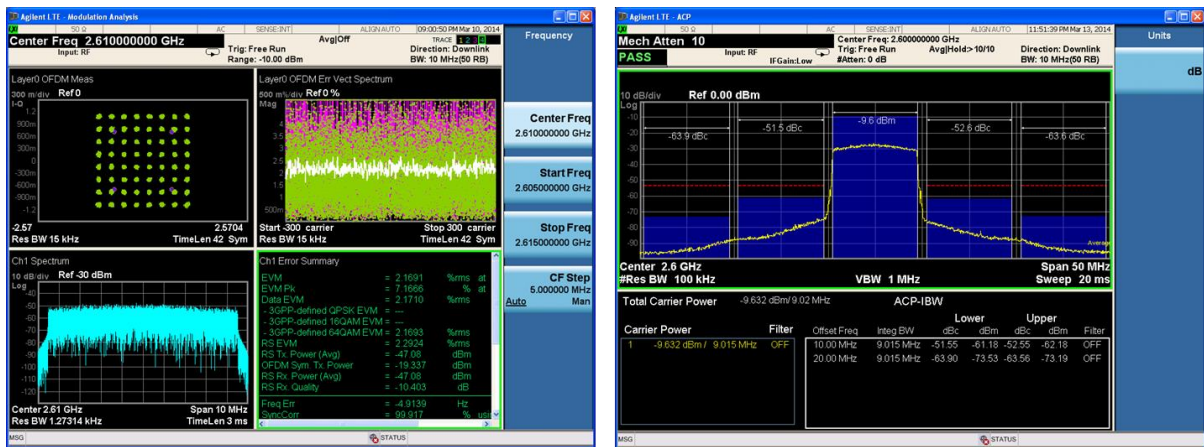
| Tx LO, MHz | Pout, dBm | Cable loss, dB | ACPR 10 MHz Offset, dBc | ACPR 20 MHz Offset, dBc | EVM, % |
|------------|-----------|----------------|-------------------------|-------------------------|--------|
| 860 | -4.9 | 1.1 | -55.1 | -61.1 | 1.8 |

Figure 31. LTE EVM Measurement at 860MHz



| Tx LO, MHz | Pout, dBm | Cable loss, dB | ACPR 10 MHz Offset, dBc | ACPR 20 MHz Offset, dBc | EVM, % |
|------------|-----------|----------------|-------------------------|-------------------------|--------|
| 2140 | -7.1 | 2.3 | -53.4 | -64.7 | 1.97 |

Figure 32. LTE EVM Measurement at 2140MHz



| Tx LO, MHz | Pout, dBm | Cable loss, dB | ACPR 10 MHz Offset, dBc | ACPR 20MHz Offset, dBc | EVM, % |
|------------|-----------|----------------|-------------------------|------------------------|--------|
| 2610 | -9.6 | 2.8 | -51.5 | -63.9 | 2.17 |

Figure 33. LTE EVM Measurement at 2610MHz

3.9 TX Output Power vs Frequency

The LMS7002M evaluation board can be used as a broadband software defined radio with default matching components, without any tuning of the transmitter output for a particular frequency. A test bench shown in Figure 34 was used to make the measurements. The MXG was programmed with a single carrier CW signal (should be in the TXLPF pass band range). The measurements presented in Figure 35 shows a typical power with frequency for broadband operation for both the lowband and highband transmitter outputs. The MXG common mode voltage is set to 0.3V. The TXLPF resistors and TXIAMP are set to a specific bandwidth (TXBB tab of the GUI).

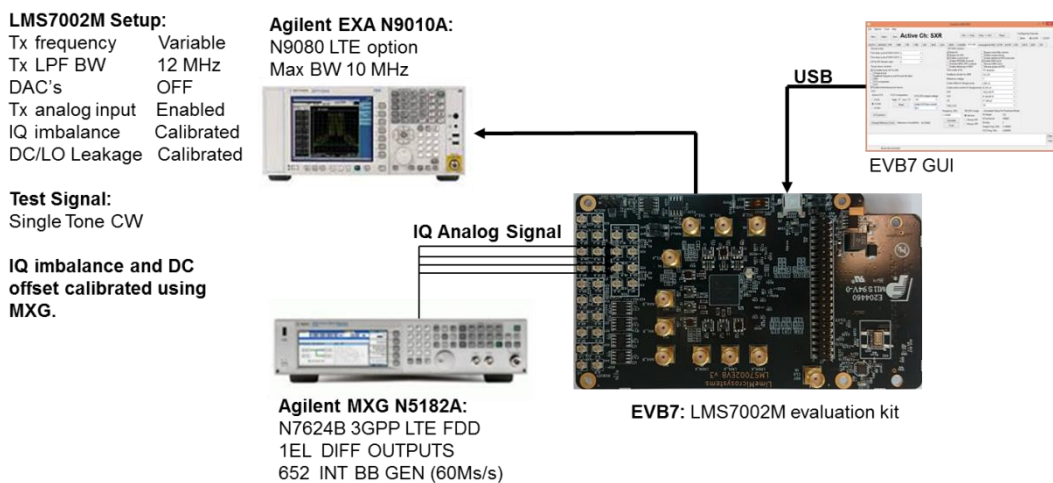


Figure 34. Test bench for broadband software defined radio output power measurements.

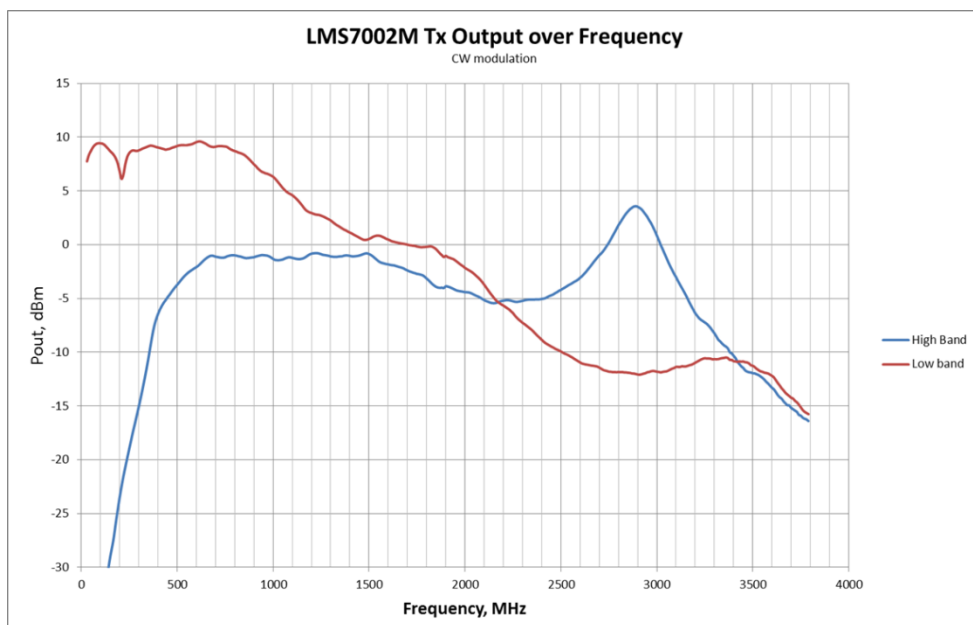


Figure 35. TX power output vs frequency for an unmatched evaluation board in broadband operation with W-CDMA signal with -50dBc ACPR.

3.10 TX Noise Leakage into RX Band

Transmit noise from the TX can leak into the RX band leading to a reduction of sensitivity in receiver under FDD operation. For typical small cell applications it is limited by the far out phase noise of the TX PLL and the isolation of the duplexer. We measure here the far out noise contribution of the transmitter by using a duplexer to separate the receive noise from the TX signal using the test set shown in Figure 36. A duplexer is used to isolate the RX band noise from the TX output. The RX band noise is amplified with an LNA to give better sensitivity in the spectrum analyser. Results for Band V and Band I are presented in Table 11 and Table 12 respectively.

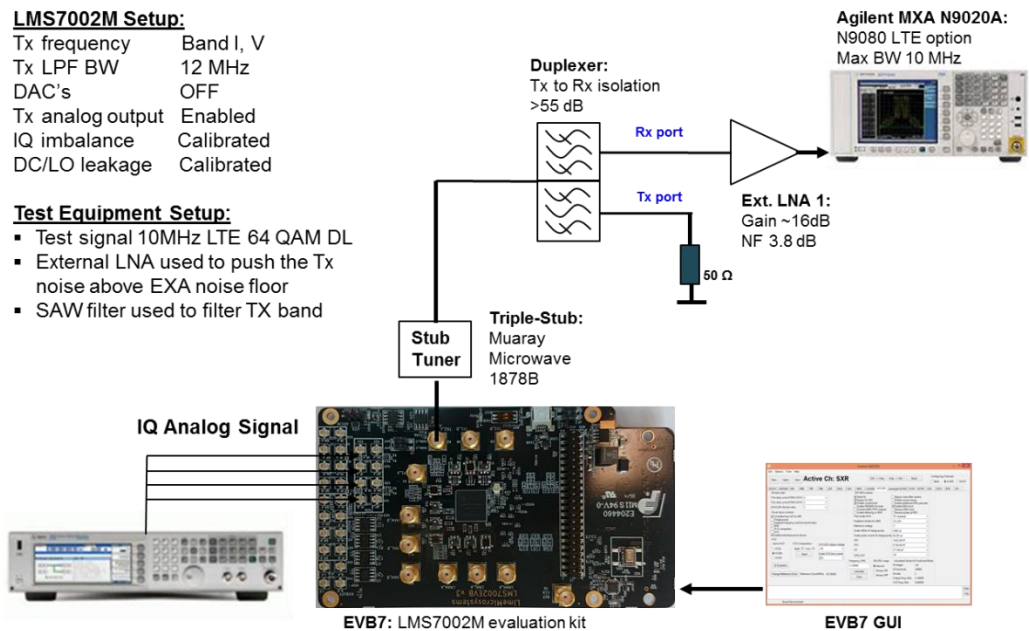


Figure 36. Test bench for measuring TX Noise in the RX band.

Table 11. TX noise leakage into RX band for Band V LTE

| Setup | Transmitter Frequency 880MHz | | Receiver Band Frequency 830MHz | | | |
|--------|------------------------------|--------------------|-------------------------------------|----------------------------------|---|---------------------------|
| | TxPAD Gain, dB | TxOUT, dBm/8.89MHz | Measured Noise@Rx Band, dBm/8.89MHz | External System Gain@Rx Band, dB | De-embedded Tx Noise@Rx Band, dBm/8.89MHz | Tx Noise @RX Band, dBm/Hz |
| ANT-Rx | 5 | -12 | -62.6 | 24.2 | -86.8 | -156.28 |
| ANT-Rx | 7 | -14 | -64 | 24.2 | -88.2 | -157.68 |
| ANT-Rx | 10 | -17.11 | -65.9 | 24.2 | -90.1 | -159.58 |
| Tx-Rx | 5 | -12 | -80 | 18.8 | < -98.8 | < -168.28 |
| Tx-Rx | 7 | -14 | -80 | 18.8 | < -98.9 | < -168.28 |

Table 12. TX noise leakage into RX band for Band I LTE

| | Transmitter Frequency 880MHz | | Receiver Band Frequency 830MHz | | | |
|---------------|---------------------------------|-----------------------|---|--|---|---------------------------------|
| Setup | TxPAD Gain, dB | TxOUT, dBm/8.89MHz | Measured Noise@Rx Band, dBm/8.89MHz | External System Gain@Rx Band, dB | De-embedded Tx Noise@Rx Band, dBm/8.89MHz | Tx Noise @RX Band, dBm/Hz |
| ANT-Rx | 0 | -12.9 | -69.7 | 21 | -90.7 | -160.18 |
| ANT-Rx | 2 | -14.9 | -70.8 | 21 | -91.8 | -161.29 |
| ANT-Rx | 5 | -17.9 | -72.2 | 21 | -93.2 | -162.69 |
| Tx-Rx | 0 | -12.9 | -80.7 | 15.4 | < -96.1 | < -165.58 |
| Tx-Rx | 2 | -14.9 | -80.7 | 15.4 | < -96.2 | < -165.59 |

3.11 TX Peak Detector Measurements

The LMS7002M includes an ‘on chip’ peak detector at the output of each transmitter output. This is to provide a measure of the RF output power level from the LMS7002M. The test bench shown in Figure 37 was used to measure the peak detector. The peak detector was measured by varying the gain and load controls. The results can be seen in Figure 38 and Figure 39 respectively. A typical GUI setup for the measurement mode is shown in Table 13.

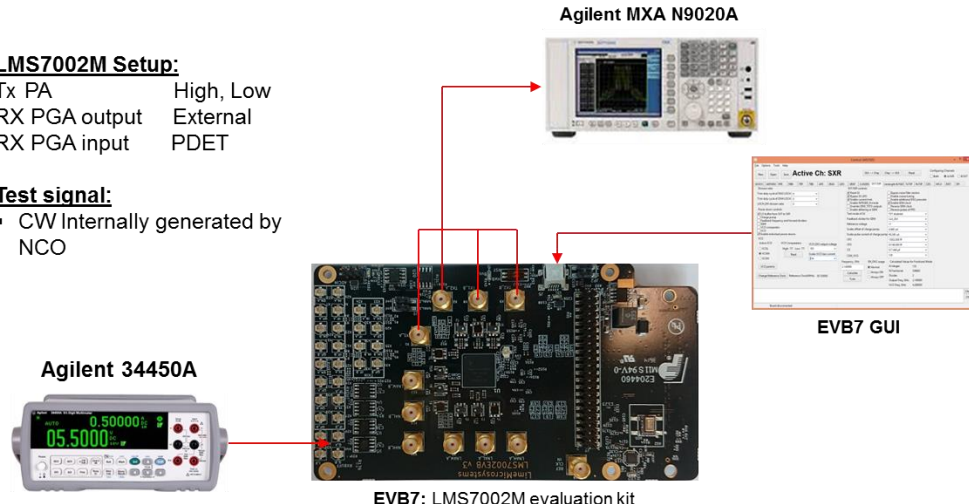


Figure 37. Test bench used to measure peak detector performance.

Table 13. Peak detector measurement GUI setup

| Channel A | Channel B |
|---|-----------|
| RBB | |
| PGA input connected to = Loopback path from peak detector | |
| PGA output connected to = output pads | |
| LPFL block = <input checked="" type="checkbox"/> | |
| PGA gain = 0 dB | |
| TBB | |
| Reference bias current of IAMPA cascade transistor gate voltage = 5 | |
| TRF | |
| TXFE output selection = Band2 | |
| Enable TX MIMO mode = Enabled | |
| Power detector = <input type="checkbox"/> | |
| AFE | |
| ADC ch. 2 = <input type="checkbox"/> | |
| DAC ch. 2 = <input type="checkbox"/> | |
| CLKGEN | |
| Execute VCO tune procedure | |
| SXR | |
| SXT | |
| VCO = <input type="checkbox"/> | |
| Set frequency = 0.5 | |
| Execute VCO tune procedure | |
| TxTSP | |
| GFIR3 = <input checked="" type="checkbox"/> | |
| GFIR2 = <input checked="" type="checkbox"/> | |
| GFIR1 = <input checked="" type="checkbox"/> | |
| FCW active tab = 1 | |
| Upload NCO = click | |
| Calibration | |
| TX DC offset = calibrated | |
| TX IQ imbalance = calibrated | |

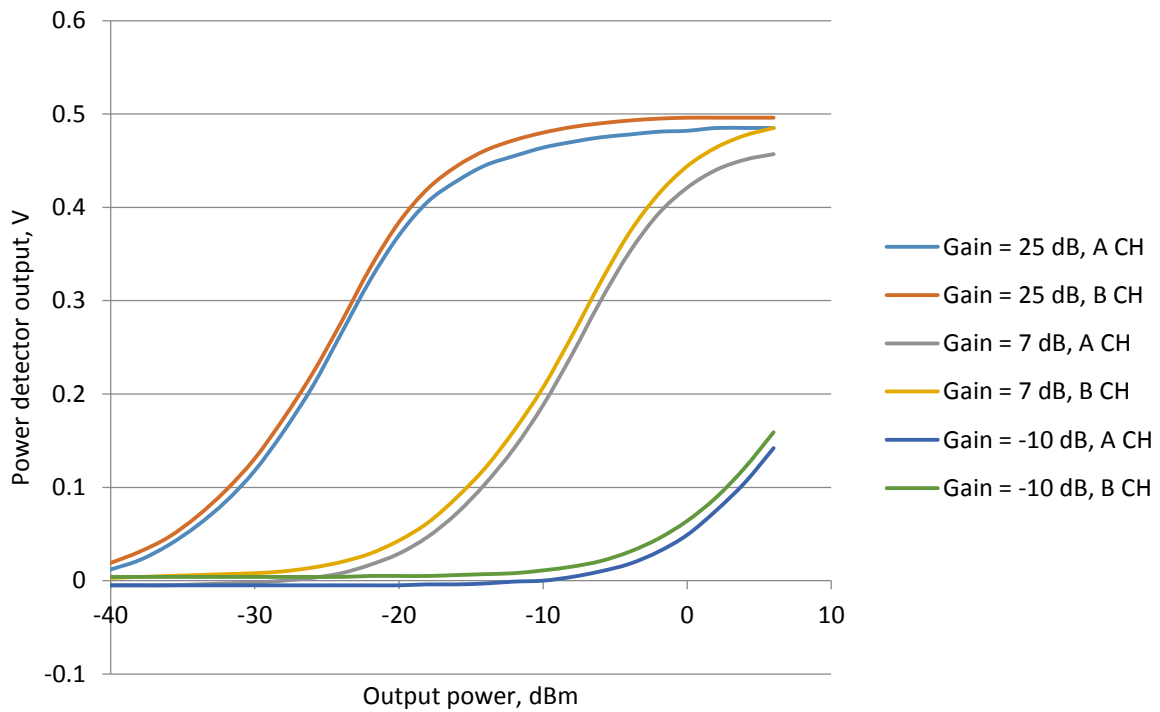


Figure 38. Typical output of peak detector with TX output power while varying the peak detector preamplifier gain.

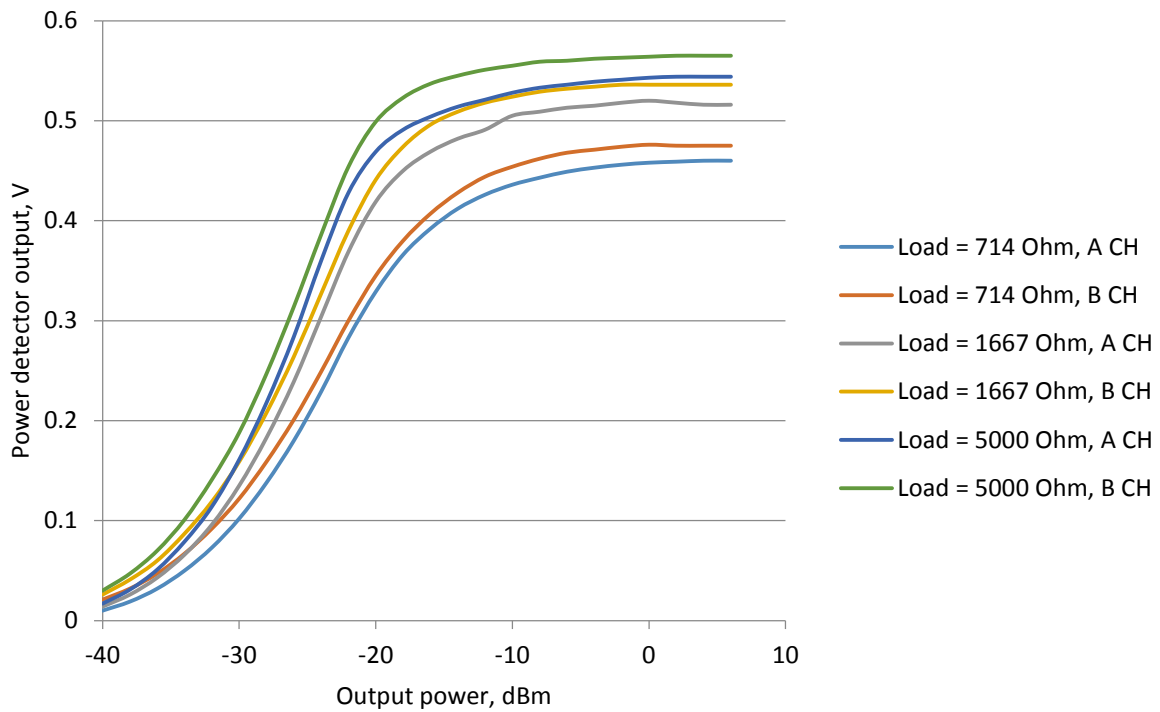


Figure 39. Typical output of peak detector with TX output power while varying the peak detector load.

3.12 TX-TX TX-RX Isolation at RF Port

A key performance parameter of a MIMO transceiver is the level of coupling between MIMO channels. Coupling between adjacent TX channels can arise through 3 main coupling mechanisms. Electromagnetic (EM) coupling either on the PCB or in the package, or capacitive coupling on the chip. Use of differential TX RF lines minimizes coupling to adjacent ports. Use of a thin substrate microstrip environment on the PCB minimizes EM coupling on the PCB. The use of a standard conductive silicon substrate, good layout practice and good grounding reduces the effect of capacitive coupling effects with other parts of the chips

Using the test set of Figure 40 the LMS7002M evaluation board is programmed into MIMO operation with 2140MHz LO applied to the high frequency TX outputs, and 1950MHz LO applied to the high frequency RX mixers. The NCOs are used to generate a large test signal at 1MHz from the TX LO. The spectrum analyzer is connected to the port being measured, all other active ports are terminated with 50R. The measurements results are given in Table 14. It can be seen that for adjacent RF ports (i.e. LF and HF ports) coupling is about 25dB at 2140MHz. However coupling to adjacent MIMO RF ports (i.e. TXA HF to TXB HF or TXA LF to TXB LF) is 40dB at 2140MHz. Figures presented are illustrative, and can change if TX frequency, matching networks, PCB microstrip substrate thickness or track routing are altered.

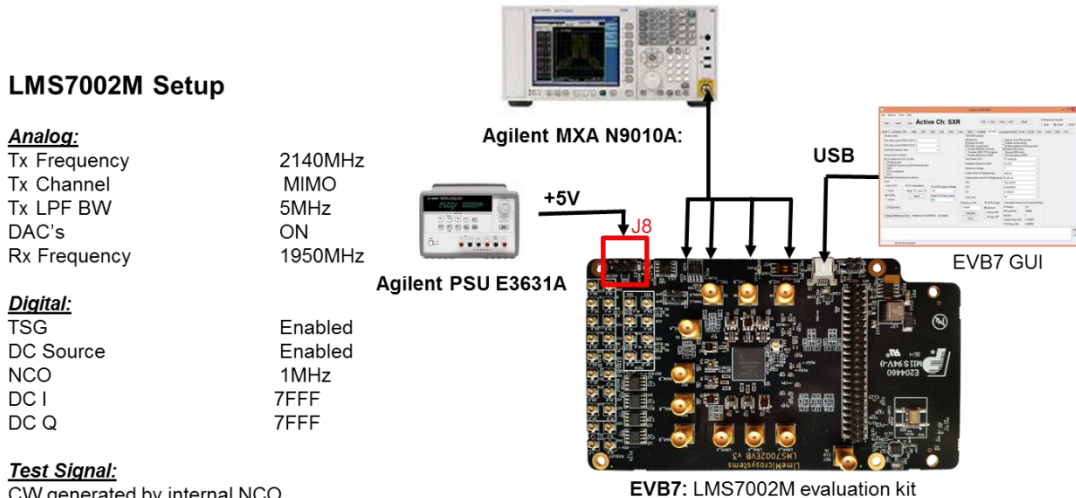


Figure 40. Test bench for TX-TX and TX-RX coupling using the LMS7002M evaluation board.

Table 14. Measurements of TX-TX and TX-RX coupling on the LMS7002M Evaluation board at 2140MHz.

| MIMOA | MIMOB | Frequency | NCO | TXLO | RXLO | TXA1 | TXA2 | TXB1 | TXB2 | RXAH | RXAL | RXAW | RXBH | RXBL | RXBW |
|-------|----------|-----------|-----|------|------|------|--------|-------|--------|------|------|------|------|------|------|
| Ch1 | Ch1 | 2141 | 1 | 2140 | 1950 | 2.05 | -24.23 | 2.26 | -26.43 | -85 | -76 | -78 | -76 | -79 | -68 |
| Ch1 | Disabled | 2141 | 1 | 2140 | 1950 | 2.34 | -27.78 | -41.4 | -59.3 | -81 | -84 | -83 | -79 | -84 | -68 |
| MHz | | | | | | dBm | | | | | | | | | |

4

RX Measurements

A receiver must be able to receive signals with the widest range of amplitudes as possible with minimum loss of signal quality. Noise Figure (NF) or sensitivity and Error Vector Magnitude (EVM) provide a measure of signal quality. In particular the receiver should preserve as much sensitivity as possible even in the presence of large out of band blocking signals.

Through the combination of good phase noise, programmable filtering and high dynamic range design, the LMS7002M can fulfil these requirements. Additionally the LMS7002M has a wide range of gain control which enables it to work with applications requiring automatic gain control AGC. We also show that EVM is sufficient for QAM based OFDM signals.

The receiver channel consists of several analog blocks shown in the simplified block diagram of Figure 41. The channel includes three selectable programmable gain low noise amplifiers (LNA), programmable gain transimpedance amplifier (TIA), unity gain low pass filter (LPF) with programmable bandwidth, a programmable gain amplifier (PGA). Additionally the receiver signal processing block (RSP) can provide additional functionality such as adaptive dc offset cancellation, gain and phase correction for image rejection, decimation, automatic gain control, digital filtering and digital down conversion with the NCO. The testing of the RSP blocks is covered in another document.

Section 4.1 describes the frequency response of the low pass filters. Section 4.2 describes the noise figure and in band IIP3 measurements. Section 4.3 describes the out of band IIP2 and IIP3 measurements. Section 4.4 describes the variation of RX gain and noise figure with temperature. Section 4.5 describes the LTE EVM measurements. Section 4.6 describes the GSM blocker EVM measurements. Section 4.7 describes results from a W-CDMA blocker test. Section 4.8 describes out of band 1dB compression point. Section 4.9 compares the performance of the 3 LNAs of each MIMO channel. Section 4.10 describes the performance of the Received Signal Strength Indicator (RSSI). Section 4.11 describes the RX gain step accuracy. Section 4.12 describes the LO leakage at the RF RX ports.

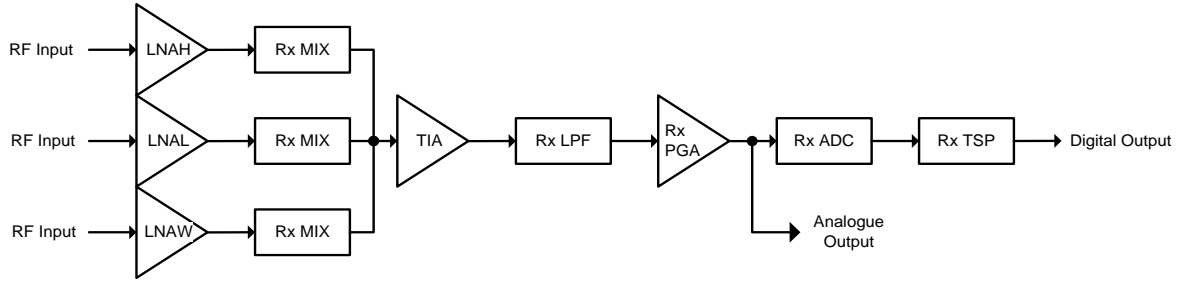


Figure 41. Simplified block diagram of a single receiver channel.

4.1 RX Low Pass Filters

The ability of a software defined radio to achieve good performance in the presence of blocker signals relies on the use of a programmable low pass filter to prevent blocker signals overloading the IF. The LMS7002M includes a programmable low frequency low pass filter (LPFL) covering 600kHz to 14MHz, and a programmable high frequency high (LPFH) pass filter covering 10MHz to 70MHz.

The low pass filters are tested with the configuration shown in Figure 42. The low frequency low pass filter bandwidth is controlled by the TIA Feedback capacitor in the RXRF tab of the GUI and the LPFL capacitor in the RXBB tab of the GUI. Changing the ratio of the two capacitance changes the ripple of the low pass filter. The TIA gain must be set to maximum (0dB) or middle settings (-3dB). The filter is intended to be a 3rd order Chebychev filter with nominally 0.5dB ripple. Figure 44 shows a typical 600kHz low pass filter response. Figure 43 shows the low frequency low pass filter tuning range. Figure 45 shows a typical 2.5MHz low pass filter response.

The high frequency low pass filter bandwidth is controlled by the TIA Feedback capacitor in the RXRF tab of the GUI and the LPFL capacitor in the RXBB tab of the GUI. The TIA gain must be minimum (-12dB). Changing the ratio of the two capacitance changes the ripple of the low pass filter. The TIA gain must maximum (0dB) or mid (-3dB). The filter is intended to be a 3rd order Chebychev filter with nominally 0.5dB ripple. Figure 46 shows the high frequency low pass filter control range.

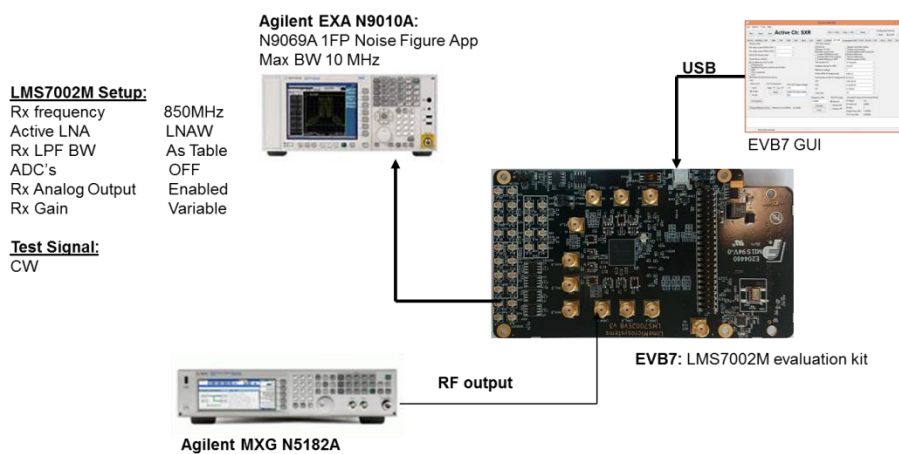


Figure 42. Test bench for testing low pass filters.

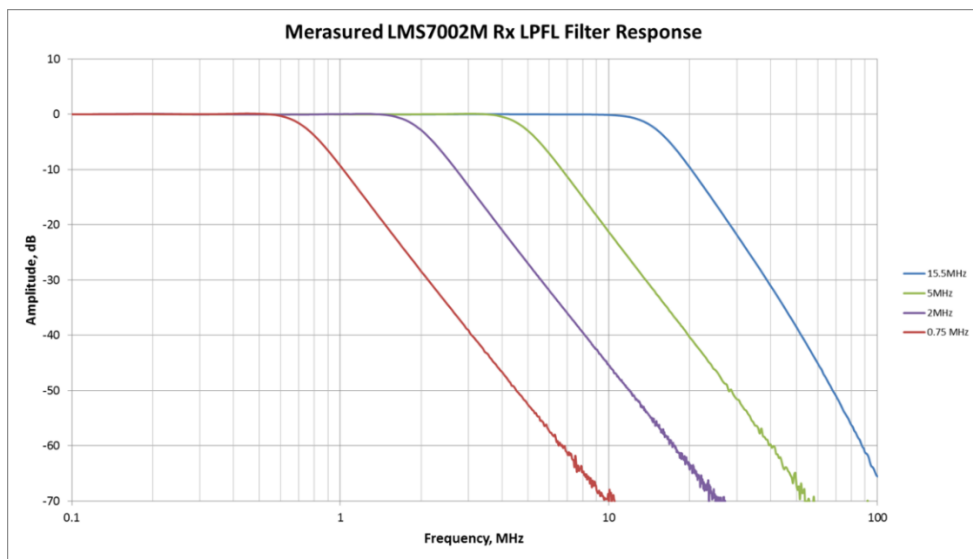


Figure 43. Variable bandwidth of low frequency low pass filter (LPFL)

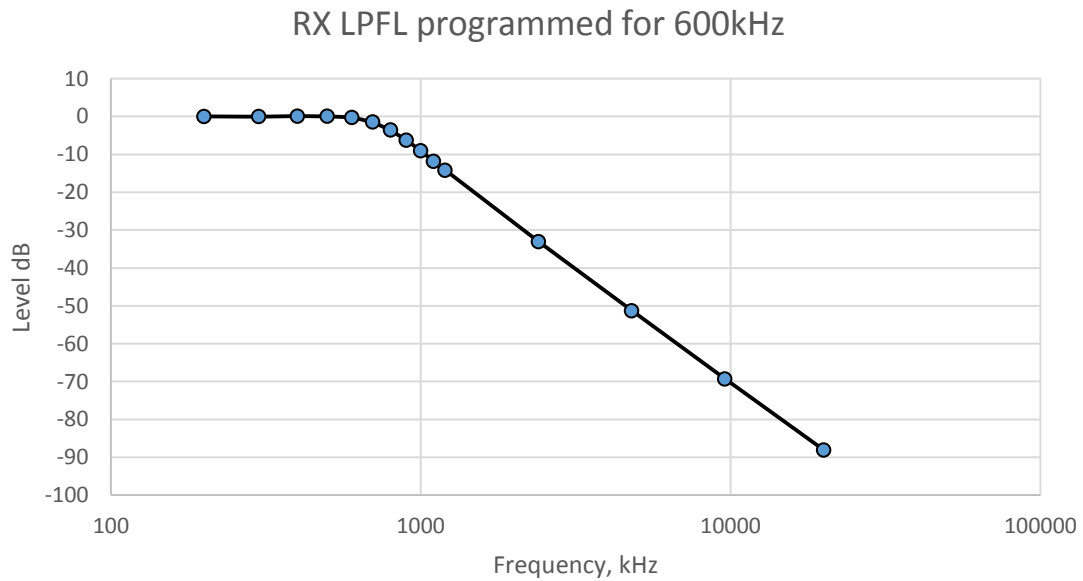


Figure 44. 600kHz Low pass filter (LPFH)

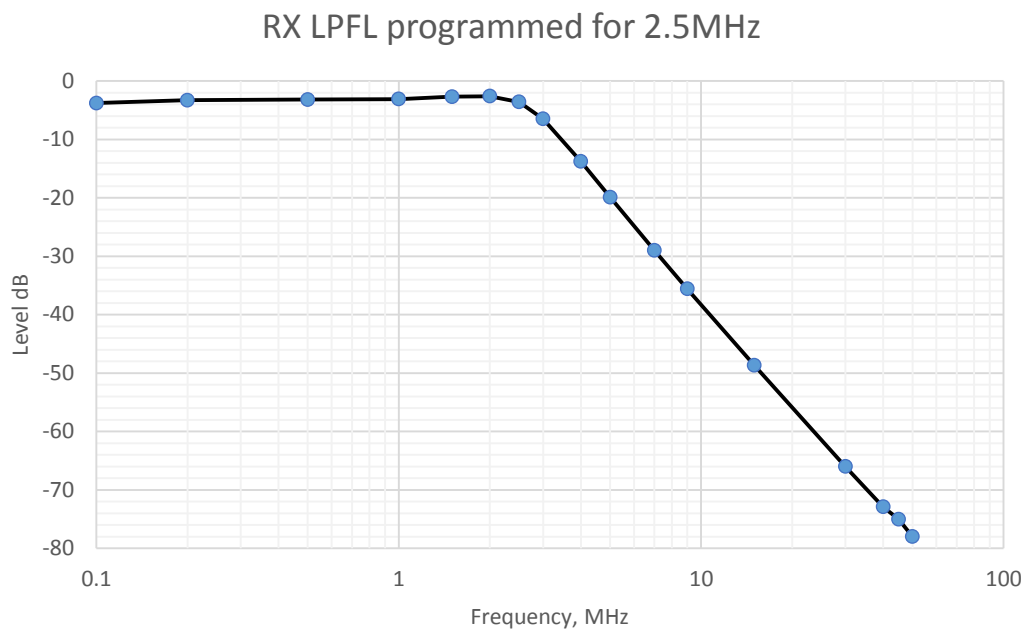


Figure 45. 2.5MHz Lowpass filter (LPFL)

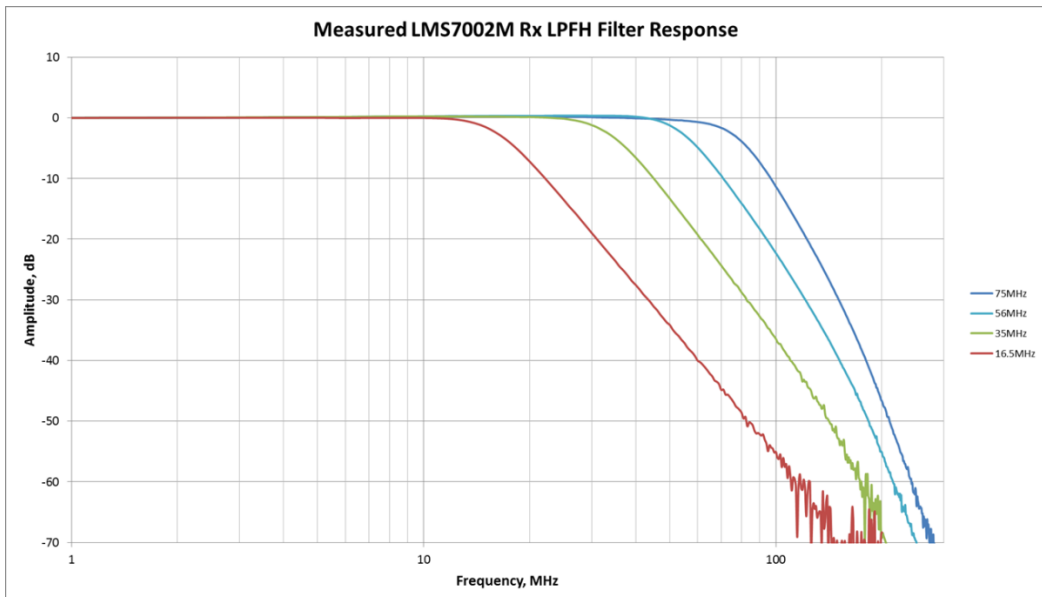


Figure 46. Variable bandwidth of the high frequency low pass filter (LPFH)

4.2 RX Noise Figure and Inband IIP3 Measurement

Noise figure (NF) defines how sensitive a receiver can be. When the receiver is operated at its highest gain it will normally have its maximum sensitivity. The test bench for measuring noise figure is shown in Figure 47. A tuner is used to match the evaluation board at the frequency being measured. A noise source is used with the y-factor noise measurement technique on either the I or Q channel output to obtain the SSB-NF. When the receiver is operated as an image reject receiver, the DSB-NF is a more useful measure of performance. The measured NF is converted from SSB-NF to DSB-NF by adding 3dB. Figure 48 shows the variation of NF and inband IIP3 with total receiver gain at 800MHz. Figure 49 shows the variation of NF and inband IIP3 with total receiver gain at 1850MHz. Figure 50 shows the variation of NF and inband IIP3 with total receiver gain at 2600MHz.

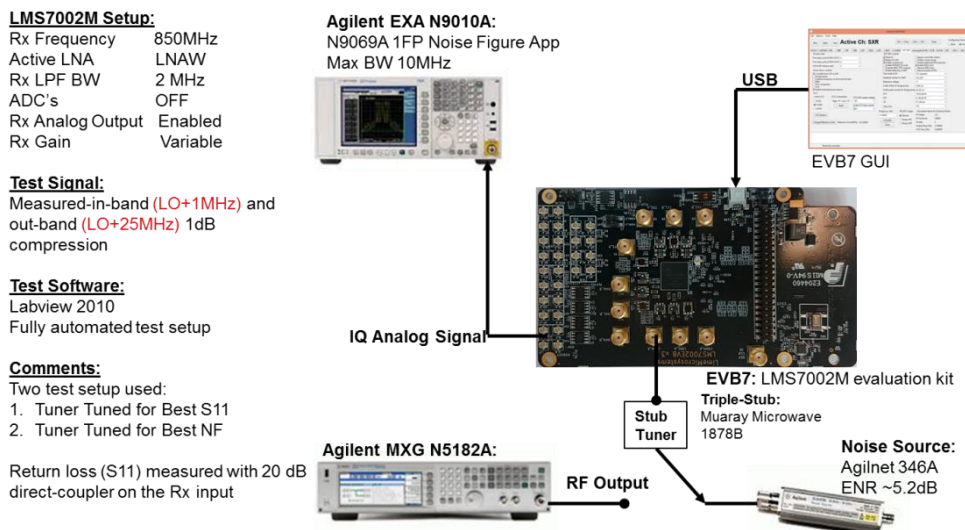


Figure 47. Test Bench for Noise Figure and Inband Linearity

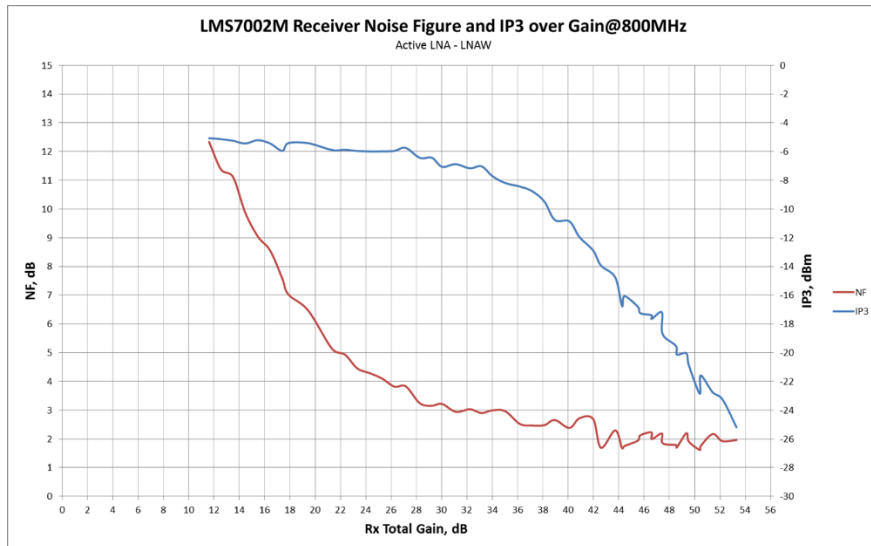


Figure 48. DSB Noise figure and inband IIP3 measurements vs gain at 800MHz

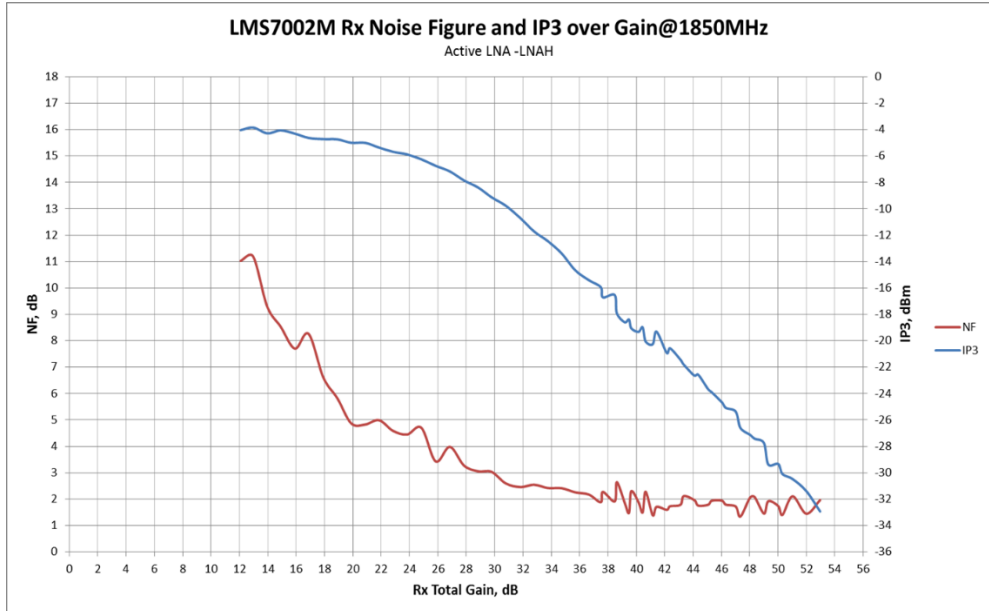


Figure 49. DSB Noise figure and inband IIP3 measurements vs gain at 1850MHz

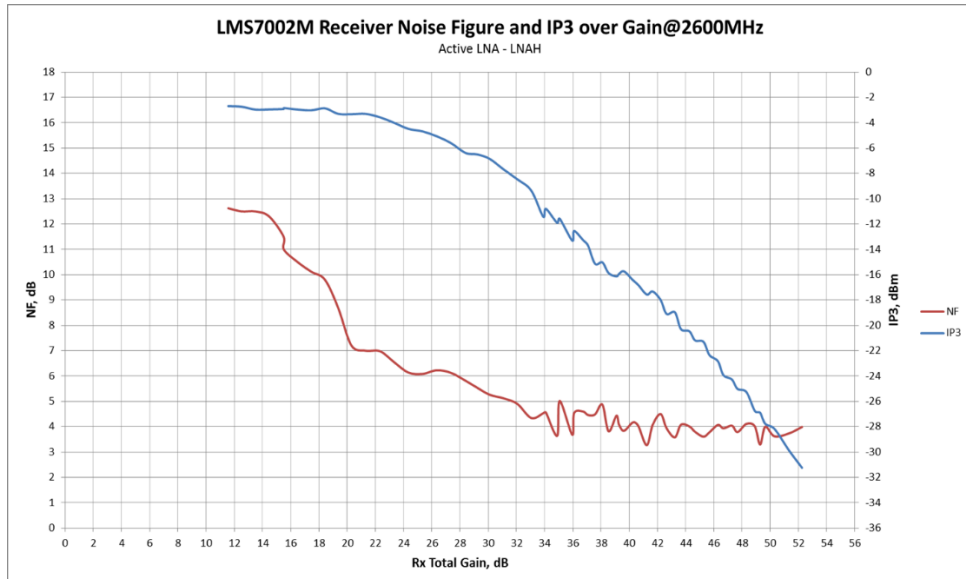


Figure 50. DSB Noise figure and inband IIP3 measurements vs gain at 2600MHz

Figure 51 and Figure 52 shows NF and S₁₁ vs frequency for different matching conditions. Figure 51 is matched for best S₁₁ at 850MHz. Figure 52 is matched for lowest noise figure at 850MHz. It can be see that matching for best return loss does not always lead to minimum noise figure. Since the LMS7002M is a broadband software defined radio, it is not possible to simultaneously give minimum noise figure at best match for all frequencies. However it is possible for designers to optimize noise figure at a critical frequency for each LNA.

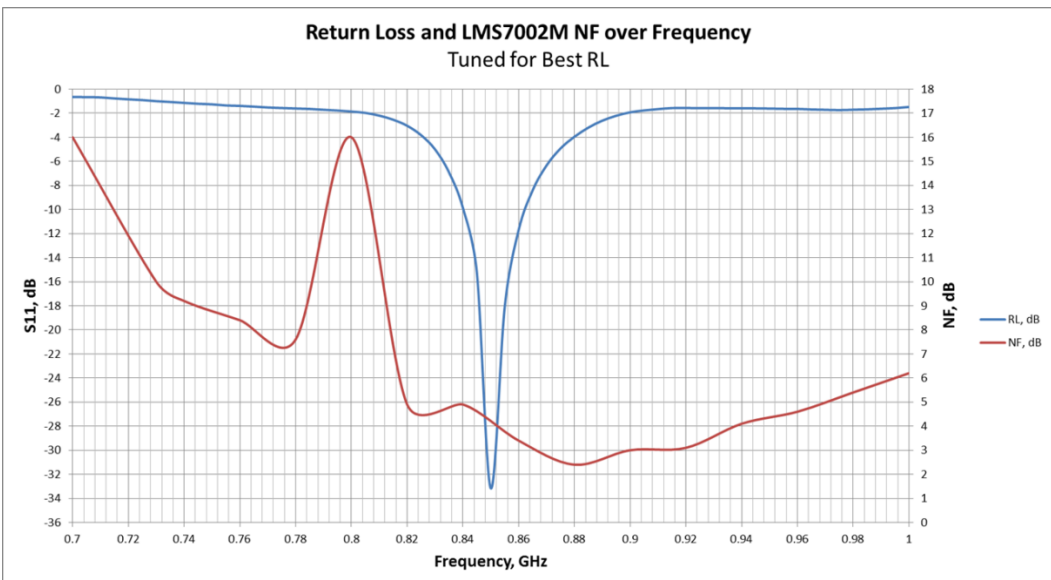


Figure 51. Noise figure and S₁₁ vs frequency for best match at 850MHz.

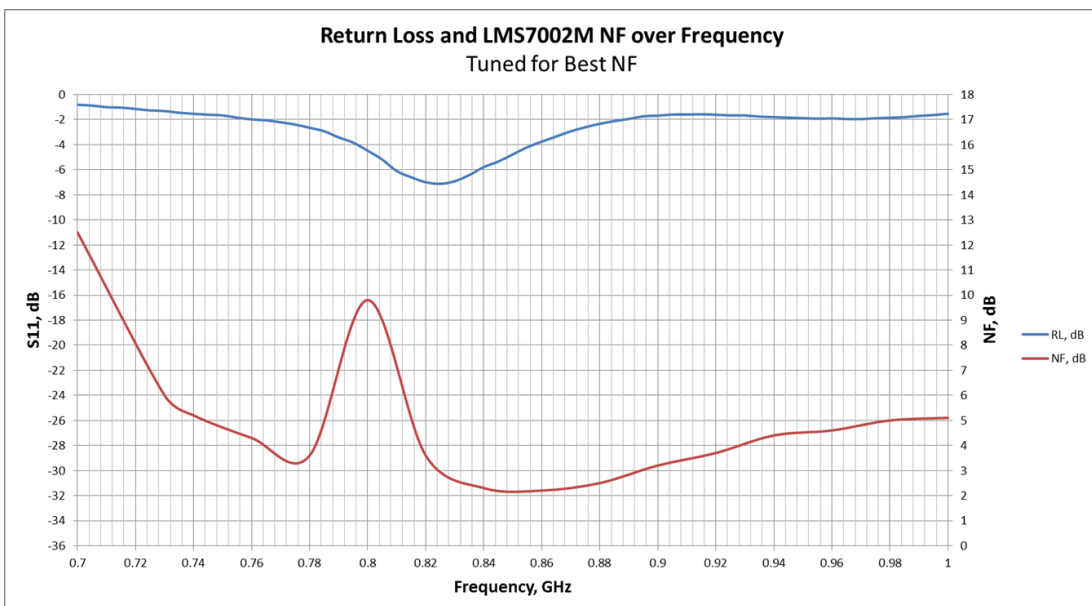


Figure 52. Noise figure and S₁₁ vs frequency for minimum noise at 850MHz.

4.3 RX Out of band IIP2 and IIP3 Measurement

The sensitivity of the receiver in the presence of large blocker signals is achieved by optimizing the IIP2 and IIP3 behavior of the transceiver. Optimization is largely done by limiting the magnitude of the blocker in the IF through the use of the RX low pass filter. This enables the transceiver to run close to full gain. Some further improvement in IIP2 and IIP3 is possible by reducing gain. The test bench used for the out of band two tone receiver measurements is shown in Figure 53. A summary table of IIP2 and IIP3 measurements with various gain settings is shown in

Table 15. A comparison of IIP3 performance with gain for the LMS7002M and a competing part is shown in Figure 54 at 850MHz with 600kHz LPF, Figure 55 at 915MHz with 600kHz LPF, Figure 56 1850MH with 2.5MHz LPF, Figure 57 2400MHz with 2.5MHz LPF.

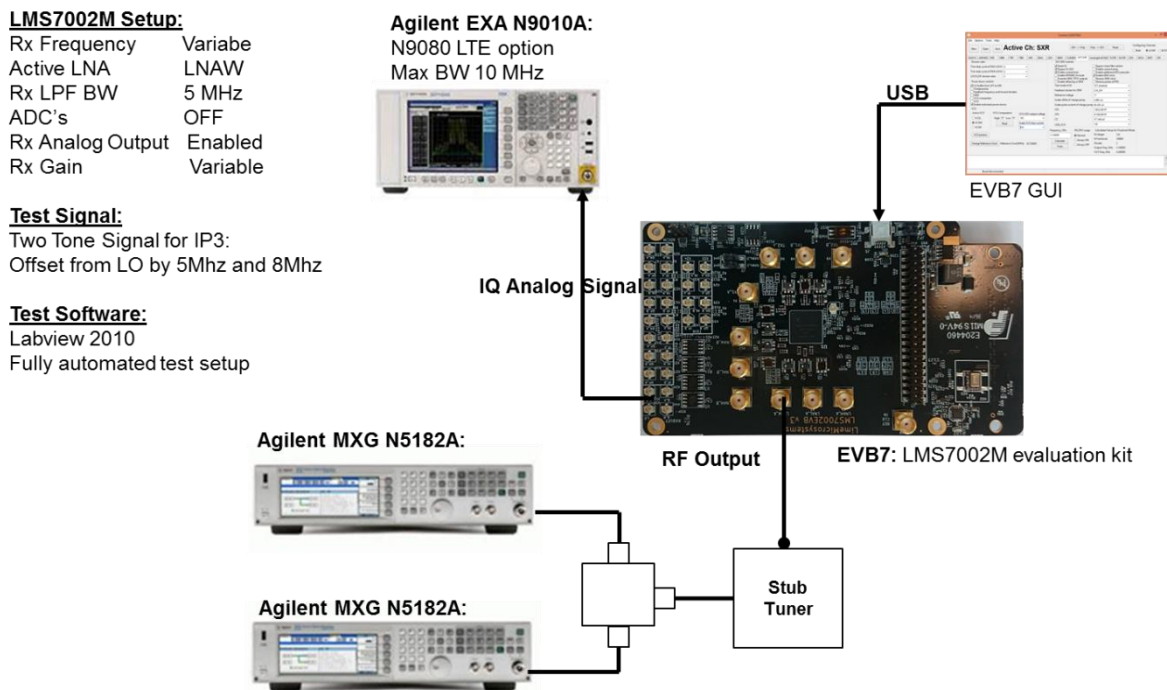


Figure 53. Test bench for the out of band two tone receiver measurements

To calculate IIP3 for a receiver whose LPF filters the input tones f_1 and f_2 , but passes the lower frequency intermodulation produce $2f_1-f_2$, the following formula is used.

$$IIP3 = \frac{2V_i(f_1) + V_i(f_2) + G_{dB} - V_o(2f_1 - f_2 - f_{LO})}{2}$$

Where:

$V_i(f)$ is the input voltage at frequency f in dBm. This signal level should take into account cable and combiner losses. Whilst it is common for the two input tones to be of equal amplitude, the equations still gives a valid result if the two tones are unequal in amplitude.

$V_o(f)$ is the output voltage at frequency f in dBm.

G_{dB} is the small signal gain at a frequency lower than the cut off frequency of the filter (typically 500kHz for a 2.5MHz low pass filter. Lower frequencies could be used, but some spectrum analyzers have measurement inaccuracy below 500kHz).

Likewise to calculate IIP2 for a receiver LPF filters the input tones f_1 and f_2 , but passes the lower frequency intermodulation produce f_2-f_1 , the following formula is used.

$$IIP2 = V_i(f_1) + V_i(f_2) + G_{dB} - V_o(f_2 - f_1)$$

Table 15. Summary of IIP2 and IIP3 measurements.

| LNA | LO, MHz | RF1, MHz | RF2, MHz | RF1, dBm | RF2, dBm | LNA Gain | TIA Gain | PGA Gain | LPF, MHz | Gain, dB | IIP2, dBm | IIP3, dBm |
|------|---------|----------|----------|----------|----------|----------|----------|----------|----------|----------|-----------|-----------|
| LNAL | 850 | 851.9 | 852.1 | -39.3 | -39.3 | 0 | 0 | 19 | 0.6 | 67.7 | 48.9 | n/a |
| | 850 | 851.9 | 852.1 | -33.3 | -33.3 | -9 | 0 | 19 | 0.6 | 60.3 | 52 | n/a |
| | 850 | 851.9 | 852.1 | -12.3 | -12.3 | -30 | 0 | 19 | 0.6 | 38.2 | 81.1 | n/a |
| | 850 | 851.5 | 852.5 | -46.3 | -46.3 | 0 | 0 | 19 | 0.6 | 67.7 | n/a | -5.5 |
| | 850 | 851.5 | 852.5 | -39.3 | -39.3 | -9 | 0 | 19 | 0.6 | 60.3 | n/a | 3.6 |
| | 850 | 851.5 | 852.5 | -34.3 | -34.3 | -30 | 0 | 19 | 0.6 | 38.2 | n/a | 3.2 |
| | 915 | 916.2 | 917.2 | -41.3 | -41.3 | 0 | 0 | 19 | 0.6 | 69.1 | 48.1 | n/a |
| | 915 | 916.2 | 917.2 | -33.3 | -33.3 | -9 | 0 | 19 | 0.6 | 60.8 | 57.1 | n/a |
| | 915 | 916.2 | 917.2 | -13.3 | -13.3 | -30 | 0 | 19 | 0.6 | 38.4 | 78.9 | n/a |
| | 915 | 916.4 | 917.4 | -46.3 | -46.3 | 0 | 0 | 19 | 0.6 | 69.1 | n/a | -2.4 |
| LNAH | 915 | 916.4 | 917.4 | -41.3 | -41.3 | -9 | 0 | 19 | 0.6 | 60.8 | n/a | 5.5 |
| | 915 | 916.4 | 917.4 | -31.3 | -31.3 | -30 | 0 | 19 | 0.6 | 38.4 | n/a | 4.3 |
| | 1980 | 2010 | 2011 | -33.3 | -33.3 | 0 | 0 | 19 | 2.5 | 56.4 | 40.6 | n/a |
| | 1980 | 2010 | 2011 | -25.3 | -25.3 | -9 | 0 | 19 | 2.5 | 48.3 | 54.1 | n/a |
| | 1980 | 2010 | 2011 | -10.3 | -10.3 | -30 | 0 | 19 | 2.5 | 27.9 | 65 | n/a |
| | 1980 | 2010 | 2041 | -34.3 | -34.3 | 0 | 0 | 19 | 2.5 | 56.4 | n/a | 8.3 |
| LNAL | 1980 | 2010 | 2041 | -31.3 | -31.3 | -9 | 0 | 19 | 2.5 | 48.3 | n/a | 9 |
| | 1980 | 2010 | 2041 | -24.3 | -24.3 | -30 | 0 | 19 | 2.5 | 27.9 | n/a | 10.8 |
| | 2400 | 2460 | 2461 | -31.3 | -31.3 | 0 | 0 | 19 | 2.5 | 55.2 | 58.1 | n/a |
| | 2400 | 2460 | 2461 | -18.3 | -18.3 | -15 | 0 | 19 | 2.5 | 41.1 | 72 | n/a |
| | 2400 | 2460 | 2461 | -11.3 | -11.3 | -30 | 0 | 19 | 2.5 | 26.3 | 68.8 | n/a |
| | 2400 | 2430 | 2461 | -31.3 | -31.3 | 0 | 0 | 19 | 2.5 | 55.2 | n/a | 8.8 |
| LNAH | 2400 | 2430 | 2461 | -31.3 | -31.3 | -9 | 0 | 19 | 2.5 | 47 | n/a | 9.4 |
| | 2400 | 2430 | 2461 | -23.3 | -23.3 | -30 | 0 | 19 | 2.5 | 26.3 | n/a | 9.3 |
| | 2535 | 2618.5 | 2619.5 | -33 | -33 | 0 | 0 | 0 | 5 | 41.3 | 44.2 | -4.5 |
| | 3050 | 3056 | 3057 | -33 | -33 | 0 | 0 | 0 | 5 | 40.4 | 41.4 | -3.9 |
| | 3050 | 3096 | 3097 | -33 | -33 | 0 | 0 | 0 | 5 | 40.4 | 44.8 | n/a |
| | 3450 | 3456 | 3457 | -36 | -36 | 0 | 0 | 0 | 5 | 38.7 | 44.7 | -1.1 |
| | 3450 | 3496 | 3497 | -36 | -36 | 0 | 0 | 0 | 5 | 38.7 | 41 | n/a |
| LNAL | 3750 | 3756 | 3757 | -39 | -39 | 0 | 0 | 0 | 5 | 34.4 | 50.8 | 3.25 |
| | 3750 | 3796 | 3797 | -39 | -39 | 0 | 0 | 0 | 5 | 34.4 | 55.8 | n/a |

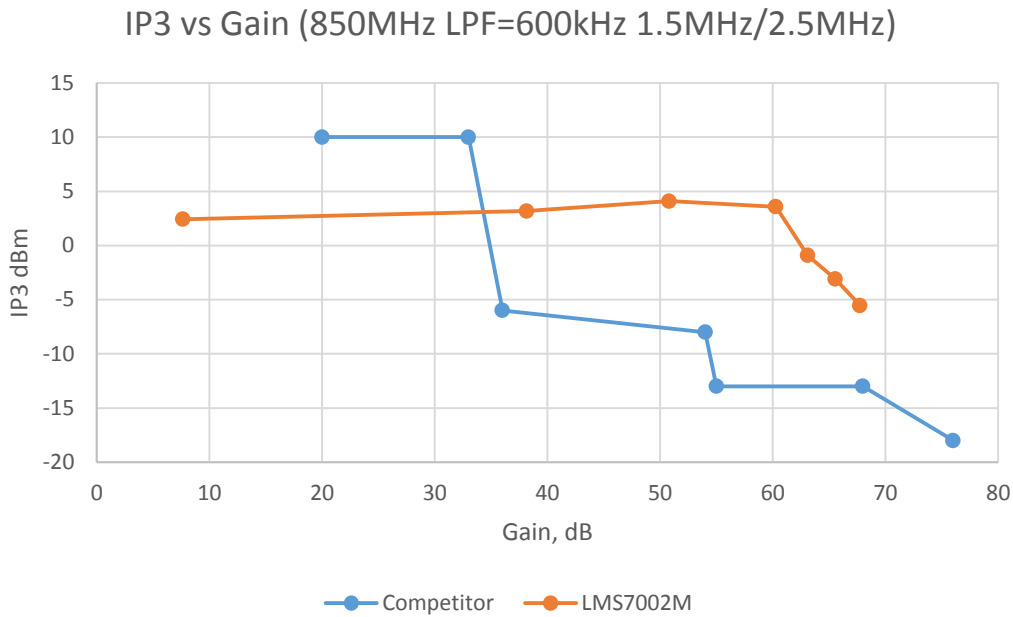


Figure 54. Comparsion of out of band IIP3 with gain of LMS7002M with a competing part at 850MHz with 600kHz LPF.

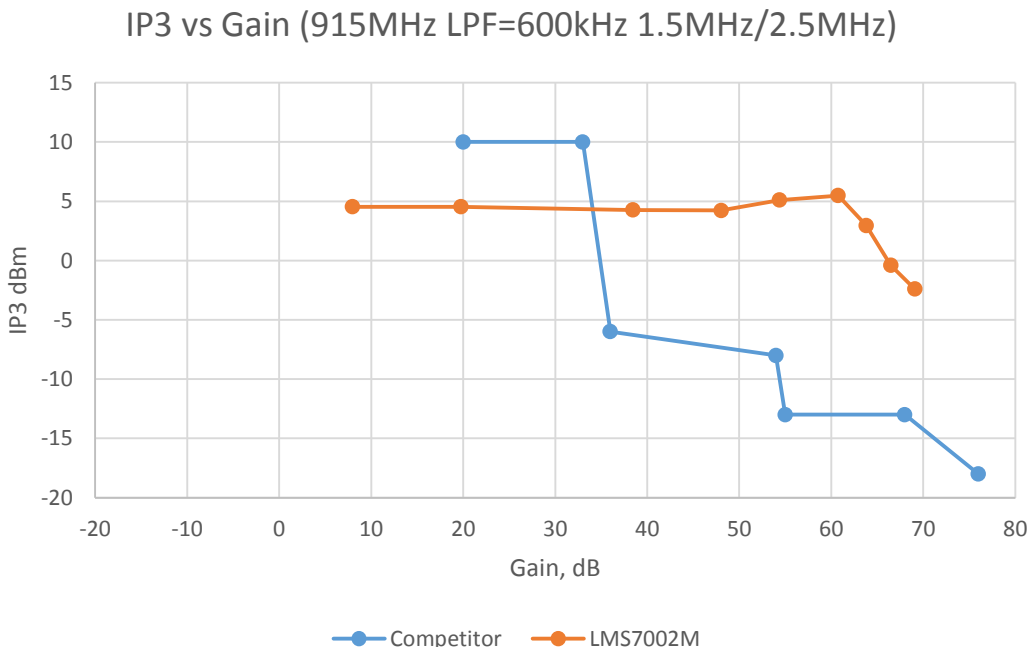


Figure 55. Comparsion of out of band IIP3 with gain of LMS7002M with a competing part at 915MHz with 600kHz LPF

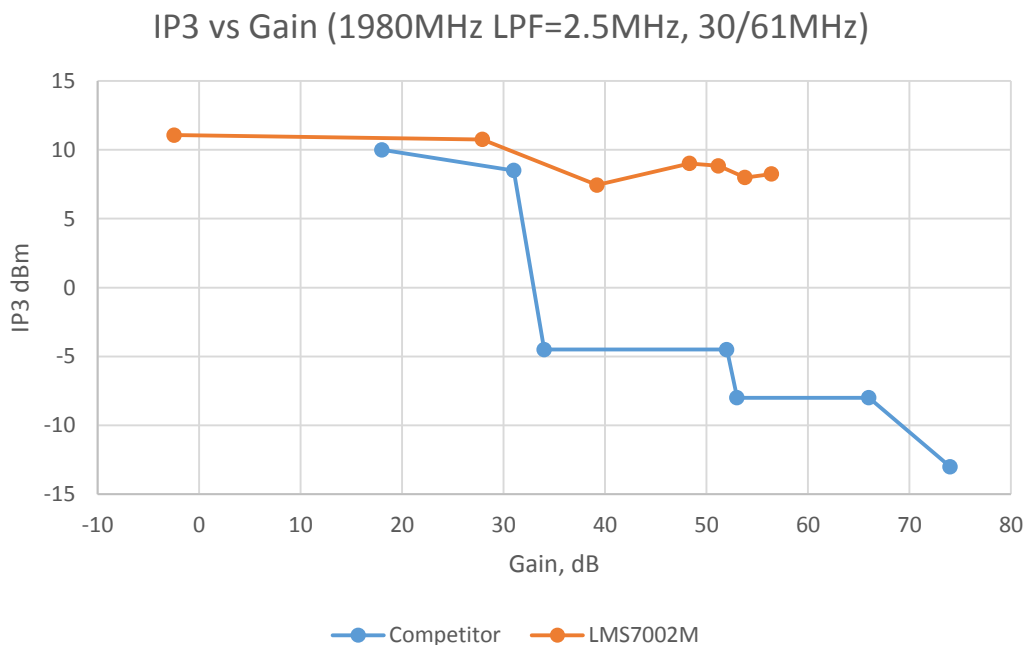


Figure 56. Comparsion of out of band IIP3 with gain of LMS7002M with a competing part at 1980MHz with 2.5MHz LPF

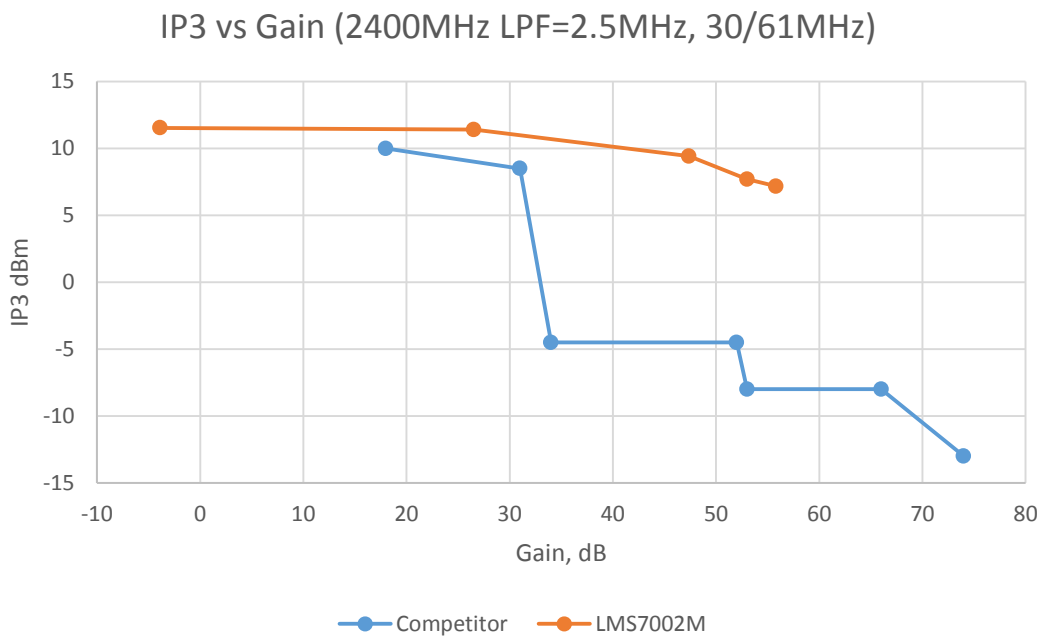


Figure 57. Comparsion of out of band IIP3 with gain of LMS7002M with a competing part at 2400MHz with 2.5MHz LPF

4.4 Variation of RX Gain and Noise Figure with Temperature

The gain and noise figure of the LMS7002M Receiver have been measured over temperature using the test set shown in Figure 58 and Figure 59. Note that the noise source is kept outside of the oven, and the cable loss calibrated out with the MXA noise personality. In Figure 60 it can be seen the RX gain varies by 6dB between -50°C and 110°C. In Figure 61 it can be seen the RX noise figure varies by 2dB between -50°C and 110°C.

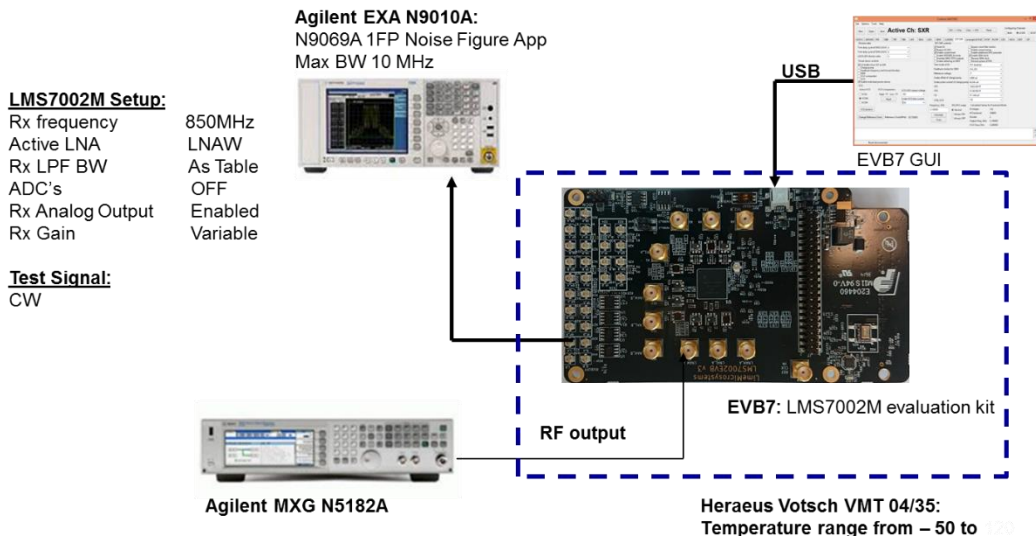


Figure 58 Test bench for gain over temperature measurements

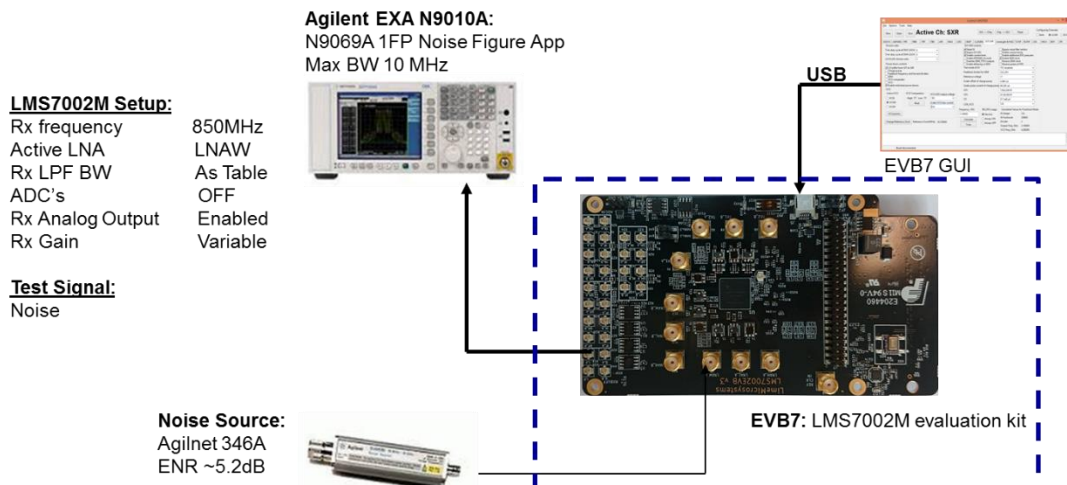


Figure 59 Test Bench for noise figure over temperature measurements

LMS7002M Total Receiver Gain over the Temperature

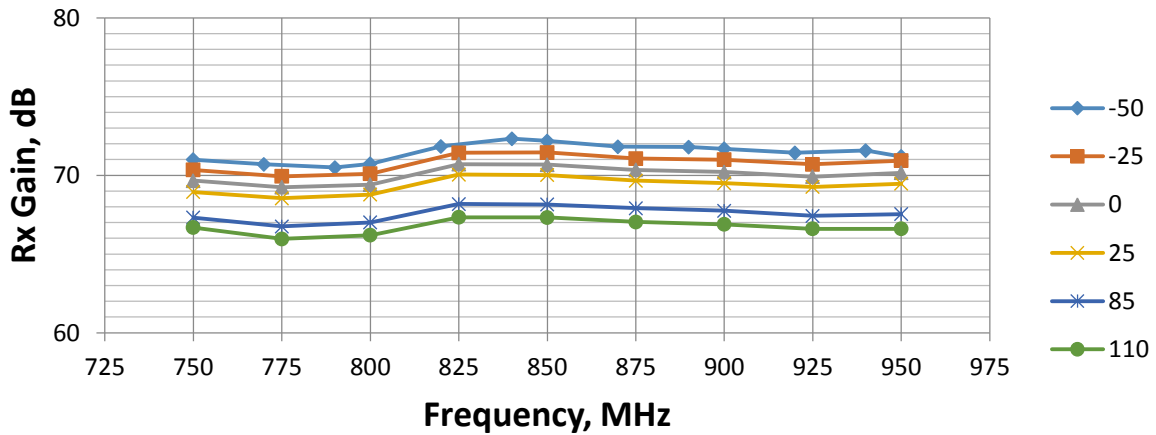


Figure 60 Gain vs Frequency for different temperatures

Noise Figure vs Frequency

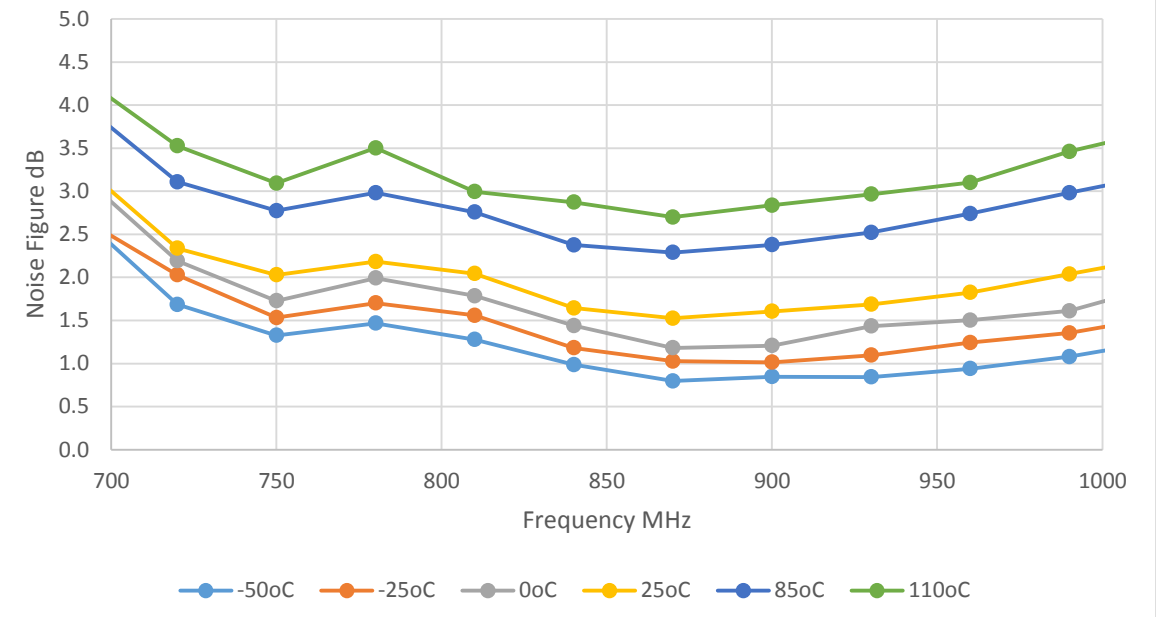


Figure 61 Noise Figure vs Frequency for different temperatures

4.5 RX LTE EVM Measurement

The quality of the received LTE signal can be measured using error vector magnitude (EVM). This includes effects such as plateau phase noise, filter noise, nonlinearity etc. The test bench used to measure EVM of the LTE signal is shown in Figure 62. The signal is generated with an Agilent MXG with LTE personality. The signal is demodulated with an Agilent EXA with LTE personality using a ‘low IF’ approach. The low IF approach is where the signal is demodulated on either the I or Q output of the receiver with a nonzero IF frequency. EVM measurements were made at 860MHz (Figure 63), 2400MHz (Figure 64) and 2600MHz (Figure 65).

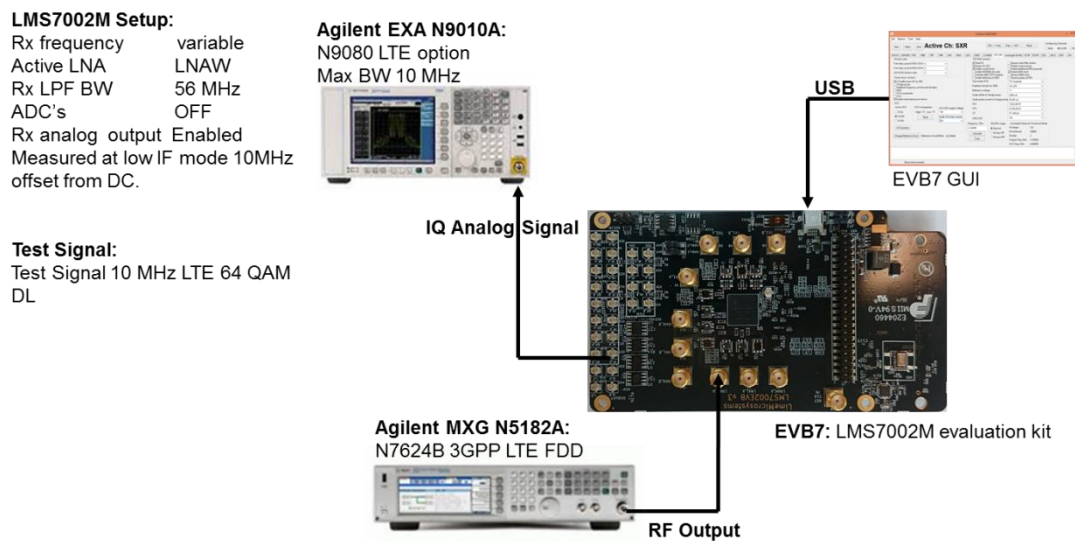


Figure 62. Test bench for RX EVM measurements

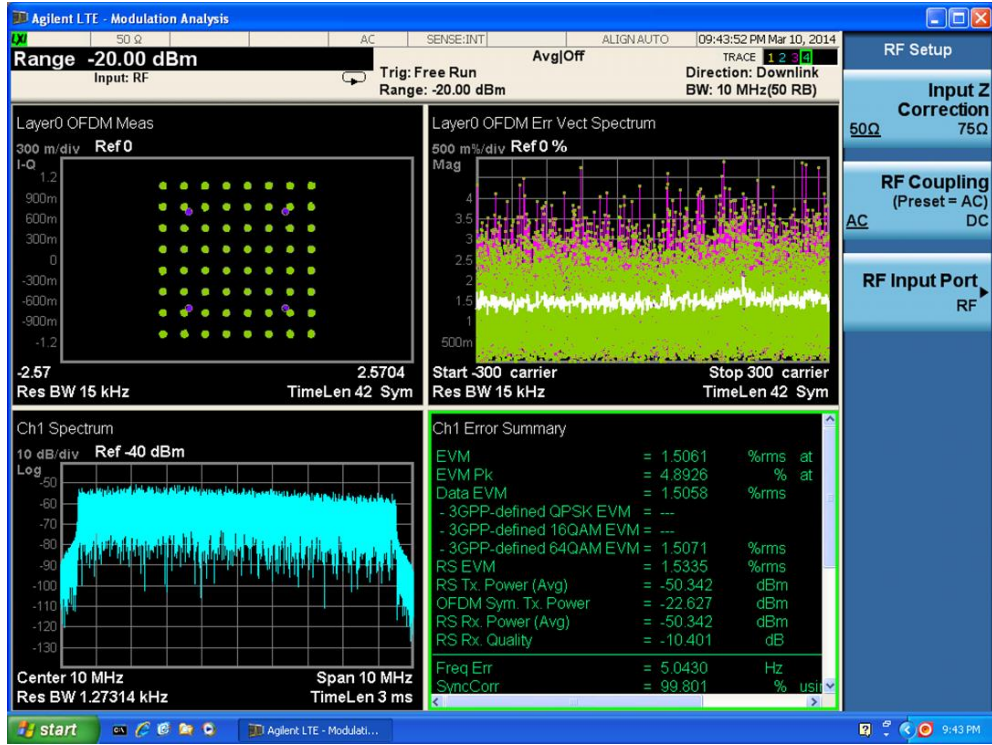


Figure 63. Low IF EVM performance at 860MHz

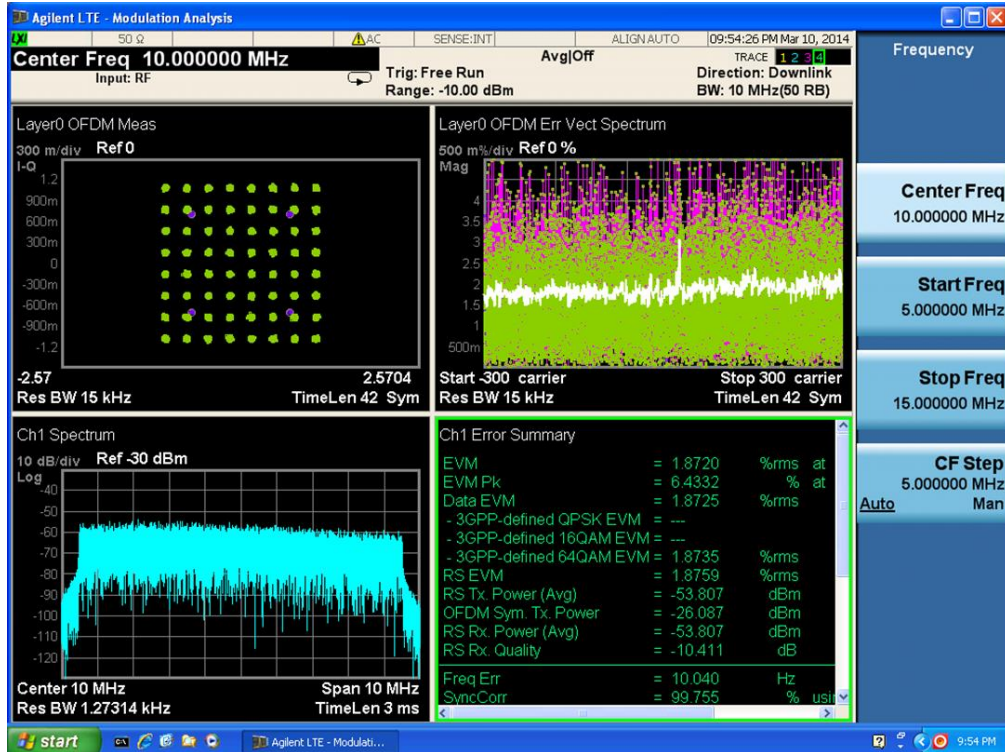


Figure 64. Low IF LTE EVM at 2140MHz

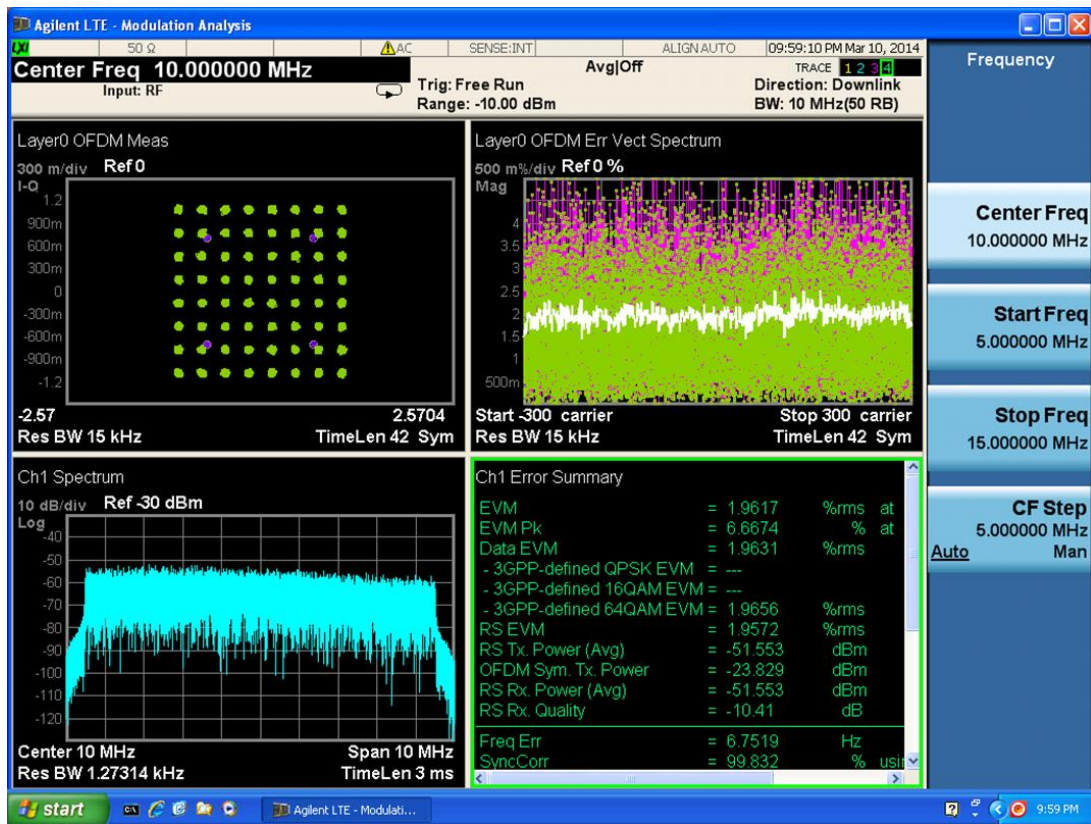


Figure 65. Low IF LTE EVM at 2600MHz

4.6 RX GSM Blocker EVM Measurements

The GSM receiver is required to operate with CW blockers at 600kHz away from the channel centre, where close in phase noise from the receiver synthesizer can affect sensitivity and error vector magnitude (EVM) [1]. This measurement was carried out with the configuration shown in Figure 66. The CW blocker was generated with a low phase noise source (MXG). The GSM signal was generated with a 2nd MXG. The signal was demodulated with a PXA spectrum analyzer with GSM personality. The GSM signal is demodulated with “Low IF” approach. The low IF approach is where the signal is demodulated on either the I or Q output of the receiver with a nonzero IF frequency. The measured GSM results are shown in Figure 67 to Figure 70.

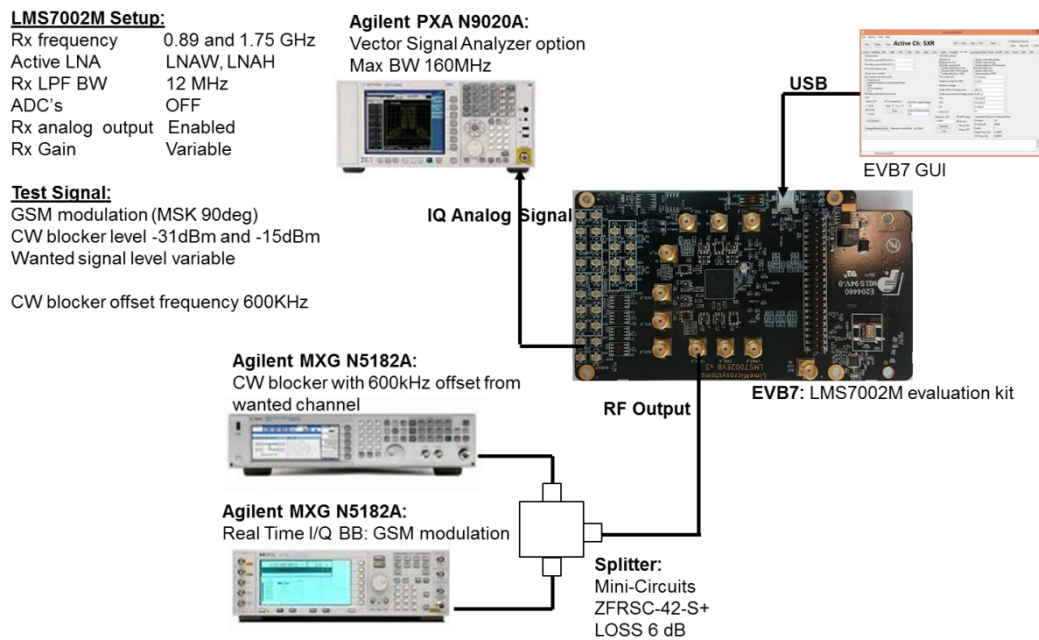


Figure 66. Test bench used to measure RX EVM with CW blocker.

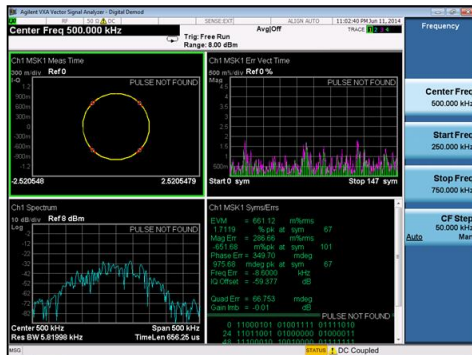
LMS7002M Setup:

| | |
|------------------|---------------|
| Rx frequency | 0.89GHz |
| Active LNA | LNAW |
| Rx LPF BW | 12 MHz |
| ADC's | OFF |
| Rx analog output | Enabled |
| LNA Gain | MAX |
| TIA Gain | MAX-12 |
| PGA Gain | -4 dB |

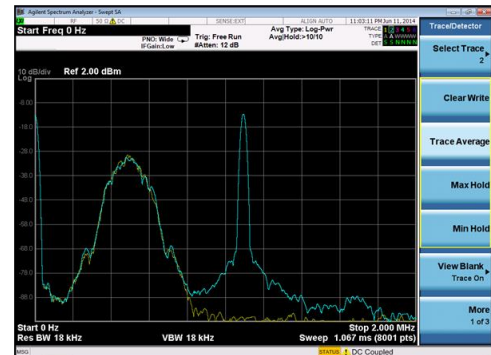
| EVM % | | | | | |
|---------------------|------|------|-----|-----|-----|
| Pin, dBm | -40 | -50 | -60 | -70 | -80 |
| No Blocker | 0.66 | 0.75 | 1.3 | 3.3 | 10 |
| With Blocker | 0.72 | 0.98 | 1.9 | 5.4 | # |

Test Setup:

Blocker level -31dBm



Measured EVM 0.66%, No blocker



Spectrum of Rx IF stage with GSM modulation and CW blocker

Figure 67. RX GSM 900 EVM with CW blocker

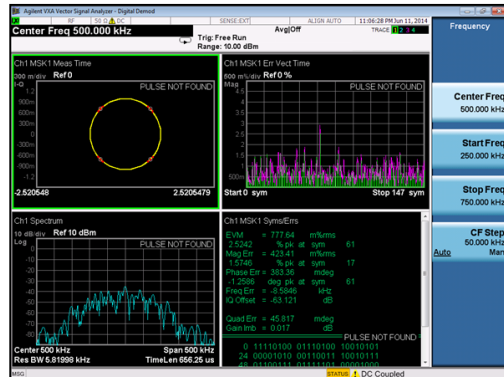
LMS7002M Setup:

| | |
|------------------|---------------|
| Rx frequency | 0.89GHz |
| Active LNA | LNAW |
| Rx LPF BW | 12 MHz |
| ADC's | OFF |
| Rx analog output | Enabled |
| LNA Gain | MAX-15 |
| TIA Gain | MAX-12 |
| PGA Gain | 2 dB |

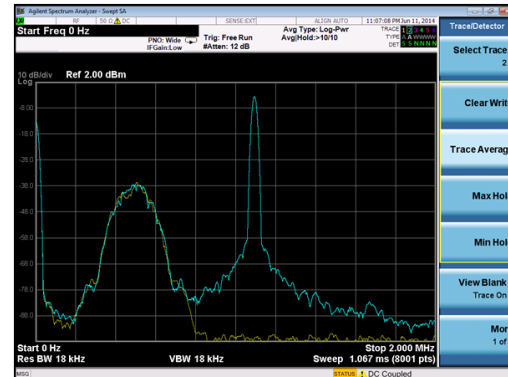
| EVM % | | | | | |
|---------------------|------|-----|-----|-----|-----|
| Pin, dBm | -40 | -50 | -60 | -70 | -80 |
| No Blocker | 0.77 | 1 | 2.6 | 7.3 | # |
| With Blocker | 1.1 | 2.8 | 8.7 | # | # |

Test Setup:

Blocker level -15dBm



Measured EVM 0.77%, No blocker



Spectrum of Rx IF stage with GSM modulation and CW blocker

Figure 68. RX GSM 900 EVM with CW blocker

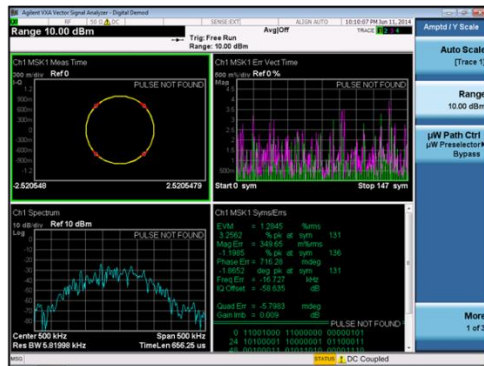
LMS7002M Setup:

| | |
|------------------|---------------|
| Rx frequency | 1.75GHz |
| Active LNA | LNAH |
| Rx LPF BW | 12 MHz |
| ADC's | OFF |
| Rx analog output | Enabled |
| | |
| LNA Gain | MAX |
| TIA Gain | MAX-12 |
| PGA Gain | 4 dB |

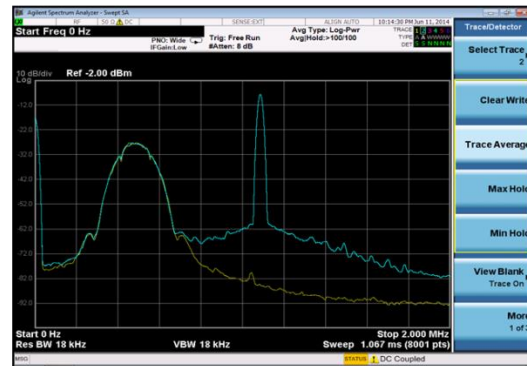
| EVM % | | | | | |
|---------------------|------|------|------|-----|-----|
| Pin, dBm | -40 | -50 | -60 | -70 | -80 |
| No Blocker | 1.28 | 1.35 | 1.89 | 3.3 | 9 |
| With Blocker | 1.6 | 3.4 | 10.4 | # | # |

Test Setup:

Blocker level -31dBm



Measured EVM 1.28%, No blocker



Spectrum of Rx IF stage with GSM modulation and CW blocker

Figure 69. RX GSM 1850 EVM with CW blocker

LMS7002M Setup:

| | |
|------------------|---------------|
| Rx frequency | 1.75GHz |
| Active LNA | LNAH |
| Rx LPF BW | 12 MHz |
| ADC's | OFF |
| Rx analog output | Enabled |
| | |
| LNA Gain | MAX-12 |
| TIA Gain | MAX-12 |
| PGA Gain | 4 dB |

| EVM % | | | | | |
|---------------------|-----|-----|-----|-----|-----|
| Pin, dBm | -40 | -50 | -60 | -70 | -80 |
| No Blocker | 1.4 | 2.3 | 6.4 | 10 | # |
| With Blocker | 6.5 | # | # | # | # |

Test Setup:

Blocker level -15dBm

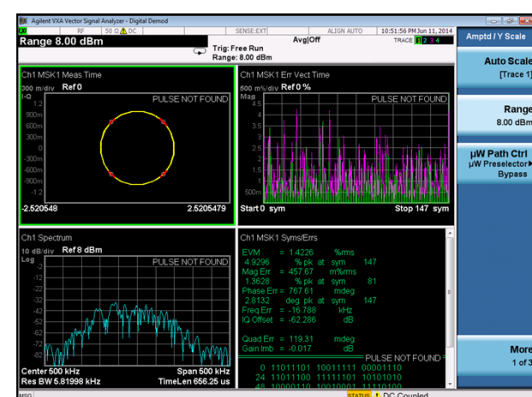
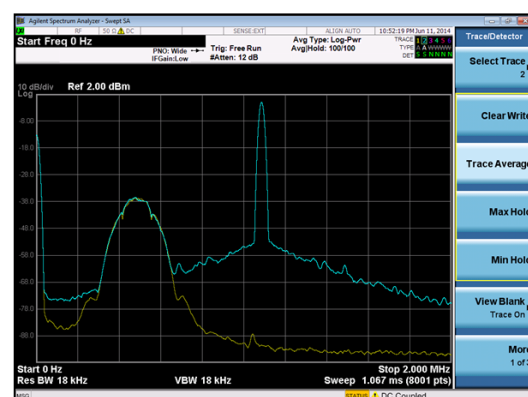


Figure 70. RX GSM 1850 EVM with CW blocker



4.7 RX W-CDMA Blocker Test

Perhaps one of the most demanding blocker cases in the W-CDMA specifications is the -15dBm CW blocker test, where sensitivity has to be better than -101dBm when a CW blocker is 20MHz away from the edge of the up band. Only receivers with very low far out phase noise and high dynamic range are able to operate under these conditions.

Using the test set shown in Figure 71, a sensitivity measurement is made with and without the blocker with the receiver optimized for blocker sensitivity using the Low IF technique. The experiment set up procedure is as follows.

First the tuner is tuned to give good return loss at 849MHz.

Next the ESG is loaded with a W-CDMA Up Link (UL) signal. The MXA is set with W-CDMA personality operating in the “Mobile” mode. The bandwidth of the LPF of the receiver is adjusted (approx. 5MHz) to give reasonable EVM with a W-CDMA signal of around -50dBm with a low IF frequency centered on 3MHz. It is assumed that the RX PLL settings have been already optimized for EVM.

The low frequency TX output of the LMS7002M is adjusted to 869MHz using the internal NCO and set to approximately -15dBm. Note that it is necessary to use an LMS7002M to generate the blocker signal as many commercial signal generators only have a phase noise of about -135dBc at 20MHz offset which would give incorrect measurement results, whereas the LMS7002M far out phase is around -160dBc at 20MHz.

The gain of the receiver LNA is slightly reduced from maximum to improve large signal performance with only a slight increase of noise figure and loss of sensitivity. This allows successful demodulation of the received signal with the blocker present. The PGA gain is adjusted to ensure the blocker does not saturate the IF output. The exact value of PGA gain is not usually critical providing the IF is not overloaded.

Figure 72 shows typical output with -94dBm W-CDMA UL input signal without the CW blocker signal being present. Figure 73 shows the same W-CDMA input signal with the -15.6dBm CW blocker signal present. The receiver noise floor rises by only 7 to 8dB due to the combined far out phase noise from both the RX and TX synthesizers of the LMS7002M. Figure 74 shows a -94dBm W-CDMA UL signal being correctly demodulated in the MXA spectrum analyzer with a -15.6dBm blocker present. The receiver sensitivity without the blocker present was -97dBm with the receiver optimized for the blocker. With the receiver operating at full gain, the sensitivity was around -100dBm.

It is thought that the Agilent MXA does not take advantage of the 18dB code spreading gain and error correction codes in the modulation, so sensitivity with a fully functioning baseband is anticipated to be over 18dB better. This would suggest the LMS7002M has a W-CDMA Up Link sensitivity of -118dBm, which reduces to -112dBm with the -15dBm blocker present as shown in Table 16. Further improvements in blocker performance can be obtained using a duplexer to help reduce the amplitude of the blocker reaching the receiver, typically by 3 to 20dB, depending on duplexer quality. It is also thought that using a zero IF configuration will give further improvement as this reduces unwanted sideband noise by 3dB and gives better LPFL roll off.

Table 16. Measured and interpolated sensitivity of LMS7002M with and without CW blocker.

| LNA | LO Freq | IF Freq | RF Freq | Blocker Freq | LNA Gain | TIA Gain | PGA Gain | CLPF | CTIA | Measured Sensitivity | Blocker | Correct Sensitivity |
|-------|---------|---------|---------|--------------|----------|----------|----------|------|------|----------------------|---------|---------------------|
| LNA L | 846 | 3 | 849 | 870 | Max-6dB | Max-3dB | 5 | 110 | 320 | -97 | -70 | -115 |
| LNA L | 846 | 3 | 849 | 870 | Max-6dB | Max-3dB | 5 | 110 | 320 | -94 | -15.3 | -112 |
| MHz | | | | | dB | | | | | dBm | | |

LMS7002M Setup

Analog:

Rx Frequency 849MHz
Rx LPF BW 5MHz
Tx Frequency 869MHz
Mode SISO FDD
Rx LPF BW 5MHz
DAC's ON

Digital:

TSG Enabled
DC Source Enabled
NCO 1MHz
DC I 7FFF
DC Q 7FFF

Test Signal:

CW generated by internal NCO

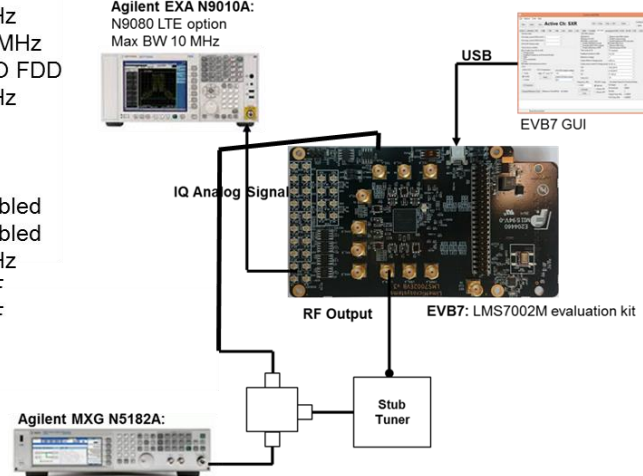


Figure 71. Test bench configuration for W-CDMA blocker case.



Figure 72. Spectrum of IF output without blocker present (signal -94dBm).

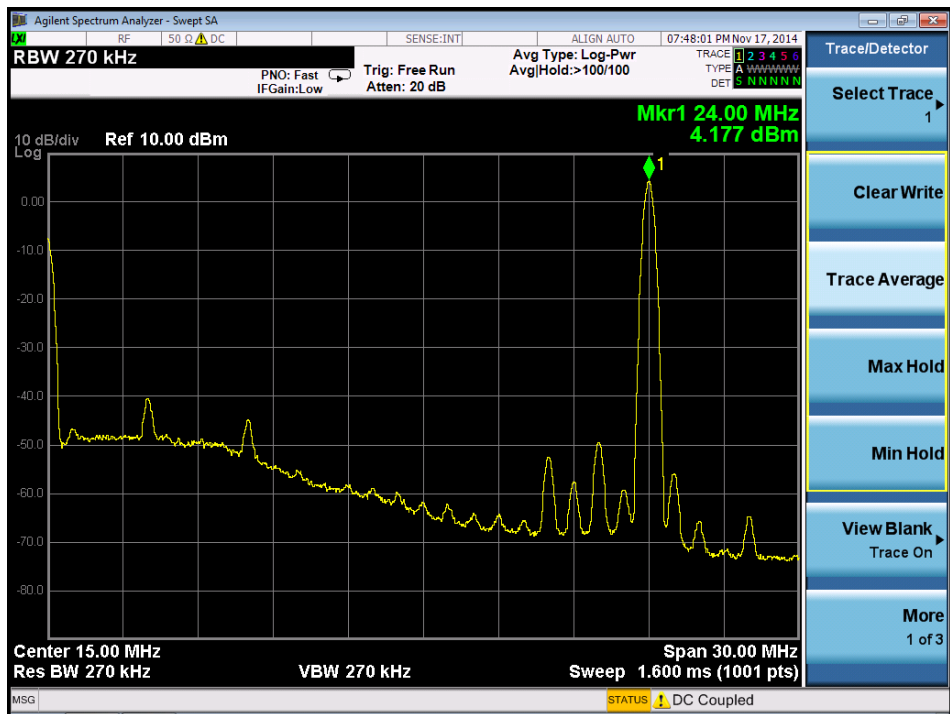


Figure 73. Spectrum of IF output with blocker present (signal -94dBm, blocker -15.6dBm).

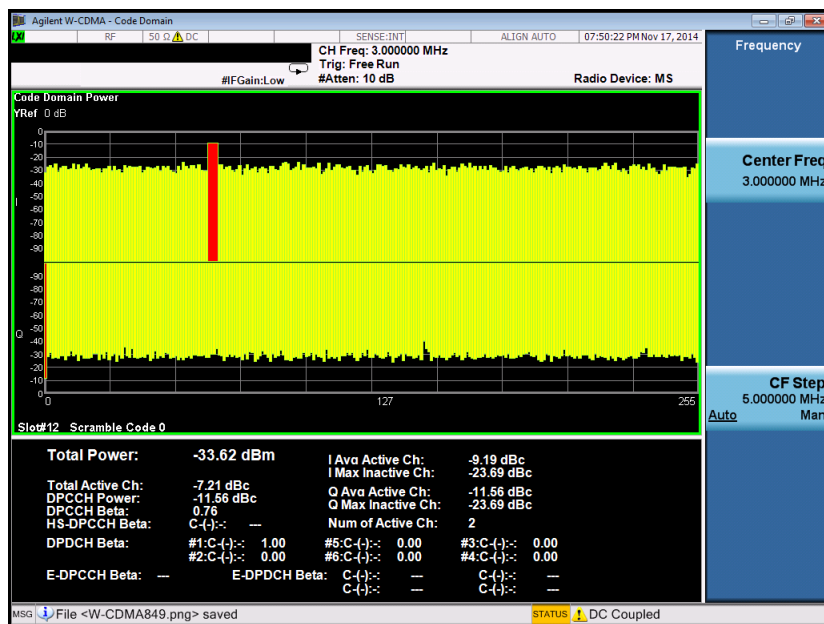


Figure 74. W-CDMA Code Domain View (signal -94dB, blocker -15.6dBm)

4.8 Out of Band P1dB

For W-CDMA applications, one of the key blocker requirements is for the receiver to have only slightly reduced sensitivity in the presence of a -15dBm CW blocker 20MHz away from the band edge. Part of this requirement is fulfilled by the duplex filter, part of this requirement is fulfilled by a high dynamic range LNA/Mixer with a programmable LPF in the IF chain, and part of this requirement is fulfilled by very low far out phase noise in the synthesizer.

The test bench of Figure 47 was used to measure P1dB compression of an out of band blocker with LNA gain control code. The measurements are shown in Figure 75. It can be seen that the LNA gain has to be reduced by just over 7dB to directly withstand a -15dBm blocker without a duplexer filter. Since gain is high, the degradation in noise figure is relatively low, only a few dBs. If a good quality duplexer is used, the system could be run at full gain with negligible loss of sensitivity.

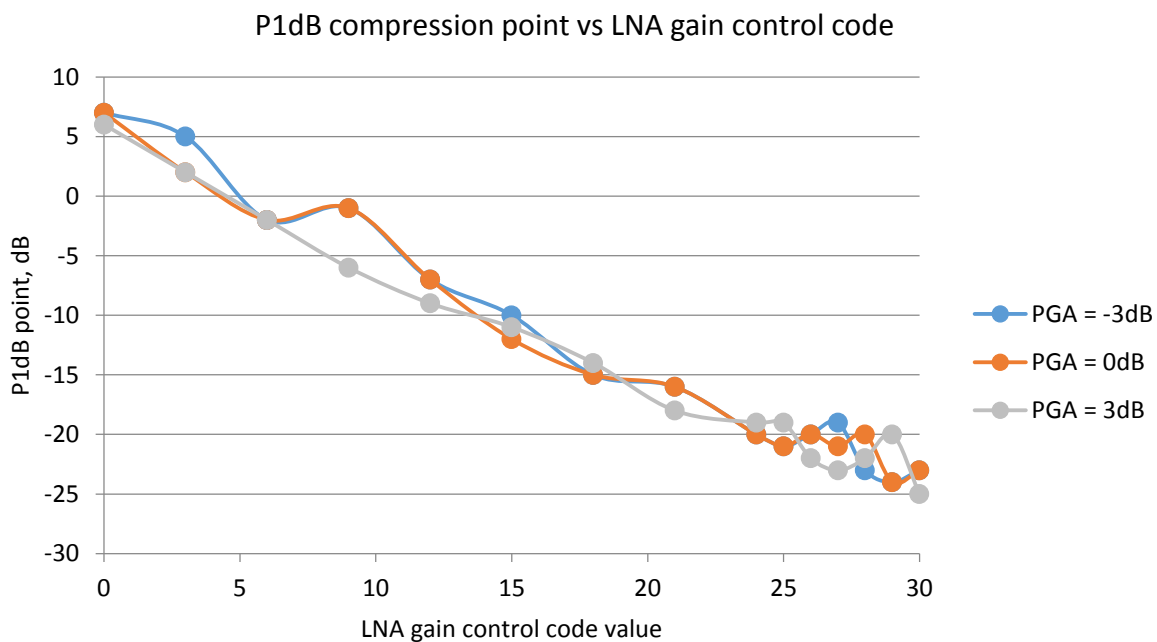


Figure 75. Out of band P1dB compression point vs LNA gain control code. Measured with 2.5MHz LPF and blocker at 20MHz offset for different PGA gains.

4.9 Comparison of LNA gains

The LMS702M has been optimised for low power consumption. This means the mixer of LNAL and LNAW use less power than the mixer of LNAH, leading to a lower maximum frequency of operation. Additionally LNAL uses a different bondwire configuration to improve noise and matching at low frequency. Figure 76 shows the variation of gain with frequency of the LMS7002M evaluation board. The LNAs are matched with the stub tuner for each frequency. The programmable gain blocks were set as follows: LNA=Max Gain, TIA=Mid Gain (-3dB) and PGA=5dB. The test bench of Figure 42 was used for the measurements.

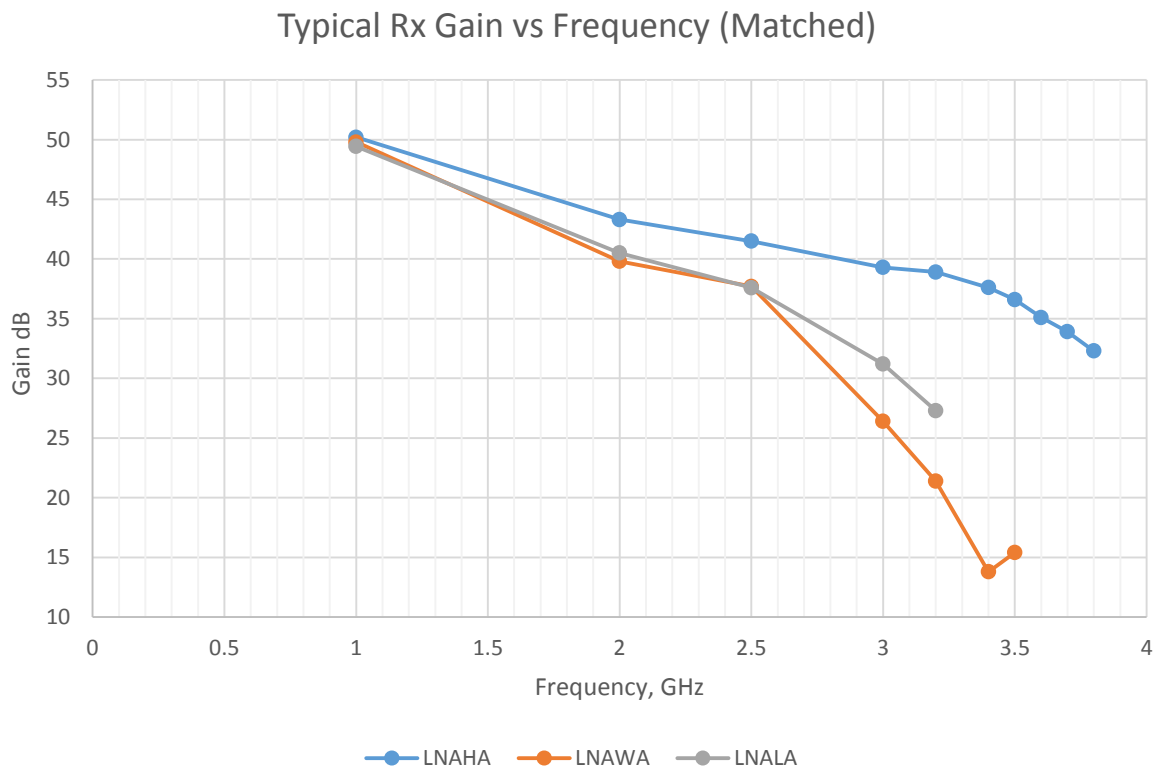


Figure 76. Variation of gain vs frequency of LNAH, LNAW and LNAL on LMS7002M evaluation board with each input matched at each frequency.

4.10 RSSI

The two wideband low noise amplifiers (LNAW) in the receiver inputs have received signal strength indicators (RSSI) at their inputs. These can be used to detect large signals at the input of the LNA to help set the AGC loop for best sensitivity. The RSSI outputs are digitised using the main ADC and the output is read by SPI. Additionally there is a digital RSSI implemented in the RX digital signal processing block (RxTSP) and is documented in another document.

The test configuration used to test the RSSI input is shown in Figure 77. The GUI setup is shown in Table 17. RSSI was measured at 2.14GHz the measurements are shown in Figure 78. The RSSI output value is a differential voltage between its output and a stable reference which is also generated by the RSSI.

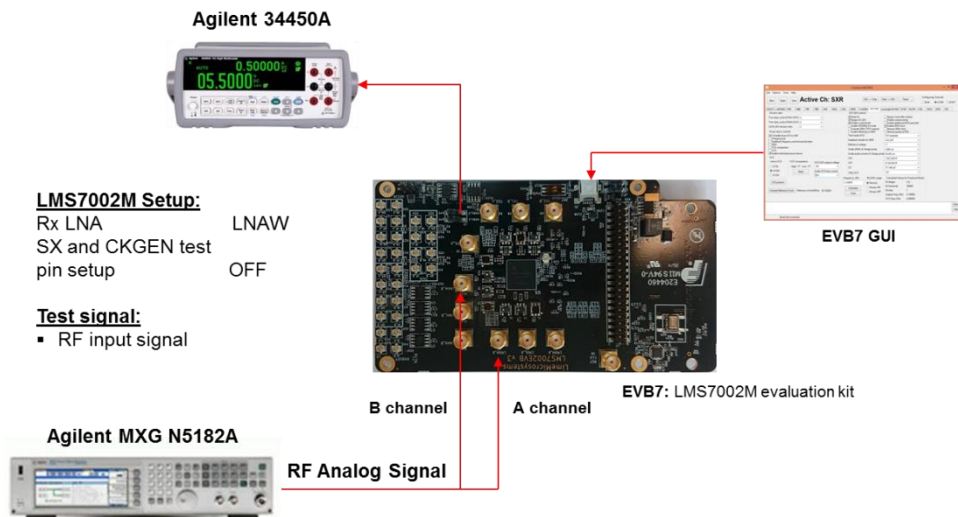


Figure 77. RSSI measurement test setup

Table 17. RSSI GUI setup

| Channel A | Channel B |
|---|---|
| RFE | |
| RXFE RSSI = <input type="checkbox"/> Input of LNAW = <input checked="" type="checkbox"/> | RXFE RSSI = <input type="checkbox"/> Input of LNAW = <input checked="" type="checkbox"/> |

Note: for testing Channel B RSSI with reference voltage, disable Channel A RSSI

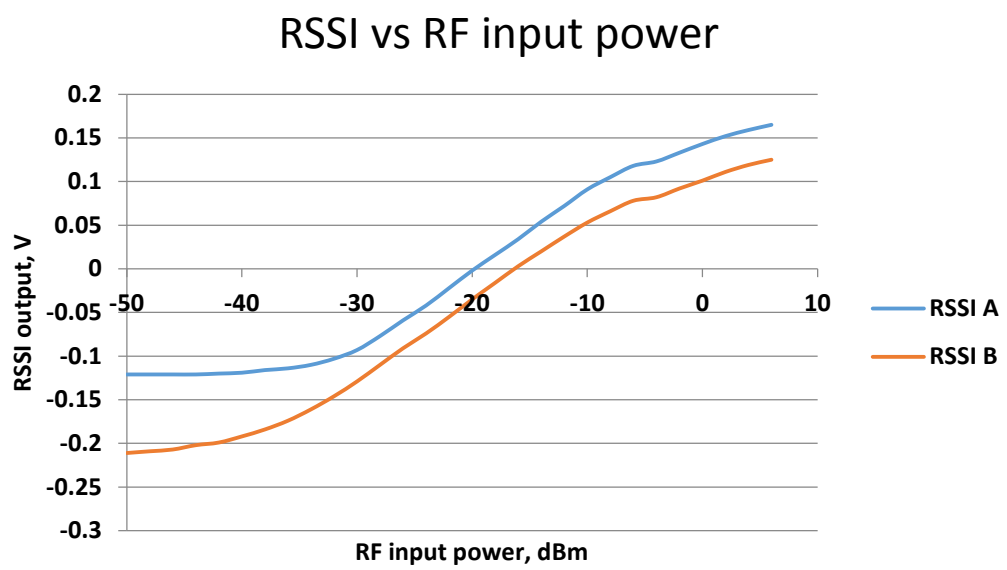


Figure 78. RSSI output value vs input power @ 2.14GHz

4.11 RX Gain step accuracy

The LMS7002M receiver channels include a number of blocks with programmable gain. These blocks include the low noise amplifier (LNA), the transimpedance amplifier (TIA) and the programmable gain amplifier (PGA). The LNA gain is important for optimizing the signal level at the mixer to achieve best dynamic range. The PGA gain can be used for optimizing level to the ADC for achieving AGC. The TIA gain control depends on the IF bandwidth. The TIA is used in minimum gain only for the high band low pass filter (LPFH). The TIA is used in maximum or mid gain only for low band low pass filter (LPFL). The two gain steps for the TIA with LPFL can be used to optimize linearity.

The test bench used to measure the receiver gain steps is shown in Figure 79. The measured variation of LNA gain steps with control code are shown in Figure 80. It can be seen that the first 6 gain steps are 1dB steps. The following steps are 3dB steps. The accuracy of the steps can be affected by the matching networks. Step accuracy depends on frequency and matching sensitivity. The measured variation of TIA gain steps with control code are shown in Table 18. The measured variation of PGA gain steps with gain code is shown in Figure 81. Step accuracy is within 0.1dB and frequency insensitive.

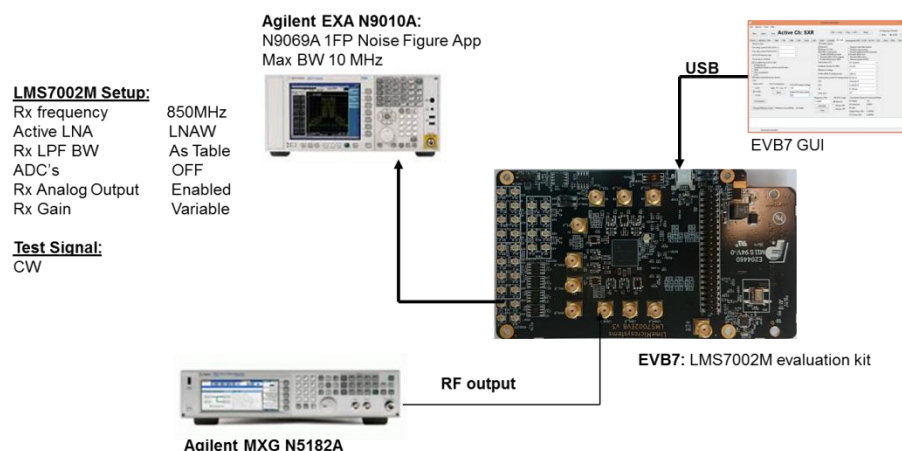


Figure 79. Test bench for measuring RX gain step accuracy

Table 18. Measurements Measured TIA gain step size for different IF frequencies.

| Gain | 1MHz | 10MHz | Active filters |
|------|--------|--------|----------------|
| 0 | 0 | 0 | LPFL |
| -3 | -2.78 | -2.78 | |
| -12 | -11.12 | -10.89 | LPFH |

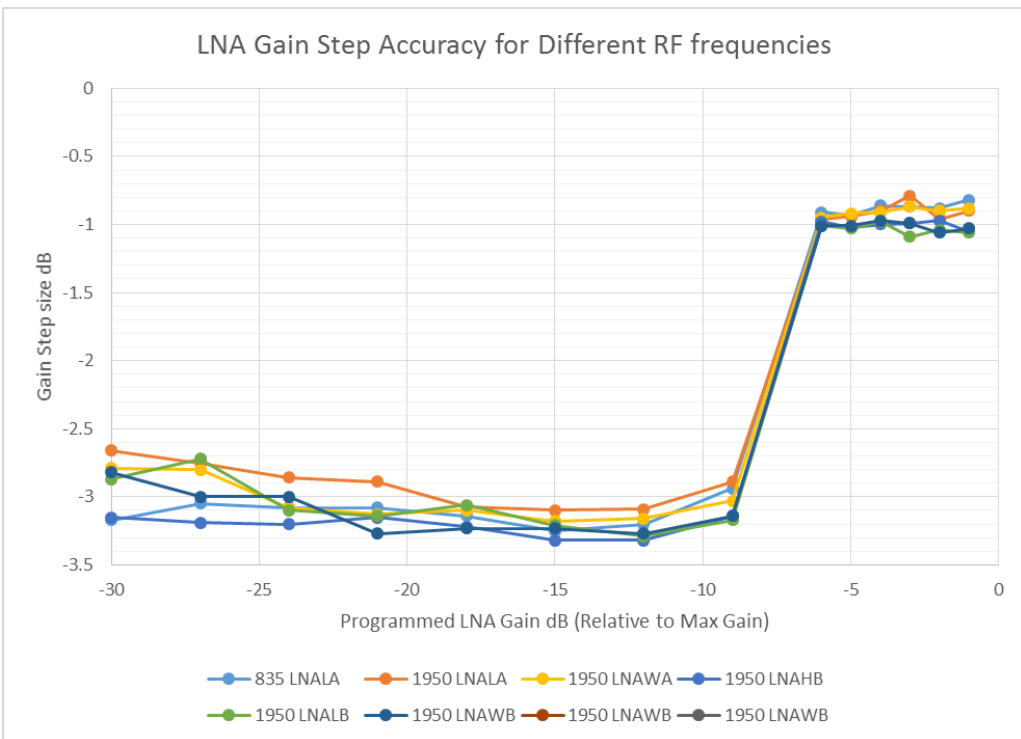


Figure 80. LNA Gain step accuracy for different RF frequencies

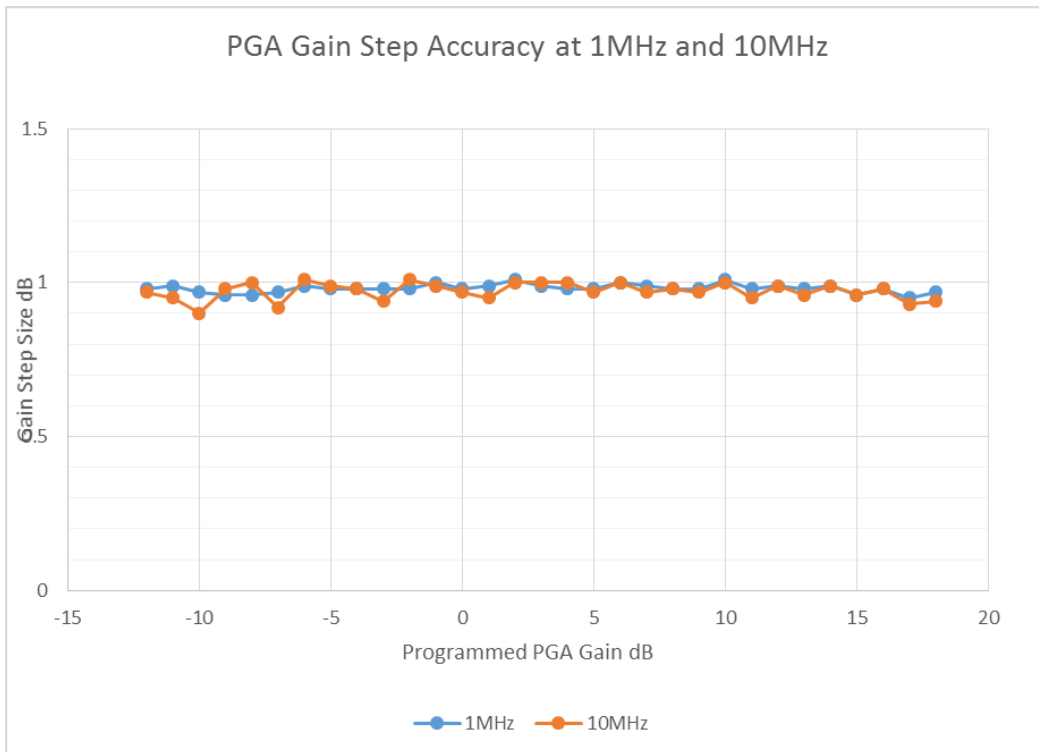


Figure 81. Gain step accuracy for PGA at 1MHz and 10MHz.

4.12 RX LO Leakage at RF Port

Most telecommunication standards specify a maximum LO leakage output at the input of the receiver within the receiver operating band. For example, for 3G it is below -78dBm within the operating band. In a receiver such as the LMS7002M, the topology of having an LNA before a fully differential RX mixer inherently gives a high attenuation of the LO leakage.

Using the test set of Figure 82 the LMS7002M evaluation board is programmed into MIMO RX only operation with 1950MHz LO applied to the RX mixers. The spectrum analyzer is connected to the port being measured. The measurements for each LNA are repeated with the selected LNA on and off. The measurements results are given in Table 19. It can be seen the LO leakage from the RX ports is very low, below -85dBm.

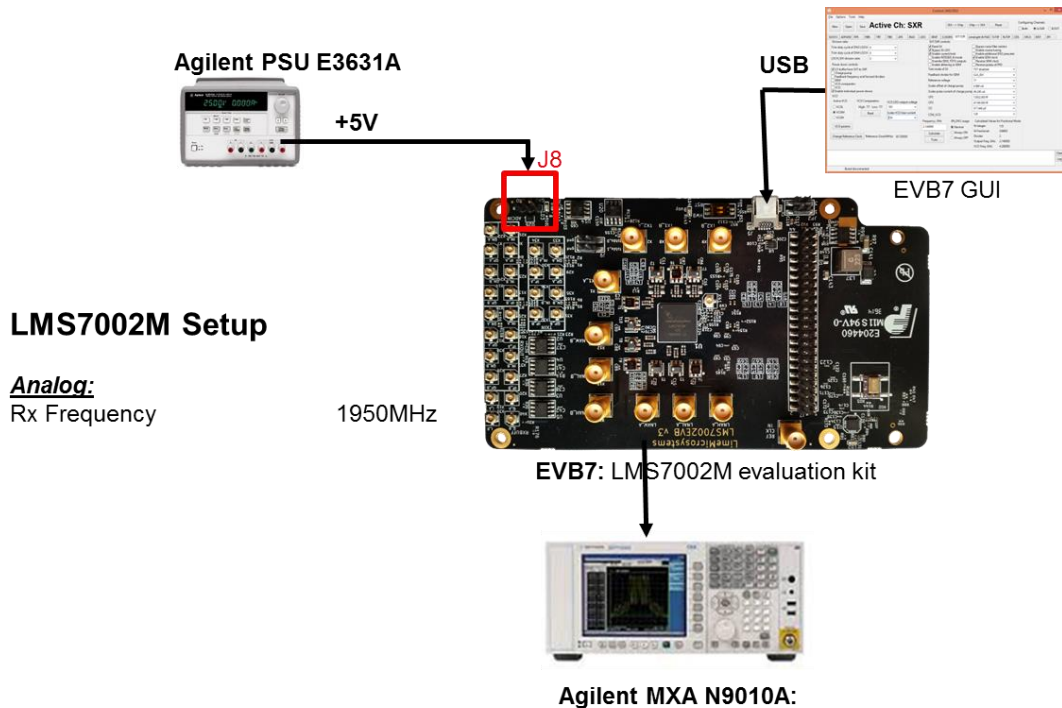


Figure 82. Test bench for measuring RX LO leakage.

Table 19. Measurements of RX LO leakage at RX RF ports.

| LNA | Frequency | TXLO | RXLO | TXA1 | TXA2 | TXB1 | TXB2 | RXAH | RXAL | RXAW | RXBH | RXBL | RXBW |
|----------|-----------|------|------|------|------|------|------|------|------|------|------|------|------|
| Enabled | 1.95 | 2.14 | 1.95 | -102 | -105 | -103 | -102 | -94 | -90 | -91 | -97 | -92 | -98 |
| Disabled | 1.95 | 2.14 | 1.95 | -102 | -105 | -103 | -102 | -97 | -98 | -92 | -99 | -99 | -99 |
| MHz | | | | dBm | | | | | | | | | |

5

Loop Back Measurements

The LMS7002M provides 3 types of loop back for the purpose of calibration and testing. These are RF loopback, baseband analog loopback and digital loopback. Section 5.1 describes the performance and set up of the baseband loopback. Section 5.2 describes the performance and set up of the RF loopback. Digital loopback will be discussed in a separate document.

5.1 Baseband Loopback

The baseband loopback is primarily intended to be used for calibration. This includes LO leakage, image rejection and the frequency response of the TX low band and high band low pass filters. The filters require calibration as ‘on chip’ resistors and capacitors are vulnerable to significant variation of absolute value (up to about +/-20%).

The baseband loopback can also be used to implement various self test functions. It provides a flexible means to route low frequency baseband signals without using the RF outputs or RF loopback. It allows various combinations of low pass filters to be either selected or bypassed. The most useful combinations of the available routing are given in Table 20.

Baseband loopback requires significant set up. The TSP is configured to generate test signals from 1MHz to 50MHz by means of the DAC, CLKGEN PLL and the TSP NCO. The CLKGEN PLL is programmed for 240MHz clocking to allow tone generation up to 60MHz. The DAC is generally set with a current of 625uA. For calibrating the TX low pass filters, it is best to route the baseband loopback directly to the RX programmable gain amplifier.

The baseband test bench is shown in Figure 83. Typical frequency responses of the baseband loopback are shown in Figure 84. In this case, the TXLPFL was programmed for 10MHz, with the TX real pole set to 2MHz. The RXLPFL was programmed for 5MHz. The TXLPFH and RXLPFH were programmed for a cut off frequency greater than 70MHz. The PGA is set with 0dB gain. The IAMP is set with a gain of 32.

Although the baseband loopback allows access to the RX low pass filters, they cannot be fully calibrated in baseband loopback as the TIA includes a pole necessary to produce the full 3rd

order chebychev response. The RX low pass filters should be calibrated using RF loopback described in Section.

Table 20 Baseband Loopback Modes for the LMS7002M

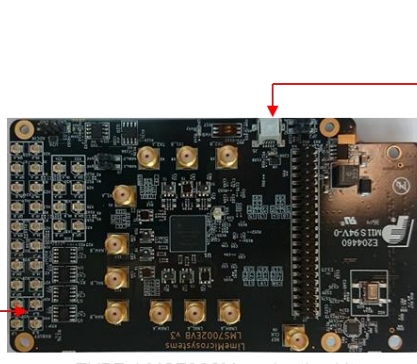
| | | IAMPF | IAMPL | IAMPL | IAMPL | IAMPF | IAMPL | IAMPF | IAMPL | IAMPF | IAMPL |
|---------|----------------------|------------------|------------------|------------------|------------------|------------------|------------------|------------|------------|-------------|------------|
| | | no TXLPF | no TXLPF | TXLPFL+RP | TXLPFL | TXLPFH | TXRP | no TXLPF | no TXLPF | TXLPFL | TXLPFH |
| | | no RXLPF | RXLPLF | RXLPLF | RXLPLF | RXLPLF |
| | | PGA | PGA | PGA | PGA | PGA | PGA | PGA | PGA | PGA | PGA |
| GUI Tab | GUI Parameter | | | | | | | | | | |
| TBB | Tx BB Loopback | TBB Output | TBB Output | TBB Output | LPFLAD Output | TBB Output | TBB Output | TBB Output | TBB Output | PFLAD Outpu | TBB Output |
| TBB | PD LPFH Biquad | y | y | y | y | | y | y | y | y | y |
| TBB | PD LPFH IAMP | | | | | | | | | | |
| TBB | PD LPFLAD | y | y | | | y | y | y | y | y | y |
| TBB | PD LPFS5 | y | | | | y | | y | | | y |
| TBB | Bypass LPF Ladder | | | | | | y | | | | |
| RBB | BB Loopback to RXLPF | Disabled | Disabled | Disabled | Disabled | Disabled | Disabled | LPFL_RBB | LPFH_RBB | LPFL_RBB | LPFH_RBB |
| RBB | PGA input | Loopback from TX | LPFL_RBB | LPFH_RBB | LPFL_RBB | LPFH_RBB |
| RBB | PD LPFH Block | y | y | y | y | y | y | | y | | y |
| RBB | PD LPFL Block | y | y | y | y | y | y | | y | | y |
| RBB | PD PGA Block | | | | | | | | | | |

LMS7002M Setup:

TX/RX RB
loopbacks Enabled
TX PA Disabled
TX LPF BW 10 MHz
RX LPF BW 5MHz
RX LNA Disabled
RX PGA To external

Test signal:

CW Internally generated by NCO



EVB7 GUI

Figure 83 Test bench for baseband loop back testing.

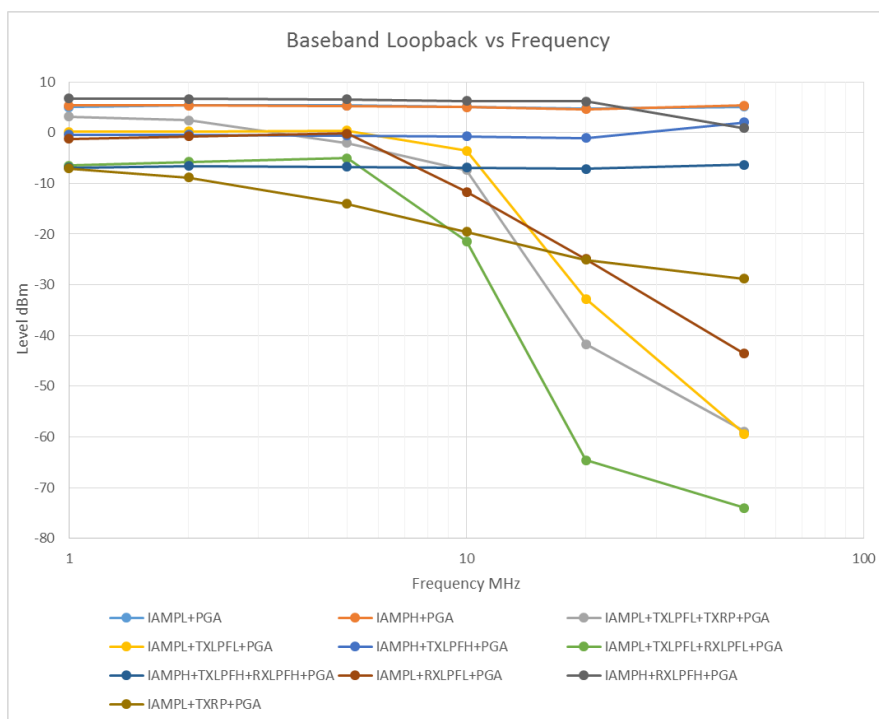


Figure 84 Frequency response of baseband loopback.

5.2 RF Loopback

The RF loopback is primarily intended to be used for calibration of the TX LO leakage, and image rejection. It can also be used to tune the RX low band and high band lowpass filters. The RF loopback occurs ‘on chip’ through internal switches and the level of gain in the RF loopback is programmable in both the TX and RX. Typical settings used for RF loopback are shown in Table 21. The TSP NCO can be used to generate test signals for RF loopback calibration.

The RF loopback occurs ‘on chip’ through internal switches and the level of gain in the RF loopback is programmable. Figure 86 shows how the level of loopback can be controlled by the RF loopback gain control code for two different frequencies, 500MHz and 2.5GHz. The test bench that was used for the measurement is shown in Figure 85.

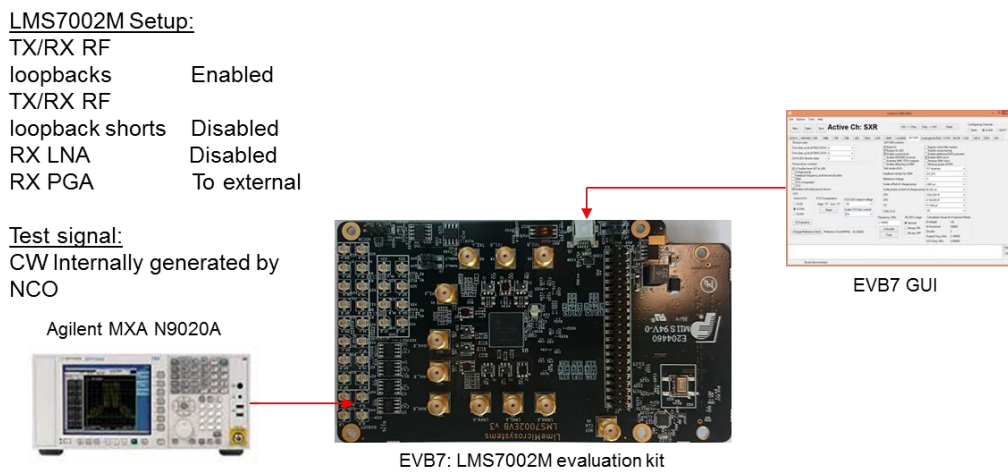


Figure 85. Test bench used to measure RF loopback.

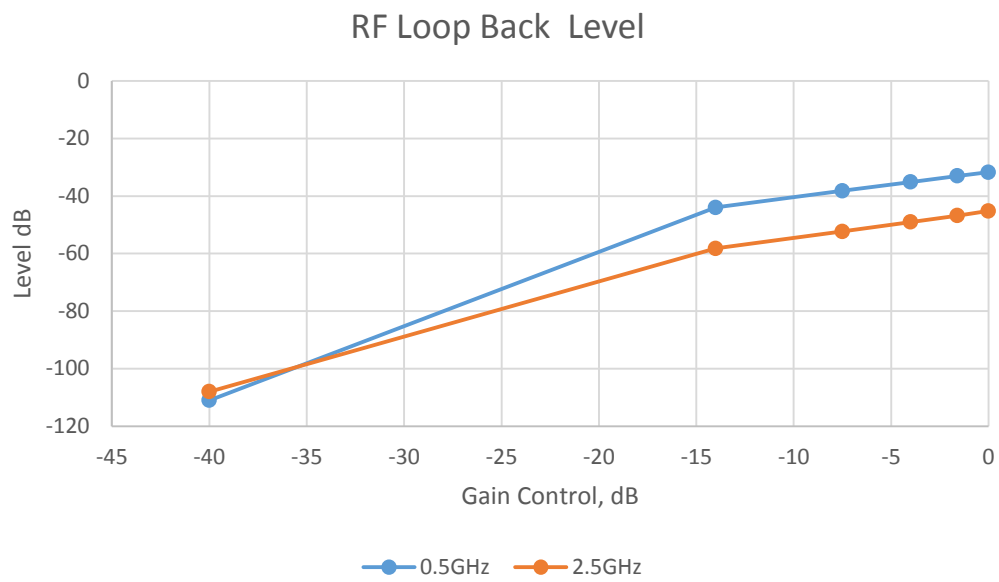


Figure 86. Variation of RF loopback gain for two different frequencies.

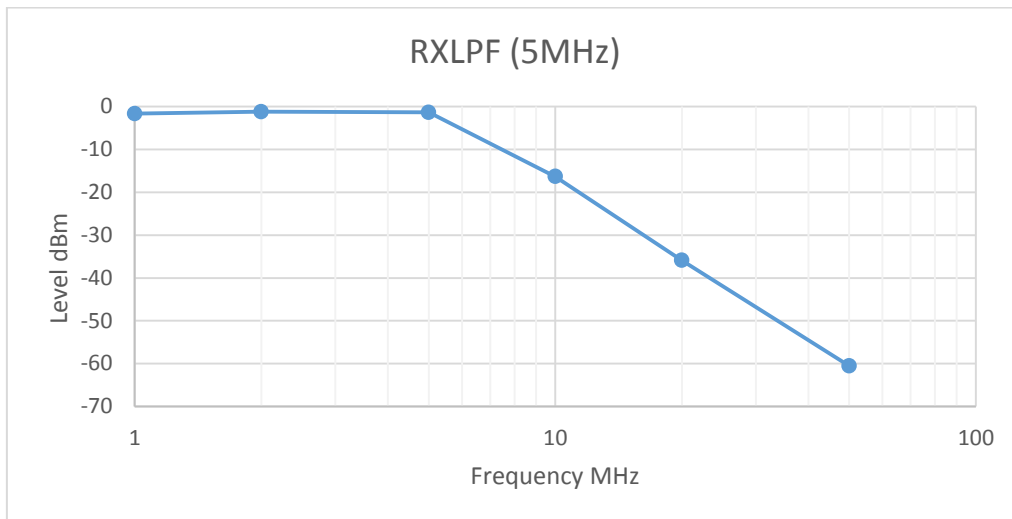


Figure 87 Typical RX LPF response measured with RF loop back.

Table 21 Typical RF Loop Back Settings

| | | |
|-----|---|---------|
| RFE | PD_LNA_RFE | y |
| RFE | PD_RXFE loopback 1 | |
| RFE | PD_RXFE loopback 2 | y |
| RFE | Active path to RXFE | LNAW |
| RFE | short switch loopback 1 | |
| RFE | short switch loopback 1 | y |
| RFE | input of LNAW | y |
| RFE | LNA Gain | GMAX-30 |
| RFE | Loopback Gain | GMAX |
| RFE | TIA | GMAX |
| | | |
| TRF | Enable TXPAD loopback path | y |
| TRF | Loopback loss | 13.9 |
| TRF | TXPAD gain control | 2 |
| TRF | TXPAD linearizing part | 0 |
| TRF | Linearizing bias | 48.3 |
| TRF | Maing gm bias | 12 |
| | | |
| SXT | SXT Frequency (LO and IIR Calibration) | 878 |
| SXT | SXT Frequency (RX LPF Filter Calibration) | 875 |
| SXR | SXR Frequency | 875 |
| | | |
| RFE | TIA 1st Stage | 3 |
| RFE | TIA 2nd Stage | 3 |
| RFE | Feedback Cap TIA | 350 |
| RFE | Feedback resistor TIA | 13 |
| | | |
| RBB | LPFH Capacitance | 12 |
| RBB | LPFL Capacitance | 165 |
| RBB | Resistance | 13 |
| RBB | PD LPFH block | y |
| RBB | PD LPFL block | |
| RBB | PD PGA block | |
| RBB | PGA gain | 0 |
| | | |
| TBB | IAMP Gain | 32 |
| TBB | IAMP Reference | 3 |
| TBB | IAMP Cascode | 12 |
| TBB | PD LPFH Biquad | |
| TBB | PD IAMP | |
| TBB | PDLPFLAD | y |
| TBB | PD LPFS5 real pole | y |

6

Miscellaneous Measurements

This chapter presents a number of measurements. Section 6.1 describes DC power dissipation for different modes of operation. Section 6.2 describes the variation of the internal Low Drop Out Regulators (LDO) voltage with control code. Section 6.3 describes the measurement of the noise of the internal LDOs.

6.1 Power dissipation

The LMS7002M uses low voltage CMOS technology which leads to low power operation. The LMS7002M is highly reconfigurable, capable of operating in a number of modes including RX only, TX only, Frequency Division Duplexing (FDD), Time Division Duplex (TDD) which use both RX and TX simultaneously. Additionally there are single in single out (SISO) or multiple in or multiple out (MIMO) modes. The MIMO mode uses two RX or TX channels simultaneously.

Power dissipation is measured with the test bench shown in Figure 88.

Table 22 shows the power dissipation when the LMS7002M operates in SISO mode, as an RX or TX only. Generally the RX alone in SISO mode uses 160-260mW depending on routing and operating frequency. Generally the TX alone in SISO mode uses 240-380mW at maximum output power, depending on routing and operating frequency. Power can be reduced by reducing output power in TPAD. Note, although the B channel is intended for MIMO operation, it is possible to operate the transceiver with the B channel in SISO operation, e.g. to provide matching for additional bands.

Table 23 shows the power dissipation when the LMS7002M operates in SISO mode, in either FDD or TDD mode. Generally FDD in SISO mode uses between 404-650mW at maximum output power, depending on routing and operating frequency. Power can be reduced by reducing output power in TPAD. Generally TDD in SISO mode uses between 325-650mW at maximum output power, depending on routing and operating frequency. Power can be

reduced by reducing output power in TPAD. The TDD power dissipation is lower than FDD power dissipation as only one PLL is active.

Table 24 shows the power dissipation when the LMS7002M operates in MIMO mode, as an RX or TX only. Generally the RX alone in SISO mode uses 220-330mW depending on routing and operating frequency. Generally the TX alone in SISO mode uses 380-550mW at maximum output power, depending on routing and operating frequency. Power can be reduced by reducing output power in TPAD.

Table 25 shows the power dissipation when the LMS7002M operates in MIMO mode, in either FDD or TDD mode. Generally FDD in SISO mode uses between 595-870mW at maximum output power, depending on routing and operating frequency. Power can be reduced by reducing output power in TPAD. Generally TDD in SISO mode uses between 510-865mW at maximum output power, depending on routing and operating frequency. Power can be reduced by reducing output power in TPAD. The TDD power dissipation is lower than FDD power dissipation as only one PLL is active.

Note that these tests used only the analog part of the transceiver. The digital power dissipation will be presented in a separate document and depends on both clock frequency and functionality.

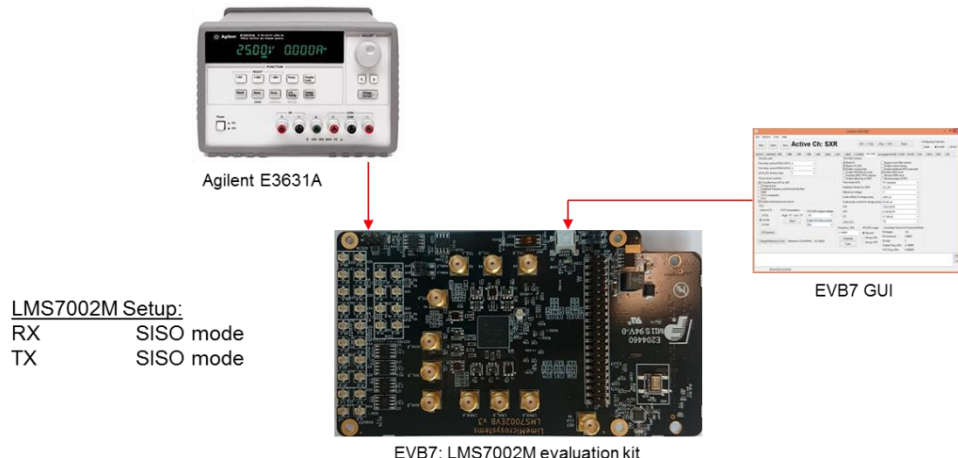


Figure 88. Test bench used to measure power dissipation

Table 22. Comparison of power dissipation of LMS7002M operating either in TX or RX SISO mode for different frequencies.

| Mode | RXA | RXB | TXA | TXB | RX/TX PLL | PDISS mW |
|------------|------|------|-----|-----|-----------|----------|
| Power down | OFF | OFF | OFF | OFF | OFF | 0 |
| SISO-RX | LNAH | OFF | OFF | OFF | 30 | 161.98 |
| SISO-RX | LNAH | OFF | OFF | OFF | 835 | 183.54 |
| SISO-RX | LNAH | OFF | OFF | OFF | 1950 | 166.18 |
| SISO-RX | LNAH | OFF | OFF | OFF | 3800 | 214.76 |
| SISO-RX | LNAL | OFF | OFF | OFF | 835 | 185.08 |
| SISO-RX | LNAL | OFF | OFF | OFF | 1950 | 172.34 |
| SISO-RX | LNAW | OFF | OFF | OFF | 1950 | 182.84 |
| SISO-RX | OFF | LNAH | OFF | OFF | 1950 | 187.74 |
| SISO-RX | OFF | LNAH | OFF | OFF | 3800 | 255.22 |
| SISO-RX | OFF | LNAL | OFF | OFF | 835 | 191.94 |
| SISO-RX | OFF | LNAL | OFF | OFF | 1950 | 193.76 |

| Mode | RXA | RXB | TXA | TXB | RX/TX PLL | PDISS mW |
|-------------|------------|------------|------------|------------|------------------|-----------------|
| SISO-RX | OFF | LNAW | OFF | OFF | 1950 | 202.3 |
| SISO-TX | OFF | OFF | TX1 | OFF | 30 | 241.92 |
| SISO-TX | OFF | OFF | TX1 | OFF | 875 | 273.28 |
| SISO-TX | OFF | OFF | TX1 | OFF | 2140 | 271.04 |
| SISO-TX | OFF | OFF | TX1 | OFF | 3800 | 335.86 |
| SISO-TX | OFF | OFF | TX2 | OFF | 2140 | 275.52 |
| SISO-TX | OFF | OFF | OFF | TX1 | 2140 | 318.22 |
| SISO-TX | OFF | OFF | OFF | TX1 | 3800 | 388.92 |
| SISO-TX | OFF | OFF | OFF | TX2 | 2140 | 312.2 |

Table 23. Comparison of power dissipation of LMS7002M operating either in SISO FDD and TDD mode for different frequencies.

| Mode | RXA | RXB | TXA | TXB | RX/TX PLL | PDISS mW |
|-------------|------------|------------|------------|------------|------------------|-----------------|
| SISO-FDD | LNAH | OFF | TX1 | OFF | 1950/2140 | 514.36 |
| SISO-FDD | LNAH | OFF | TX1 | OFF | 3450/3550 | 647.64 |
| SISO-FDD | LNAL | OFF | TX2 | OFF | 30/40 | 412.3 |
| SISO-FDD | LNAL | OFF | TX2 | OFF | 835/875 | 480.48 |
| SISO-FDD | LNAL | OFF | TX2 | OFF | 1950/2140 | 504.7 |
| SISO-FDD | LNAW | OFF | TX2 | OFF | 1950/2140 | 506.24 |
| SISO-FDD | OFF | LNAH | OFF | TX1 | 1950/2140 | 504.98 |
| SISO-FDD | OFF | LNAH | OFF | TX1 | 3450/3550 | 627.2 |
| SISO-FDD | OFF | LNAL | OFF | TX2 | 30/40 | 404.6 |
| SISO-FDD | OFF | LNAL | OFF | TX2 | 835/875 | 472.22 |
| SISO-FDD | OFF | LNAL | OFF | TX2 | 1950/2140 | 505.12 |
| SISO-FDD | OFF | LNAW | OFF | TX2 | 1950/2140 | 505.26 |
| SISO-TDD | LNAH | OFF | TX1 | OFF | 2140 | 499.8 |
| SISO-TDD | LNAH | OFF | TX1 | OFF | 3800 | 649.6 |
| SISO-TDD | LNAL | OFF | TX2 | OFF | 30 | 325.78 |
| SISO-TDD | LNAL | OFF | TX2 | OFF | 2140 | 507.64 |
| SISO-TDD | OFF | LNAH | OFF | TX1 | 2140 | 485.94 |
| SISO-TDD | OFF | LNAH | OFF | TX1 | 3800 | 621.18 |
| SISO-TDD | OFF | LNAL | OFF | TX2 | 30 | 309.26 |
| SISO-TDD | OFF | LNAL | OFF | TX2 | 2140 | 486.5 |
| SISO-TDD | OFF | LNAW | OFF | TX2 | 2140 | 495.32 |

Table 24. Comparison of power dissipation of LMS7002M operating either in TX or RX MIMO mode for different frequencies.

| Mode | RXA | RXB | TXA | TXB | RX/TX PLL | PDISS mW |
|-------------|------------|------------|------------|------------|------------------|-----------------|
| MIMO-RX | LNAH | LNAH | OFF | OFF | 30 | 219.52 |
| MIMO-RX | LNAH | LNAH | OFF | OFF | 835 | 256.06 |
| MIMO-RX | LNAH | LNAH | OFF | OFF | 1950 | 256.62 |
| MIMO-RX | LNAH | LNAH | OFF | OFF | 3800 | 330.96 |
| MIMO-RX | LNAL | LNAL | OFF | OFF | 1950 | 260.68 |
| MIMO-RX | LNAW | LNAW | OFF | OFF | 1950 | 271.18 |
| MIMO-TX | OFF | OFF | TX1 | TX1 | 30 | 382.9 |
| MIMO-TX | OFF | OFF | TX1 | TX1 | 875 | 446.6 |
| MIMO-TX | OFF | OFF | TX1 | TX1 | 2140 | 487.06 |
| MIMO-TX | OFF | OFF | TX1 | TX1 | 3800 | 554.96 |
| MIMO-TX | OFF | OFF | TX2 | TX2 | 875 | 438.2 |
| MIMO-TX | OFF | OFF | TX2 | TX2 | 2140 | 473.9 |

Table 25. Comparison of power dissipation of LMS7002M operating either in MIMO FDD and TDD mode for different frequencies.

| Mode | RXA | RXB | TXA | TXB | RX/TX PLL | PDISS mW |
|-------------|------------|------------|------------|------------|------------------|-----------------|
| MIMO-FDD | LNAH | LNAH | TX1 | TX1 | 835/875 | 694.54 |
| MIMO-FDD | LNAH | LNAH | TX1 | TX1 | 1950/2140 | 745.36 |
| MIMO-FDD | LNAH | LNAH | TX1 | TX1 | 3450/3550 | 869.82 |
| MIMO-FDD | LNAL | LNAL | TX2 | TX2 | 30/40 | 596.12 |
| MIMO-FDD | LNAL | LNAL | TX2 | TX2 | 835/875 | 684.74 |
| MIMO-FDD | LNAL | LNAL | TX2 | TX2 | 1950/2140 | 733.74 |
| MIMO-TDD | LNAH | LNAH | TX1 | TX1 | 875 | 623 |
| MIMO-TDD | LNAH | LNAH | TX1 | TX1 | 2140 | 729.26 |
| MIMO-TDD | LNAH | LNAH | TX1 | TX1 | 3800 | 864.22 |
| MIMO-TDD | LNAL | LNAL | TX2 | TX2 | 30 | 510.86 |
| MIMO-TDD | LNAL | LNAL | TX2 | TX2 | 2140 | 720.72 |
| MIMO-TDD | LNAW | LNAW | TX2 | TX2 | 2140 | 730.24 |

6.2 ‘On Chip’ LDO Measurements

The LMS7002M includes 30 on chip LDOs, which can allow the chip to be powered from a single 1.8V supply. The LDOs can either be switched off and the chip powered from external voltage regulators, or switched on with only off chip decoupling capacitors connected to the power pins. The voltage of each LDO can be programmed via the SPI control, although the exact voltage may also depend on SPI settings and current consumption. In Table 26 output voltages for several LDOs are presented.

Table 26. Measured output voltage for selected LDOs

| LDO Setting | Voltage, V | | | | | | | |
|-------------|------------|------------|---------|-----------|-----------|-----------|---------|---------|
| | LDO_CPSXT | LDO_DIVSXT | LDO_AFE | LDO_LNA12 | LDO_LNA14 | LDO_MXRFE | LDO_RBB | LDO_TBB |
| 0 | 0.855 | 0.889 | 0.833 | 0.906 | 0.930 | 0.826 | 0.862 | 0.850 |
| 5 | 0.874 | 0.906 | 0.852 | 0.922 | 0.947 | 0.844 | 0.881 | 0.868 |
| 10 | 0.894 | 0.928 | 0.872 | 0.936 | 0.971 | 0.860 | 0.901 | 0.885 |
| 15 | 0.913 | 0.947 | 0.891 | 0.952 | 0.994 | 0.877 | 0.921 | 0.903 |
| 20 | 0.933 | 0.966 | 0.909 | 0.965 | 1.011 | 0.894 | 0.942 | 0.922 |
| 25 | 0.954 | 0.988 | 0.928 | 0.980 | 1.032 | 0.910 | 0.962 | 0.938 |
| 30 | 0.972 | 1.007 | 0.947 | 0.993 | 1.052 | 0.926 | 0.982 | 0.957 |
| 35 | 0.993 | 1.026 | 0.967 | 1.007 | 1.071 | 0.943 | 1.000 | 0.973 |
| 40 | 1.010 | 1.049 | 0.984 | 1.020 | 1.093 | 0.957 | 1.022 | 0.991 |
| 45 | 1.029 | 1.069 | 1.004 | 1.032 | 1.112 | 0.974 | 1.041 | 1.008 |
| 50 | 1.051 | 1.088 | 1.023 | 1.046 | 1.133 | 0.989 | 1.061 | 1.025 |
| 55 | 1.068 | 1.108 | 1.042 | 1.058 | 1.153 | 1.004 | 1.080 | 1.042 |
| 60 | 1.091 | 1.130 | 1.061 | 1.071 | 1.174 | 1.020 | 1.101 | 1.060 |
| 65 | 1.109 | 1.148 | 1.079 | 1.084 | 1.195 | 1.034 | 1.120 | 1.076 |
| 70 | 1.128 | 1.169 | 1.098 | 1.095 | 1.214 | 1.049 | 1.140 | 1.093 |
| 75 | 1.149 | 1.190 | 1.116 | 1.108 | 1.233 | 1.063 | 1.160 | 1.111 |
| 80 | 1.167 | 1.210 | 1.136 | 1.121 | 1.257 | 1.077 | 1.179 | 1.127 |
| 85 | 1.186 | 1.229 | 1.154 | 1.134 | 1.274 | 1.089 | 1.198 | 1.144 |
| 90 | 1.207 | 1.251 | 1.173 | 1.145 | 1.300 | 1.102 | 1.217 | 1.161 |
| 95 | 1.225 | 1.271 | 1.191 | 1.160 | 1.322 | 1.114 | 1.237 | 1.178 |
| 100 | 1.246 | 1.288 | 1.211 | 1.172 | 1.338 | 1.124 | 1.255 | 1.195 |
| 105 | 1.263 | 1.310 | 1.229 | 1.186 | 1.354 | 1.137 | 1.275 | 1.212 |
| 110 | 1.283 | 1.331 | 1.248 | 1.199 | 1.380 | 1.146 | 1.294 | 1.228 |
| 115 | 1.304 | 1.348 | 1.265 | 1.212 | 1.398 | 1.155 | 1.312 | 1.244 |
| 120 | 1.322 | 1.371 | 1.285 | 1.225 | 1.420 | 1.166 | 1.333 | 1.261 |
| 125 | 1.343 | 1.390 | 1.303 | 1.241 | 1.444 | 1.174 | 1.351 | 1.277 |
| 130 | 1.360 | 1.407 | 1.320 | 1.252 | 1.462 | 1.181 | 1.367 | 1.291 |
| 135 | 1.378 | 1.428 | 1.338 | 1.265 | 1.478 | 1.187 | 1.385 | 1.307 |
| 140 | 1.398 | 1.448 | 1.357 | 1.278 | 1.499 | 1.195 | 1.405 | 1.323 |
| 145 | 1.417 | 1.467 | 1.373 | 1.293 | 1.519 | 1.200 | 1.421 | 1.338 |
| 150 | 1.436 | 1.487 | 1.392 | 1.305 | 1.539 | 1.206 | 1.441 | 1.353 |
| 155 | 1.456 | 1.508 | 1.412 | 1.320 | 1.558 | 1.211 | 1.456 | 1.367 |
| 160 | 1.475 | 1.528 | 1.428 | 1.334 | 1.580 | 1.216 | 1.474 | 1.382 |
| 165 | 1.496 | 1.547 | 1.445 | 1.347 | 1.599 | 1.220 | 1.487 | 1.390 |

| LDO Setting | Voltage, V | | | | | | | |
|-------------|------------|------------|---------|-----------|-----------|-----------|---------|---------|
| | LDO_CPSXT | LDO_DIVSXT | LDO_AFE | LDO_LNA12 | LDO_LNA14 | LDO_MXRFE | LDO_RBB | LDO_TBB |
| 170 | 1.513 | 1.568 | 1.462 | 1.361 | 1.618 | 1.223 | 1.502 | 1.404 |
| 175 | 1.532 | 1.586 | 1.480 | 1.371 | 1.636 | 1.227 | 1.515 | 1.415 |
| 180 | 1.552 | 1.606 | 1.492 | 1.388 | 1.656 | 1.229 | 1.526 | 1.427 |
| 185 | 1.571 | 1.629 | 1.509 | 1.397 | 1.671 | 1.232 | 1.535 | 1.436 |
| 190 | 1.591 | 1.646 | 1.521 | 1.411 | 1.687 | 1.235 | 1.542 | 1.446 |
| 195 | 1.607 | 1.664 | 1.529 | 1.422 | 1.699 | 1.237 | 1.550 | 1.452 |
| 200 | 1.627 | 1.686 | 1.540 | 1.433 | 1.708 | 1.240 | 1.556 | 1.461 |
| 205 | 1.646 | 1.703 | 1.549 | 1.447 | 1.716 | 1.241 | 1.561 | 1.468 |
| 210 | 1.664 | 1.722 | 1.556 | 1.458 | 1.723 | 1.243 | 1.564 | 1.474 |
| 215 | 1.684 | 1.743 | 1.564 | 1.468 | 1.728 | 1.244 | 1.568 | 1.479 |
| 220 | 1.701 | 1.759 | 1.570 | 1.480 | 1.732 | 1.245 | 1.571 | 1.485 |
| 225 | 1.716 | 1.774 | 1.573 | 1.489 | 1.734 | 1.247 | 1.574 | 1.489 |
| 230 | 1.730 | 1.780 | 1.577 | 1.499 | 1.738 | 1.247 | 1.576 | 1.494 |
| 235 | 1.736 | 1.780 | 1.581 | 1.505 | 1.740 | 1.249 | 1.578 | 1.497 |
| 240 | 1.746 | 1.781 | 1.582 | 1.516 | 1.742 | 1.250 | 1.580 | 1.501 |
| 245 | 1.749 | 1.780 | 1.584 | 1.522 | 1.743 | 1.250 | 1.581 | 1.504 |
| 250 | 1.750 | 1.781 | 1.587 | 1.530 | 1.745 | 1.251 | 1.583 | 1.506 |
| 255 | 1.752 | 1.781 | 1.588 | 1.535 | 1.746 | 1.251 | 1.584 | 1.510 |

6.3 LMS7002M Internal LDO Noise Measurement

The LMS7002M contains 28 internal low drop out voltage regulators (LDOs). The LDOs are intended to reduce the bill of materials (BOM) of a design using the LMS7002M by eliminating external LDOs below 1.8V. This section describes noise measurement of the LDO.

An evaluation board was modified so that the LDO output from VDD_CP_SXR (pin AL19) was measured. The external power was disconnected by removing R172. An additional network was added which provides AC coupling to an external LNA and spectrum analyser as shown in Figure 90. The external LNA is a low frequency design based on the BFG541. The LDOs are controlled by the LDO tab in the GUI software. EN_LDO_CPSXR is required to be checked to power up the LDO. SPDUP_LDO_CPSXR enables the speed up option for faster settling. The second ‘sub tab’ sets the voltage using RDIV_SPSXR.

The measurements were processed to include the effect of spectrum analyser resolution bandwidth, LNA gain, loss in the AC coupling circuit. It was not possible to calibrate the spectrum analyser and external LNA below 100kHz due to limits of the available signal source. The LDO was measured in normal operation, with the ‘speed up’ option used for fast settling, and in power down. Additionally the noise of the LNA with a 50R termination at the input was measured to show the noise floor of the measurements. The measurements are shown in Figure 91. The integrated noise from 100Hz to 100kHz is about 180uV. The speed up mode of the LDO had very little effect on output noise.

LMS7002M Setup:

LDO_CPSXR Enabled

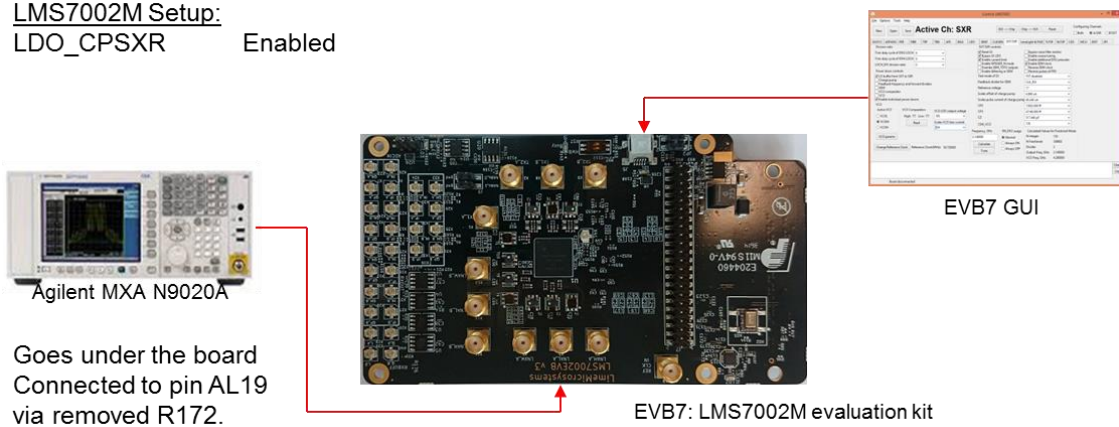


Figure 89 Test configuration used to measure noise.

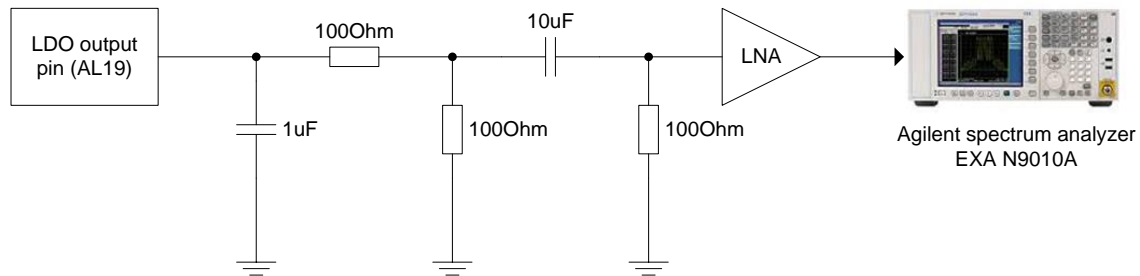


Figure 90 AC coupling circuit used for LDO noise measurement.

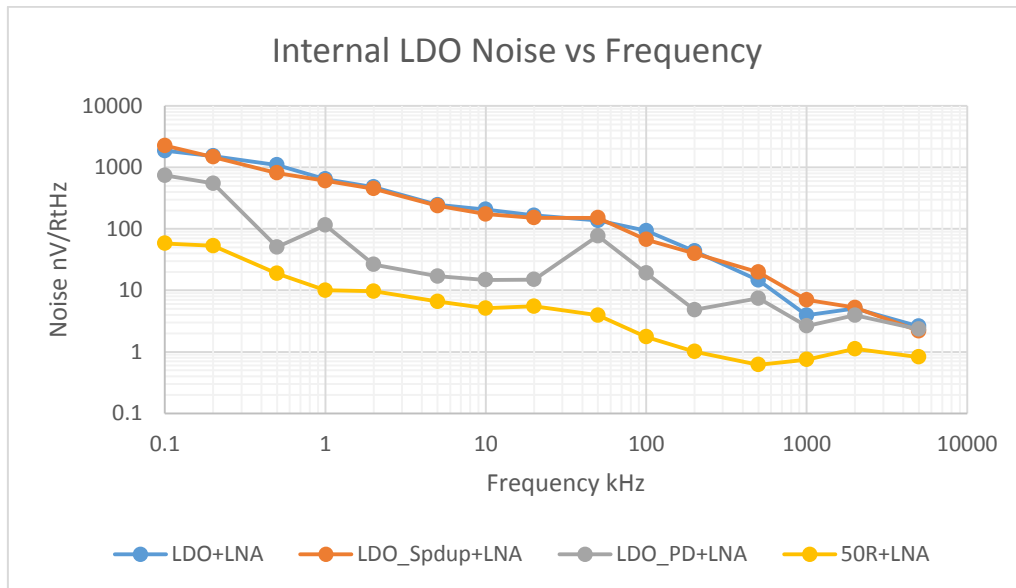


Figure 91 Measured LDO noise of the LDO with LNA for different LDO modes.